

Distribution Agreement

In presenting this thesis or dissertation as a partial fulfillment of the requirements for an advanced degree from Emory University, I hereby grant to Emory University and its agents the non-exclusive license to archive, make accessible, and display my thesis or dissertation in whole or in part in all forms of media, now or hereafter known, including display on the world wide web. I understand that I may select some access restrictions as part of the online submission of this thesis or dissertation. I retain all ownership rights to the copyright of the thesis or dissertation. I also retain the right to use in future works (such as articles or books) all or part of this thesis or dissertation.

Signature:

Elizabeth L. Frost

Date

**CD8 T CELL IMMUNOSURVEILLANCE OF THE POLYOMAVIRUS-
INFECTED CENTRAL NERVOUS SYSTEM**

By

Elizabeth L. Frost

Doctor of Philosophy

Graduate Division of Biological and Biomedical Sciences

Immunology and Molecular Pathogenesis

Aron E. Lukacher, Advisor

Brian D. Evavold, Advisor

Daniel Kalman, Committee Member

William R. Tyor, Committee Member

Ifor R. Williams, Committee Member

Accepted:

Lisa A. Tedesco, Ph.D.
Dean of the James T. Laney School of Graduate Studies

Friday, March 4, 2016

**CD8 T CELL IMMUNOSURVEILLANCE OF THE POLYOMAVIRUS-
INFECTED CENTRAL NERVOUS SYSTEM**

By

Elizabeth L. Frost

B.S., University of Alabama, 2009

Advisors: Brian D. Evavold, Ph.D.

and

Aron E. Lukacher, M.D., Ph.D.

An abstract of

A dissertation submitted to the Faculty of the
James T. Laney School of Graduate Studies of Emory University

in partial fulfillment of the requirements for the degree of
Doctor of Philosophy
in the Graduate Division of Biological and Biomedical Science

Immunology and Molecular Pathogenesis

2016

CD8 T CELL IMMUNOSURVEILLANCE OF THE POLYOMAVIRUS- INFECTED CENTRAL NERVOUS SYSTEM

By Elizabeth L. Frost

Progressive multifocal leukoencephalopathy (PML) is a debilitating and often fatal demyelinating disease of the central nervous system (CNS) in immunosuppressed patients infected by the ubiquitous human JC polyomavirus (JCV). Demyelination is thought to result from lytically infected oligodendrocytes, which fail to be cleared in the setting of depressed JCV-specific T cell-mediated CNS surveillance, for example as a result of natalizumab therapy (targeting very late antigen-4 (VLA-4)-mediated T cell trafficking) for multiple sclerosis. Mechanisms of PML progression and CNS anti-viral immunity are poorly understood, largely due to lack of a tractable animal model resulting from restriction of polyomaviruses to co-evolved hosts. In recent years, humanized mouse models for infection with JCV have been developed but cannot offer insight into the interplay between host immune responses and viral infection. The aim of our work is to bridge this gap, utilizing intracerebral inoculation of immunocompetent mice with mouse polyomavirus (MPyV) to understand whether anti-viral CD8 T cells are protective against demyelinating disease. We show that MPyV productively replicates in the brain, establishing a low-level persistent infection despite robust VLA-4-independent recruitment of CD8 T cells, the majority of which are directed toward a single peptide epitope. These T cells do not undergo contraction. Instead, they are stably maintained independent of replenishment from the circulation or CD4 T cell-help. Brain- as well as kidney-resident memory T (T_{RM}) cells retain high affinity T cell receptors, suggesting high antigen sensitivity is a trait of memory cells resident in multiple non-lymphoid

organs and may be critical for protective pathogen-specific surveillance. MPyV-specific brain T_{RM} cells sustain high levels of programmed cell death-1 (PD-1) receptor—regarded as a marker of T cell dysfunction resulting from chronic antigen stimulation—even as viral load declines. However, PD-1 does not prevent T cells from producing cytokines, controlling viral infection, or proliferating. Despite the presence of high-quality CD8 T cells, MPyV-infection induces CNS demyelination, which opposes what is currently accepted as the underlying cause of PML in humans. Our work raises important questions regarding present knowledge of PML pathogenesis and lays the foundation for an animal model of polyomavirus-induced CNS disease.

**CD8 T CELL IMMUNOSURVEILLANCE OF THE POLYOMAVIRUS-
INFECTED CENTRAL NERVOUS SYSTEM**

By

Elizabeth L. Frost

B.S., University of Alabama, 2009

Advisors: Brian D. Evavold, Ph.D.

and

Aron E. Lukacher, M.D., Ph.D.

A dissertation submitted to the Faculty of the
James T. Laney School of Graduate Studies of Emory University
in partial fulfillment of the requirements for the degree of
Doctor of Philosophy
in the Graduate Division of Biological and Biomedical Science
Immunology and Molecular Pathogenesis

2016

ACKNOWLEDGEMENTS

I would first like to thank my thesis advisor and mentor, Aron Lukacher, for the privilege of taking on such an exciting project and for his extensive knowledge of the literature which shaped this dissertation. Through my work with him I have gained invaluable technical experience and scientific expertise in diverse areas of immunobiology.

I am also grateful to my committee for their guidance and enthusiasm, with special thanks to Brian Evavold for his help with the difficulties that arose as I finished my dissertation long-distance.

I thank my family and friends without whom I could not have come so far. Thank you for your love, support, and compassion, and for visiting me in Hershey.

Thank you to my labmates past and present for your mentorship and making life in lab enjoyable. I am fortunate to share a lifelong scientific journey with all of you.

TABLE OF CONTENTS

CHAPTER 1: INTRODUCTION	1
1.1 Evidence that JCV-specific T cells confer protection from PML	8
1.2 CNS-resident memory CD8 T cells	10
1.3 The inhibitory PD-1 receptor balances immunity and immunopathology in the CNS	13
1.4 Using JCV to model PML in animals	15
1.5 JCV entry to the CNS	17
1.6 MPyV as a model to understand human polyomavirus pathogenesis	19
1.7 Summary	22
CHAPTER 2: RESIDENT-MEMORY CD8 T CELLS EXPRESS HIGH-AFFINITY T CELL RECEPTORS	23
Abstract	24
Introduction	25
Materials and Methods	26
Results and Discussion	29
Figures	36
CHAPTER 3: PD-1^{HI} CD8 T CELLS IN THE BRAIN REMAIN FUNCTIONAL DURING PERSISTENT MPyV INFECTION	43
Abstract	44
Introduction	45
Materials and Methods	48
Results	52
Discussion	58
Figures	63
CHAPTER 4: MPyV INDUCES CNS DEMYELINATION AND RECRUITS CD8 T CELLS INDEPENDENT OF VLA-4	72
Abstract	73
Introduction	74
Materials and Methods	78
Results	82
Discussion	88
Figures	92
CHAPTER 5: DISCUSSION	103
REFERENCES	114

LIST OF FIGURES

(in order of appearance in the chapter)

CHAPTER 2

2-1	Characterization of MPyV-specific T cell responses in the brain	36
2-2	MPyV-specific CD8 T cells survive long-term in the brain	37
2-3	Increase in tetramer binding and CD8 expression by MPyV-specific CD8 T cells in the brain	38
2-4	Comparison of TCR affinities of MPyV-specific CD8 T cells in the brain, kidney, and spleen	39
S2-1	Kidney-infiltrating CD8 T cells have elevated CD8 expression and tetramer binding, and express T _{RM} markers	40
S2-2	Adhesion frequency analyses of MPyV-specific effector and memory CD8 T cells from brain, kidney, and spleen	41

CHAPTER 3

3-1	Analysis of PD-1 expression and cytokine production by MPyV-specific CD8 T cells in brain and spleen	63
3-2	Comparison of T cell functionality in wild-type mice and mice genetically deficient for PD-L1	64
3-3	Comparison of T cell phenotype in wild-type mice and mice genetically deficient for PD-L1	65
3-4	Comparison of T cell functionality and phenotype in the brain of PD-L1-blockade or rat IgG treated mice	66
3-5	Expression of Tbet and Eomes transcription factors by LT359-specific CD8 T cells during acute and persistent MPyV infection	67
3-6	Expression of PD-L1 by hematopoietic and brain-resident non-hematopoietic cells during acute and persistent MPyV infection	68
S3-1	Expression of dendritic cell markers and antigen-presentation receptors in bone marrow-derived dendritic cell cultures	70
S3-2	Comparison of T cell functionality and phenotype in the brain of PD-L1-blockade or rat IgG treated mice	71

CHAPTER 4

4-1	Kinetic analysis of location of MPyV-infected cells and T cell infiltrate in the brain by immunohistochemistry	92
4-2	Identification of MPyV-infected CNS cell types by immunofluorescent Staining	94
4-3	Kinetic analysis of demyelination and evidence of astrogliosis in MPyV-infected mice	95
4-4	Comparison of immune responses and T cell infiltration of the brain in MPyV-infected VLA-4-deficient and wild-type mice during acute infection	97
S4-1	Comparison of viral load and immune responses following intracerebral and intravenous inoculation with MPyV	99
S4-2	Detection of MPyV replication in the brain following intracerebral inoculation	100
S4-3	Detection of anti-VLA-4 monoclonal antibody in sera	101
S4-4	Comparison of integrin expression profiles of CD4 T cells in MPyV-infected VLA-4-deficient and wild-type mice during acute infection	102

CHAPTER 1

INTRODUCTION

Originally published in *Frontiers in Immunology* as Frost EL and Lukacher AE (2015)

The importance of mouse models to define immunovirologic determinants of progressive multifocal leukoencephalopathy. *Front. Immunol.* **5**:646. doi: 10.3389/fimmu.2014.00646

<http://journal.frontiersin.org/article/10.3389/fimmu.2014.00646/full>

Progressive multifocal leukoencephalopathy (PML) is a severely debilitating and often fatal demyelinating disease of the central nervous system in immunosuppressed patients infected by the ubiquitous human JC polyomavirus (JCV). Demyelination is thought to result from lytically infected oligodendrocytes, which fail to be cleared in the setting of depressed JCV-specific T cell-mediated CNS surveillance. Although JCV mutations and genomic rearrangements, in addition to immunosuppression, are recognized risk factors, mechanisms of disease progression and CNS antiviral immunity are poorly understood, largely due to lack of a tractable animal model. Early studies using mouse polyomavirus (MPyV) in T cell-deficient mice demonstrated productive viral replication in the CNS and demyelination, but were confounded by spinal cord compression by virus-induced vertebral bone tumors. Here, we review current literature regarding animal models of PML, focusing on current trends in antiviral T cell immunity in non-lymphoid organs, including the CNS. Advances in our understanding of MPyV and human polyomavirus lifecycles, viral and host determinants of MPyV-induced tumorigenesis, and T cell immunity to viral infections in the CNS warrant revisiting the mouse-MPyV CNS infection as a bona fide animal model for JCV-PML.

The human JC polyomavirus (JCV) persists silently in >50% of the healthy adult population, with recent evidence suggesting an even higher prevalence [1, 2]. Seroepidemiological studies indicate that individuals are first exposed to JCV in late adolescence [3]. Based on detection of JCV in tonsils and sewage, the virus is thought to be acquired via respiratory or fecal-oral transmission routes [4-6]. JCV was discovered in 1971 as the etiologic agent of progressive multifocal leukoencephalopathy (PML) [7], a life-threatening demyelinating disease of the central nervous system (CNS) resulting from lysis of infected oligodendrocytes [8, 9]. PML was first described in 1958 in patients with chronic lymphocytic leukemia (CLL) and Hodgkin's lymphoma [10], and has since been diagnosed in individuals immunosuppressed by a variety of hematological malignancies. Before the advent of highly active antiretroviral therapy (HAART), approximately 5% of individuals afflicted with HIV/AIDS developed PML, such that PML became regarded as an AIDS-associated disease [11]. Profound immunosuppression, however, is not an essential prelude to PML. PML is seen in HIV-negative individuals with occult or minimal immunosuppression caused by old age, chronic liver or kidney disease, untreated dermatomyositis, and idiopathic CD4 or CD8 lymphopenia [12]. No effective anti-JCV agents are currently available, and the prognosis for PML is poor [13]. Recently, PML has emerged in patients receiving humoral immunomodulatory agents for autoimmune diseases and inflammatory disorders.

In 2005, a trilogy of articles in the *New England Journal of Medicine* described PML in patients with relapsing-remitting multiple sclerosis (RRMS) and Crohn's disease given the monoclonal antibody natalizumab (Tysabri®) [14-16]. Recent studies report that

the risk of PML increases with duration of natalizumab therapy and is as high as 11.1 cases per 1000 patients in MS patients seropositive for JCV, >24 months of infusion therapy, and a history of immunosuppression [17]. Most MS treatment regimens were designed to reduce autoreactive immune responses. Natalizumab is a humanized antibody against α_4 integrin, which complexes with the integrins β_1 (to form very late antigen-4, VLA-4) or β_7 on the surface of activated T cells [18]. VLA-4 and $\alpha_4\beta_7$ enable T cells to traffic to sites of infection/inflammation or to mucosal tissues, respectively. VLA-4 and $\alpha_4\beta_7$ are required for T cell extravasation by mediating leukocyte arrest at activated vascular endothelium expressing the VLA-4 ligand vascular cell adhesion molecule 1 (VCAM-1) or the $\alpha_4\beta_7$ ligand mucosal addressin cell adhesion molecule (MAdCAM-1). Supporting the hypothesis that natalizumab-mediated VLA-4 blockade impairs CNS immune surveillance is an early study showing that a cohort of 23 MS patients receiving natalizumab had decreased counts of CD4 and CD8 T cells, CD19⁺ B cells, and CD138⁺ plasma cells in the CSF compared to 35 untreated MS patients and 16 patients with other neurological disease. Of 14 patients available for six-month followup after cessation of natalizumab therapy, all but one had decreased counts in each of these lymphocyte populations; the one exception being a patient having a modest elevation in CD4 and CD8 T cell counts coincident with an MS relapse [19].

Other monoclonal antibody-based immunomodulatory therapies, including efalizumab (anti-LFA-1, for severe plaque psoriasis) and rituximab (anti-CD20, for B cell lymphoma), have been shown to put patients at risk for PML; because of this risk, efalizumab was taken off the market despite its efficacy in reducing rejection in kidney transplant recipients [20]. With development of more intense steroid-avoidance

immunosuppressive agents in transplantation medicine, there is concern that the incidence of PML may also rise in this patient population, as has happened for BK virus (BKV)-associated nephropathy. Recent evidence suggests that different immunosuppressive regimens that confer susceptibility to PML share inadequate T cell-mediated surveillance for JCV-infected CNS glial cells as an underlying disease mechanism. As discussed above, natalizumab interferes with trafficking of circulating effector T cells into the CNS. Rheumatoid arthritis patients receiving rituximab show marked T cell depletion, particularly in the CD4 T cell compartment, which is associated with clinical response [21]. B cell-depletion therapies, such as rituximab, may affect T cell responses by depleting B cell-derived cytokines/chemokines, by eliminating B cell in their capacity as professional antigen-presenting cells to activate CD4 T cells, or possibly by limiting availability of immune complexes to cross-present antigens to CD8 T cells by FcγR⁺ dendritic cells [22].

Immune reconstitution by HAART for AIDS or plasma exchange for monoclonal antibody therapy is the recommended treatment option for PML [23]. Such regimens predispose patients to a rapid, robust, and often fatal influx of circulating leukocytes into the CNS termed immune reconstitution inflammatory syndrome (IRIS); paradoxically, these treatments can accentuate PML lesions, cause relapse of autoimmune disease, or in the case of organ transplant recipients, lead to graft rejection [24].

In addition to underlying depressed or altered immune function, viral determinants may also increase PML risk and/or disease severity. Mutations resulting in single amino acid substitutions in the host cell receptor binding domain of the viral capsid protein VP1 and rearrangements/deletions in the non-coding control region (NCCR) were

found in most JCV sequences from cerebrospinal fluid (CSF) of PML patients [25-28]. These mutations may constitute necessary viral determinants for PML and underlie the sharp discrepancy between the high prevalence of JCV infection and the low incidence of PML. Recent work demonstrated that rearranged NCCRs conferred increased early viral gene expression and DNA replication capability in glial cells [29]. An important role for the JCV capsid protein in CNS tropism is supported by evidence that a hybrid virus containing the early genes of the monkey polyomavirus, SV40, and the late genes of the PML-JCV (Mad-1 strain) acquired the more restricted host range of JCV; i.e., the ability to infect human fetal glial cells but not monkey cells, and to hemagglutinate human type O red blood cells [30]. Recent evidence using JCV VP1 virus-like particles (VLPs) suggested that the PML-associated JCV capsid mutations alter viral tropism, retaining virion binding specificity for CNS glial cells but not to other non-CNS cell types, and differing from wild type VLPs in glycan specificity [25]. However, pseudoviruses with these VP1 mutations failed to transduce glial cells, raising the possibility that these CSF VP1 variants are noninfectious [31]. The functional role of these VP1 variants, whether they confer neurovirulence, and, if so, whether JCV acquires them in the periphery or after entry into the brain remains to be determined.

Several lines of evidence suggest that humoral immunity selects VP1 mutant polyomaviruses. Exposure of a library of VP1-mutagenized SV40 variants to a neutralizing monoclonal antibody selected viruses with mutations in solvent-exposed loops of VP1 that were resistant to neutralization by this antibody [32]. BKV serotypes have been shown to vary in their level of cross-recognition by neutralizing antibodies generated by VLP immunization [33]. Interestingly, BKV isolates from kidney transplant

patients with nephropathy and viremia also had a high frequency of VP1 substitutions [34]. These findings raise the possibility that VP1-specific neutralizing antibody responses select variant polyomaviruses with mutations in VP1 that enable escape from antiviral humoral immunity. Whether T cell immunosuppression/-modulation favors neutralizing antibody-driven selection of such polyomavirus escape variants is unknown.

Progress in understanding pathogenesis of JCV-induced PML and developing effective therapeutic approaches is handicapped by the low number of PML cases, inadequate understanding of risk factors (with only three broad risk factors described to date for natalizumab-treated MS individuals — JCV seropositivity, prior immunosuppression, and >2 years of therapy), and heterogeneity among PML patients (e.g., differences in immunosuppression regimens, HLA type, age, and gender). Additional obstacles include consistent patient compliance in clinical studies, under-reporting and under-recognition of the disease, and the rapidity of disease progression following diagnosis [35]. Because JCV replicates only in humans, we have limited understanding of the pathogenesis of PML and the immune mechanisms needed to keep persistent polyomavirus infection in check. Studying the evolution of PML pathology rather than the endpoint of disease when PML is diagnosed is essential for identifying factors that predispose only a small fraction of immunosuppressed individuals and those receiving immunomodulatory therapy to PML.

An animal model of polyomavirus-induced CNS disease that mimics pathologic hallmarks of PML would circumvent these obstacles and enable us to address important unanswered questions, including:

1. Which facets of innate and adaptive immunity control of JCV infection in the brain and how does immunosuppression/immunomodulation interfere with this control?
2. Are there circumstances in which anti-viral immune surveillance in the CNS may prove pathological rather than protective?
3. Does the pathogenesis of PML vary with different immunomodulatory regimens?
4. How/when does JCV traffic to the CNS?
5. When are PML-associated viral mutations acquired and do they confer neurotropism/neurovirulence to JCV? Are these mutations the result of immune selection/evasion?
6. Why are individuals treated with humoral immune modulatory agents susceptible to JCV encephalitis encephalitides caused by other persistent microbial pathogens (e.g., toxoplasmosis, HSV-1)?

A tractable small animal model of CNS infection by a natural host polyomavirus will provide insight into PML risk factors, mechanisms of disease, and provide a preclinical model to evaluate candidate antiviral agents. Here, we review current literature on T cell-mediated control of viral infections in non-lymphoid organs, including the CNS, describe potential mechanisms to dampen T cell function in the setting of persistent CNS infection, and advocate application of the mouse polyomavirus (MPyV) model to understand immune control of polyomavirus infection in the CNS.

1.1 Evidence that JCV-specific T cells confer protection from PML

Effective immunity to viruses typically depends on CD8 T cells and their ability to directly target and kill virally infected cells. Accordingly, presence of detectable JCV-specific CD8 T cells in peripheral blood correlated with improved prognosis and survival in PML patients [36-38], whereas anti-JCV humoral responses do not [39, 40]. In HIV⁺ patients, a detectable level of JCV-specific CD8 T cells was coincident with a higher number of CD4 T cells [41], the presence of which in peripheral blood has been positively correlated with PML survival [42]. The dominant HLA-A2-restricted CD8 T cell epitopes found in JCV-seropositive individuals are directed to determinants corresponding to VP1 residues 100-108 (p100) and 36-44 (p36), with the former being the dominant specificity [43]. Staining with HLA-A*0201-VP1p36 and -VP1p100 tetramers showed that these JCV-specific CD8 T cells have an effector-memory phenotype (CD62L^{lo}CD45RA⁻CD49d^{hi}) and can be found in the PBMCs of healthy individuals, perhaps contributing to the overall low incidence of PML [44, 45]. Indeed, when measured early after PML diagnosis, the presence of JCV-specific CD8 PBMCs predicted control of PML while the absence of these cells predicted active PML progression [41]. In HIV⁺ PML patients, CD8 T cells can be found infiltrating the brain and co-localizing with infected oligodendrocytes at the edges of PML lesions [46] where the T cell receptor ligands MHC-I and -II are upregulated [47]. Taken together, these findings suggest that JCV infection is predominantly controlled by CD8 T cells.

Studies of human JCV-specific T cell responses have been largely based on analysis of PBMCs. Because few JCV-specific cells can be isolated from healthy individuals and PML patients, JCV-specific T cells are generally subjected to extended

expansion and selection in tissue culture, which obscures conclusions regarding their *in vivo* phenotype and function, as highlighted by an early study showing long-term *in vitro* T cell proliferation can profoundly underestimate frequencies of antigen-specific T cells *in vivo* [48]. Although the development of MHC-I tetramers for detecting JCV-specific CD8 T cells has improved quantification of these cells, the low incidence of PML coupled with few described HLA-restricted JCV epitopes limits direct analyses of JCV-specific CD8 T cells in PML patients. Additionally, analysis of CNS-infiltrating T cells is hampered because PML brain lesions show minimal inflammation, which may be due to the patient's immunosuppressive state and to the late stage of disease at time of diagnosis. Only one study has analyzed CNS-infiltrating JCV-specific T cells directly *ex vivo* by flow cytometry using a fresh brain biopsy of a natalizumab-treated MS patient with a pronounced T cell infiltrate secondary to IRIS [49]. Examination of immune surveillance prior to diagnosis of PML is limited to CSF samples, which does not necessarily reflect immune infiltrates in the brain parenchyma [19]. Given the limited data available regarding the type, function, and location of cellular infiltrates in the brain parenchyma, little is known about the status of immune surveillance in the CNS for JCV-infected cells prior to PML and during its progression.

Insights into the evolution and maintenance of JCV-specific T cell responses in the human CNS would greatly benefit from a mouse model of polyomavirus CNS infection. Use of this animal model would provide insight into the kinetics of anti-polyomavirus immune surveillance in the CNS, how immune suppression alters this surveillance and the incidence of neuropathology. Inbred strains of mice simplify identification of viral peptide T cell epitopes, which is essential to monitor the

magnitude, phenotype, and function of virus-specific T cells. Incisive identification of determinants of effective CNS immune responses can be achieved using transgenic mice, mice with targeted genetic deletions, and antibody-mediated blockade of key interactions or deletion of specific cell types. Mouse models of viral infections can be optimized for pathogen dose and time postinfection to yield higher numbers of immune cells to study directly *ex vivo*. Furthermore, immune cells can be isolated from mouse tissues providing insight into potential differentiation/regulation of cells *in situ* in the CNS. Such studies using mouse models are underpinned by a newfound appreciation that circulating T cells are phenotypically and functionally distinct from those resident in non-lymphoid tissues.

1.2 CNS-resident memory CD8 T cells

Memory CD8⁺ T cells are heterogeneous in phenotype, differentiation, and function; these parameters are linked to their migration patterns and anatomic location [50]. Since the original description of nonlymphoid organ-homing “effector memory” vs lymphoid organ-homing “central memory” populations [51], evidence is quickly accumulating that memory T cell heterogeneity is integrated with tissue residence; i.e., depending on their tissue localization, memory T cells vary in expression of chemokine receptors, adhesion molecules, and effector capabilities [52]. Effector memory T cells are now thought to be comprised of circulating and non-circulating subsets. The latter “tissue resident” memory T cells or T_{rm} cells are distinguished from circulating effector memory cells by upregulation of CD69 and granzyme B (canonically indicative of TCR activation and cytotoxic effector capability, respectively) and cell surface expression of the

$\alpha_E(\text{CD103})\beta_7$ integrin. Because the $\alpha_E\beta_7$ complex binds to E-cadherin, CD103 expression implicates a role for these integrins in T cell retention in epithelium. Recent work showed that CD103 is variably expressed by CD8 T_{rm} cells in different tissues, suggesting that CD103 *per se* is not a signature T_{rm} cell marker [53]. CD69 directly antagonizes expression of S1P₁, a sphingosine-1-phosphate receptor expressed by T cells to enable their egress from peripheral lymphoid organs [54]; S1P₁ downregulation is essential for retention of T cells in tissues [53]. TGF- β is a key mediator of CD103 expression by activated CD8 T cells in the skin and intestinal mucosa, as well as the CNS, and TGF- β may also be involved in upregulating CD69 [55-57]. CD8 T_{rm} cells persist long-term in the skin and in mucosal sites such as the respiratory tract, female reproductive tract, and gut [58-61], and for the intestine at least, maintenance of CD8 T_{rm} cells is antigen-independent [56]. A rapidly expanding body of literature demonstrates that T_{rm} cells contribute to host defense against bacterial and viral reencounter at mucosal and epidermal sites [62, 63].

Antiviral CD8⁺ T cells also establish residence in the CNS but appear to differ in their requirements for function and survival compared to those in extra-CNS nonlymphoid tissues. CNS infection by vesicular stomatitis virus, an acutely infecting pathogen, resulted in the progressive accumulation in the brain of CD103⁺ CD69^{hi} granzyme B^{hi} virus-specific CD8 T_{rm} cells, whose maintenance was antigen-independent and required CD103 [64]. Differences in virus interactions with their hosts (e.g., levels of antigen persistence, cytopathic/noncytopathic cell fate, and host cell tropism) will undoubtedly influence the establishment, maintenance, and function of CNS-resident memory T cells and their immunosurveillance efficacy for infected cells.

The presence of CNS-infiltrating CD8 T cells circumscribing demyelinated lesions was associated with improved clinical outcome in HIV/AIDS-related PML patients [46]. This association has been extended to explain the development of PML in MS patients receiving natalizumab. MS progression is characterized by two distinct phases: a primary relapsing-remitting stage in which repetitive and acute infiltration of the brain by myelin-reactive T cells infiltrate occurs and inflammation resolves; and a secondary progressive phase in which little inflammation is observed but lesions of demyelination and functional disability worsen [65]. Because natalizumab acts to exclude circulating activated T cells from the CNS, it is possible that no JCV-specific T cells infiltrate the brains of natalizumab-treated MS patients with ongoing JCV replication. MS is a difficult disease to diagnose, and patients likely experience acute autoreactive inflammation prior to initiation of natalizumab therapy. Myelin-reactive inflammation may render the blood brain barrier “permeable” to JCV (as free virions or via infected cells, as discussed below) as well as JCV-reactive T cells. In this connection, it merits noting that natalizumab is typically not the first-line treatment option for MS. If JCV infection in the brain and a subsequent T cell infiltration occurred prior to the administration of natalizumab therapy, CNS-infiltrating JCV-specific cells would not be affected and could potentially establish a resident memory population. Based on data from various animal models of tissue resident memory, in the context of persistent infection in the CNS functional JCV-specific T_{rm} cells might survive long-term or be driven to dysfunction and deletion. In the former case, JCV-specific T_{rm} cells would be protective, whereas in the latter situation, exhausted T_{rm} cells may predominate and fail to limit the number of infected oligodendrocytes. Natalizumab, then, would prevent

replenishment of CNS-infiltrating JCV-specific T cells from circulating blood and result in deficient T cell-mediated immune surveillance for infected glial cells. These alternate scenarios may help explain the rarity of PML even in immunocompromised individuals. Knowing the longevity of functional T_{m} cells in the CNS, which would be most readily studied in a mouse model of polyomavirus CNS infection, may help explain the increased risk of PML with long-term natalizumab therapy.

1.3 The inhibitory PD-1 receptor balances immunity and immunopathology in the CNS

The brain is widely considered to be an “immune privileged” organ. Until recently, immune privilege was thought to result from a complete exclusion of the immune effector cells; however, healthy immune privileged sites are actually subject to active immune surveillance, but the functionality of immune effector cells is tightly regulated to protect vital and nonrenewable tissues [66]. Regulating cells of the immune response typically depends on the balance of activating and inhibitory signals. PD-1 (CD279), a CD28-family molecule, is expressed by activated T cells and counters the activation signaling cascade initiated by TCR ligation. PD-1 expression is significantly elevated on JCV-specific CD4 and CD8 T cells from peripheral blood of PML patients [67]. PD-1 is induced by TCR signaling and its expression is maintained in settings of persistent antigenic stimulation such as chronic viral infection, cancer, and autoimmunity. PD-1 binds to two ligands, PD-L1 (also called B7-H1; CD274) and PD-L2 (CD273) that differ in expression patterns: PD-L1 is broadly expressed by hematopoietic and

parenchymal cells; and PD-L2 is inducibly expressed on DCs and macrophages [68]. Recent work indicates that variable levels of PD-1 signaling translates to differentially dampening T cell functions, with low PD-1 levels inhibiting TNF- α , IL-2 production, and cell proliferation and higher levels inhibiting cytotoxicity and IFN- γ production [69]. Sustained high PD-1 expression in the setting of chronic viremic infection mediates exhaustion of virus-specific CD8 T cells [70].

Although PD-1 regulation of T cells has been intensively investigated for systemic persistent viral infections, surprisingly little is known about its role in viral encephalitis. IN mouse cytomegalovirus encephalitis, brain-localized CD8 T cells express PD-1, activated microglia and astrocytes express its ligand (PD-L1, and PD-1 blockade in microglia/astrocytes and CD8 T cell co-cultures increases IFN- γ production [71]. CD8 T cells infiltrating the CNS of mice persistently infected by the gliatropic mouse JHM coronavirus are PD-1^{hi}. IFN- γ receptor signaling by oligodendrocytes induces their expression of PD-L1, which, in turn, limits effector activity of PD-1^{hi} JHM-specific CD8 T cells [72]. Engagement of these PD-1^{hi} cells with PD-L1⁺ oligodendrocytes prevents T cell-mediated axonal bystander damage, but does so at the cost of negating viral clearance [73, 74]. Interestingly, CNS infection by VSV, a neurotropic and non-demyelinating pathogen is associated with robust virus-specific CD8 T cell brain infiltrates, but these cells lack PD-1 [64]. PD-1 is elevated on CD8 T cells from PML patients [67]. These studies raise the possibility that PD-1 upregulation is a property of T cells responding to gliatropic viral infections. These data are in line with the concept that PD-1 inhibits T cell-mediated immunopathologic demyelination, a concept supported by

studies documenting a protective role for PD-1 in the experimental autoimmune encephalomyelitis (EAE) mouse model of MS [75-78].

Because persistent polyomavirus infection establishes a low-level antigen set-point, PD-1 upregulation by polyomavirus-specific T cells is unexpected, and suggests that sustained strong TCR signaling may not be essential for PD-1 expression in the brain. In HIV-positive individuals, PD-1 expression is higher on T cells in the CSF than those in blood, despite viral RNA levels being lower in the CSF [79]. Certain common γ -chain cytokines (IL-2, IL-7, IL-15, and IL-21) and type I IFNs have been shown to induce and maintain PD-1 expression on TCR-activated cells [80-82]; and type I and type II IFNs, IL-6, IL-2, IL-7, and IL-15 upregulate PD-L1 [83]. With regard to MPyV, IFN- β transcripts have been shown to be elevated in brains of mice given MPyV i.c. [84]. This raises the possibility that the polyomavirus-induced proinflammatory environment in the CNS could complement low/intermittent TCR engagement to upregulate PD-1 on antiviral T_{RM} cells in the brain. A polyomavirus CNS infection animal model would enable investigation of the mechanisms of PD-1 upregulation by brain-resident, virus-specific T cells and the functional role(s) of PD-1 expression by T cells in the CNS.

1.4 Using JCV to model PML in animals

A tractable animal model of PML requires sufficient similarities between hallmarks of disease in humans, including cell targets for viral replication, mechanisms of immune control, associated risk factors, and neuropathology. Until recently, however, attempts to model PML in mice utilizing the etiologic agent of PML, JCV, have been handicapped by

the tight species specificity of *Polyomaviridae*. Lacking a viral DNA polymerase, polyomaviruses rely on the host cell DNA polymerase apparatus to replicate their genomes, and thus have devised strategies to override cell cycle checkpoints [85]. The species restriction for polyomaviruses is controlled at the level of binding by the host cell DNA polymerase α -primase complex to the viral origin of replication [86, 87], a molecular interaction reflective of the co-evolution of each *Polyomaviridae* family member with a particular vertebrate species. Non-productive infection by polyomaviruses can result in the integration of the viral genome into the host chromosomal DNA resulting in tumor formation [88-90]. Accordingly, experiments involving intracranial (i.c.) inoculations of animals with JCV resulted in non-productive infection and development of astrocytomas or glioblastomas but not PML-like disease [91-96]. Transgenic mice containing the early region of JCV in all cells predominantly expressed T antigens in oligodendrocytes and exhibited a dysmyelination phenotype, but did not recapitulate the demyelination associated with JCV encephalitis in humans [97]. These findings have largely obviated the use of JCV infection in unmanipulated mice to model PML.

To partially preserve the species specificity of JCV infections in animal hosts, attempts have been made to use JCV in humanized mouse models. Low levels of JCV DNA were detected in the urine and blood of JCV-infected NOD/SCID/IL-2R α ^{-/-} mice reconstituted with human fetal bone marrow, thymus, and liver, as were low numbers of IFN- γ -producing T cells [98]. In the absence of human CNS tissue to provide cellular targets for JCV replication, this system cannot recapitulate PML. This obstacle has recently been overcome. Goldman and colleagues created human glial chimeric mice by

engrafting human bipotential oligodendrocyte-astrocyte progenitor cells into congenitally hypomyelinated $Rag2^{-/-}$ $Mbp^{shi/shi}$ neonatal mice, resulting in efficient colonization of the mouse brain with human astrocytes and oligodendrocytes and myelination [99, 100]. Using these human glial chimeric mice, Kondo et al. recently reported that intracerebral delivery of Mad-1 JCV resulted in early widespread productive infection of the engrafted human astrocytes, focal demyelination, and gliosis [101]. Only rare oligodendrocytes were infected early postinfection, but at late timepoints large numbers of T antigen⁺ VP1⁻ oligodendrocytes were detected. These findings raise the provocative possibility that demyelination may in large part be accounted for by deficient trophic support for oligodendrocytes resulting from death of productively infected astrocytes rather than by elimination of oligodendrocytes by lytic JCV infection. Another notable finding in this study was the rapid emergence of a sizeable number of VP1 genomic mutations, with at least two previously seen in JCV isolates from PML patients. Thus, astrocytes may be a major site for emergence of neurovirulent VP1 variant viruses. This chimeric mouse model represents an important advance toward understanding mechanisms of pathogenesis of demyelination; however, infection of these human glia-engrafted mice cannot provide insight into the role of JCV-specific immune responses in the CNS.

1.5 JCV entry to the CNS

A major unresolved question is the mode of transit of JCV to the CNS; i.e., as free virus and/or via infected “Trojan Horse” cells. Deep sequencing of JCV NCCR in matched urine, plasma, and CSF samples from a PML patient provides strong support for a hematogenous route for viral dissemination [102], a conclusion in line with earlier

evidence that VP1 mutations are detected in blood and CSF, but not in urine, of PML patients [27]. Human brain microvascular endothelial cells have been demonstrated to be permissive for JCV infection, a finding supporting the possibility that JCV may cross the blood–brain barrier by infecting endothelial cells [103]. In favor of cell-based blood-to-brain carriage is an early study reporting detection of JCV and BKV DNA in peripheral blood leukocytes from healthy adults [104]. Subsequent work has focused attention on B cells and/or CD34⁺ hematopoietic progenitor cells (HPCs) as candidate vehicles for conveying JCV to the CNS. JCV DNA, as well as expression of T antigen and VP1, has been observed in HPC cell lines, B cell lines and primary B cells infected *in vitro* by high-dose virus inocula, and rare JCV DNA⁺ B cells have been detected in PBMCs from a PML patient [4, 105]. In addition, the rearranged NCCR contains multiple binding sites for the Spi-B and NF1-X, transcription factors that enhance JCV replication and are expressed by B cells, HPCs, and glial cells (reviewed in Ref. [13]). Notably, gene expression of unfractionated blood, and sorted CD19⁺ B cells, and CD34⁺ HPCs from MS patients receiving natalizumab revealed upregulation of genes involved in B cell activation and differentiation, including Spi-B [106, 107]. These findings are in line with a proposal that upregulation of specific transcription factors that bind JCV NCCR underlie a resurgence of JCV replication in natalizumab-treated individuals [108, 109]. Because B cells are endowed with the recombination apparatus enabling V(D)J recombination of immunoglobulin gene segments, B cells have also been proposed to provide an environment conducive for JCV genome recombination and/or rearrangement [13], despite the absence of RAG-dependent recombination signal sequence motifs in the JCV genome. Whether B cells are truly capable of supporting JCV replication remains to

be demonstrated, particularly in light of recent data suggesting that B cells may carry intact input JCV virions and transfer them to susceptible glial cells [110]. CD49d antibody-mediated blockade in mice and non-human primates is associated with elevated circulating CD34⁺ cells, an observation recapitulated in natalizumab-treated MS patients [111-113]. In humans, natalizumab has also been reported to mobilize CD34⁺ cells, pre-B cells, and B cells into the circulation [114, 115]. These observations give additional impetus to the value of an immunocompetent mouse model of PML to define the cellular vehicle by which JCV is transported to the brain parenchyma, the status of JCV replication in these cells, and investigating the possible role of VLA-4 blockade in promoting JCV spread to the CNS.

1.6 Mouse polyomavirus as a model to understand human polyomavirus pathogenesis

Mouse polyomavirus (MPyV), the founding member of the *Polyomaviridae* family, is structurally and genomically similar to JCV, BKV, and SV40 polyomaviruses. All polyomaviruses consist of a double-stranded, covalently closed circular ~5-kb DNA genome encapsidated by a nonenveloped icosahedral shell composed of 72 pentameric VP1 capsomers. The genomes of all polyomaviruses have a ~500-bp NCCR containing the origin of replication bidirectional promoters separating the genome in to early and late genes, with respect to the onset of viral DNA synthesis: an early region encoding the nonstructural small T and large T antigens; and a late region encoding the viral capsid proteins VP1, VP2, and VP3. Unlike JCV, the MPyV genome does not encode an agnoprotein in its late region and contains an additional early region sequence encoding

the non-structural middle T antigen, which mediates cellular transformation and tumor induction [116].

Mouse polyomavirus also resembles BKV and JCV with regard to infectivity and interaction with the immune system. Epidemiologic surveys of wild mice showed that MPyV, like its human counterparts, is a widely prevalent, harmless pathogen in its natural host reservoir [117, 118]. MPyV infects a variety of epithelial and mesenchymal cells [119], macrophages, and DCs, but not lymphocytes [120]. Neuroectodermal lineage cells were stated to be non-permissive for MPyV replication [119], but evidence for this host cell restriction is lacking. As described above for PML-JCV variants, strains of MPyV carrying single amino acid differences in VP1 differed in glycan specificity, which in turn altered tissue tropism and pathogenesis [121, 122]. Similar to reports of long-term persistence of JCV and BKV DNA in a variety of human tissues [6, 109, 123], MPyV DNA has been detected in multiple organs, including those of the CNS, kidney, and bone marrow, for months after acute infection in both immunodeficient and immunocompetent mice [124-126], with decline in immunologic status setting the stage for viral reactivation. Both human and mouse polyomavirus infections elicit potent neutralizing antibody responses directed toward VP1 that inhibit capsid binding to sialylated glycolipid and glycoprotein receptors on host cells. MPyV persistently infects mice in the presence of virus-neutralizing VP1 Abs [127]. Similarly, neutralizing Abs against JCV, typically present in most individuals, confer no protection against PML [128]. While neither human nor mouse polyomaviruses cause overt disease in immunocompetent adult hosts, immunosuppression provides an opportunity for both human and mouse polyomaviruses to induce a variety of disease processes [129]. MPyV-

induced rejection of mouse renal allografts has been used to understand how immunosuppression alters the evolution of polyomavirus-associated nephropathy and how the immune response to polyomavirus infection contributes to allograft injury [130, 131].

MPyV replication causes disease in the CNS. Primary glial cells derived from mouse corpus callosum showed that type 1 astrocytes, but neither type 2 astrocytes nor oligodendrocytes, were infected by MPyV [132]. This was not the case *in vivo* as infection of congenitally athymic mice with MPyV resulted in wasting disease and spinal cord demyelination consequent to infection of oligodendrocytes [133]. Demyelinated lesions were not observed in euthymic mice, emphasizing the role of immune suppression in disease progression. Infected nude mice eventually developed hind limb paralysis, which was attributed to vertebral bone tumors rather than PML-like disease [134, 135]. In each of these early studies, mice were infected by a natural route of transmission via contamination from a neighboring mouse room. In a study involving i.c. infection of adult nude mice with the LID strain of MPyV, which caused fatal kidney and brain hemorrhages in newborn C3H mice [122], paralysis and vertebral tumors developed in the absence of demyelination [135]. This publication was largely responsible for the *de facto* moratorium on use MPyV CNS infection as a model for PML. Interestingly, molecular modeling showed that the valine-to-alanine substitution at VP1 amino acid 296 in LID was orthologous to ²⁶⁹VP1 of JCV, where a serine-to-phenylalanine/tyrosine mutation was among the frequent mutations detected in VP1 genes of JCV isolates from PML patients [26]. Although an MPyV-mouse model of CNS disease cannot reproduce all aspects of JCV-PML pathology in humans, just as significant aspects of other mouse

models do not fully recapitulate human disease, new evidence for the existence of tissue-specific protective anti-viral T cells and recent work from our laboratory using i.c. inoculation of MPyV in tumor-resistant mice, suggest that MPyV may prove to be an important animal model of polyomavirus-induced CNS demyelination.

1.7 Summary

Progressive multifocal leukoencephalopathy, a rare complication of immunosuppression, is caused by infection of the CNS by JC virus, a highly ubiquitous and silent human pathogen in healthy individuals. This wide discordance between virus prevalence and disease incidence appears to stem from the coalescence of multiple predisposing factors including viral determinants that alter host cell tropism, host immune determinants that affect CNS surveillance for infected glial cells, and variability in the underlying immunosuppressive disease/treatment regimen. Lack of a tractable animal model due to the tight species specificity of *Polyomaviridae* has stymied efforts to determine the contributions of each factor to PML pathogenesis. Here, we have reviewed the literature describing previous attempts to develop animal models for PML and propose use of mouse polyomavirus to study the interplay between the host immune response and infection in the brain. Significant research using peripheral blood mononuclear cells and autopsy/biopsy tissue from PML patients implicates a role for JCV-specific T cell responses in disease outcome. The MPyV encephalitis model should provide insight into mechanisms of JCV-induced demyelination and evolution of protective/pathological immune responses to JCV CNS infection *in situ*, as well as provide a preclinical platform to evaluate strategies to prevent and control PML.

CHAPTER 2

Resident-memory CD8 T cells express high-affinity T cell receptors

Elizabeth L. Frost^{1*}, Anna E. Kersh^{1, 2*}, Brian D. Evavold², and Aron E. Lukacher³

¹Immunology and Molecular Pathogenesis Graduate Program, Emory University,
Atlanta, GA

²Department of Microbiology and Immunology, Emory University, Atlanta, GA

³Department of Microbiology and Immunology, The Pennsylvania State University
College of Medicine

*E.L.F. and A.E.K. contributed equally to this work.

Author contributions: E.L.F, A.E.K., B.D.E., and A.E.L. designed research; E.L.F. and A.E.K. performed research; E.L.F, A.E.K, B.D.E, and A.E.L. analyzed data; E.L.F., A.E.K., and A.E.L. wrote the paper.

Originally published in *The Journal of Immunology*. Frost EL, AE Kersh, BD Evavold, and AE Lukacher. 2015. Resident-memory CD8 T cells express high-affinity T cell receptors. *J. Immunol.* 195: 3520-3524. Copyright © 2015 The American Association of Immunologists, Inc.

<http://www.jimmunol.org/content/195/8/3520>

Abstract

Tissue-resident memory T (T_{RM}) cells serve as vanguards of antimicrobial host defense in non-lymphoid tissues, particularly at barrier epithelia and in organs with non-renewable cell types (e.g., brain). In this study, we asked whether an augmented ability to sense antigen complemented their role as early alarms of pathogen invasion. Using mouse polyomavirus, we show that brain-resident mouse polyomavirus-specific CD8 T cells, unlike memory cells in the spleen, progressively increase their binding to MHC class I tetramers and CD8 co-receptor expression. Using the two-dimensional micropipette adhesion-frequency assay, we show that T_{RM} cells in brain, as well as in kidney, express T cell receptors (TCRs) with up to 20-fold higher affinity than do splenic memory T cells, whereas effector cells express TCRs of similar high affinity in all organs. Together, these data demonstrate that T_{RM} cells retain high TCR affinity, which endows them with the high antigen sensitivity needed for front-line defense against infectious agents.

Introduction

Anatomic location shapes the phenotypic and functional heterogeneity that defines subsets of memory T cells. Central memory T cells reside in secondary lymphoid organs, whereas effector memory T cells travel through the vasculature and enter non-lymphoid tissues. The third and largest subset of memory T cells does not recirculate and remains in fixed position in nonlymphoid tissues [136]. These tissue-resident memory T (T_{RM}) cells inhabit cutaneous and mucosal epithelia, portals of pathogen invasion where *in situ* initiation of immune defenses may prove essential for limiting host morbidity and mortality [137]. These cells also occupy non-barrier sites [136, 138]; the CNS may especially rely on T_{RM} cells to protect the large populations of non-regenerative cells. Brain CD8 T_{RM} cell responses have been characterized for acutely cleared CNS infections, such as vesicular stomatitis virus (VSV) and West Nile virus [57, 64, 139]. JC polyomavirus (JCV) is an opportunistic pathogen in the human virome that can cause the life-threatening, demyelinating CNS disease progressive multifocal leukoencephalopathy (PML) under conditions of immunocompromise. Elevated frequencies of JCV-specific CD8 T cells correlate with improved PML prognosis in HIV/AIDS patients [36]. Using the two-dimensional micropipette adhesion-frequency assay, we identified high TCR affinity as a property of virus-specific CD8 T cells responding to persistent mouse polyomavirus (MPyV) infection in the brain. MPyV-specific T_{RM} cells in the kidney, a major site of human polyomavirus persistence, also expressed high-affinity TCRs. High TCR affinity facilitates the ability of T_{RM} cells to sense viral antigens during low-level persistent infections.

Materials and Methods

Mice and virus inoculation

C57BL/6NCr female mice, purchased from the Frederick Cancer Research and Development Center of the National Cancer Institute (Frederick, MD), were housed in accordance with the guidelines of the Institutional Animal Care and Use Committee of The Pennsylvania State University College of Medicine. Anesthetized mice (7–12 wk old) were injected intracerebrally in the right frontal lobe with 2×10^6 PFU MPyV strain A2 in 30 μ l DMEM 5% FBS. Heat-inactivated (70°C for 30 min) MPyV stock had no infectious virus by plaque assay (limit of detection 5 PFU/ml; data not shown).

Quantitation of MPyV genomes

TaqMan real-time PCR was performed with 10 μ g template DNA purified from tissue. Primers and amplification parameters were described previously [125].

mAb-mediated T cell depletion

Mice were injected i.p. with 250 μ g rat anti-CD8 (YTS169.4; Bio X Cell, West Lebanon, NH), rat anti-CD4 (GK1.5; Bio X Cell), or ChromPure whole rat IgG (Jackson ImmunoResearch, West Grove, PA) at 10 and 12 days postinfection (dpi) and then weekly until 60 dpi. Lack of staining of PBMCs by anti-CD4 (RM4-5) or anti-CD8b (53-5.8) confirmed depletion.

Cell isolation, stimulation for intracellular cytokine staining, and flow cytometry

Brains, kidneys, and spleens were harvested from transcardially perfused mice. After collagenase digestion, brain and kidney cells were isolated on Percoll gradients and exposed to Fixable Viability Dye (eBioscience, San Diego, CA) and Fc Block (BioLegend, San Diego, CA) prior to staining with D^b-LT359–368 tetramers (National Institutes of Health Tetramer Core Facility, Atlanta, GA) and Abs to the following molecules: CD8 α (53-6.7), CD4 (RM4-5), CD44 (IM7), CD69 (H1.2F3), CD103 (M290), CD62L (MEL-14), IFN- γ (XMG1.2), and IL-2 (JES6-5H4) (all from BD Biosciences, San Diego, CA) and TNF- α (TN3-19.12; eBioscience). BrdU (Sigma) was injected i.p. (1 mg/24 h), and mice were euthanized 60 h later. BrdU uptake was detected using a BrdU Flow Kit (BD Biosciences). *Ex vivo* LT359 peptide stimulation and intracellular cytokine staining were done as previously described [125]. Samples were acquired on an LSR II or LSRFortessa (BD Biosciences), and data were analyzed using FlowJo software (TreeStar, Ashland, OR).

Micropipette adhesion-frequency assay

CD8 T cells were purified by magnetic sorting of mononuclear cells isolated from brain, kidney, and spleen. Coating human RBCs with peptide-MHC (p-MHC), quantifying binding events and p-MHC and TCR surface densities, and calculating adhesion frequency and two-dimensional were as described [140, 141]. A T cell that bound a D^b-LT359–coated RBC with an adhesion frequency > 0.1 was considered antigen-reactive. No antigen-reactive binding events occurred with LCMV D^b-NP396–coated RBCs (Supplemental Fig. 2B, 2C).

Statistical analysis

The p values were determined by an unpaired Student t test or one-way ANOVA using GraphPad Prism software (La Jolla, CA). All p values < 0.05 were considered significant.

Results and Discussion

Brain-infiltrating MPyV-specific CD8 T cells are stably maintained

CD8 T cells likely check progression of JCV-PML disease [36] and are important for control of systemic MPyV infection [124]. To investigate CD8 T cell responses to MPyV CNS infection, mice were inoculated intracerebrally, a route commonly used in neurotropic virus–infection models [72, 142]. To determine whether the brain supports MPyV replication, mice received infectious or heat-inactivated virus, resulting in a 100-fold increase in viral genomes from days 1 to 4 post-infection or no increase, respectively (data not shown). Viral genome numbers in the brain contracted ~100-fold from peak replication at 4 to 8 dpi, followed by a low-level persistent infection phase (Fig. 2-1A); similar kinetics were observed in the spinal cord, kidney, and spleen, as with i.p. and s.c. inoculation routes. Next, we asked whether antiviral T cell responses correlated with declining MPyV levels in the brain. Approximately half of brain-isolated cells at 8 days post-infection (dpi) were CD8 T cells, of which nearly 75% bound D^b-LT359 tetramers (Fig. 2-1B), the immunodominant epitope [125]. After peak infiltration at 8 dpi, both the magnitude of total CD8 T cells (Fig. 2-1C) and the frequency of D^b-LT359–specific CD8 T cells in the brain remained stable into the persistent phase, unlike the response in the spleen, which contracted ~30% (Fig. 2-1D). Most LT359-specific CD8 T cells in the brain produced IFN- γ at 30 dpi, with ~25% coproducing TNF- α (Fig. 2-1E). The CD4 T cell response in the brain mirrored that of CD8 T cells, although it was ~10-fold lower in magnitude throughout infection (Fig. 2-1C). These data show that brain-infiltrating CD8 T cells are predominantly directed to a single MPyV epitope, are functional, and are stably maintained in the setting of a nearly 3-log decrease in viral load.

MPyV-specific CD8 T cells in the brain are TRM cells

We asked whether CD4 T cell help or continuous infiltration by circulating CD8 T cells in response to ongoing infection contributed to stability of this population. We depleted circulating cells by administering anti-CD4, anti-CD8, or control rat IgG at 10 dpi, to allow peak infiltration of CD8 T cells into the brain, and then weekly until 60 dpi. Total numbers of brain-infiltrating CD8 T cells decreased in anti-CD4-treated mice, demonstrating their recruitment from the circulation during persistent infection (Fig. 2-2A). No change in numbers of total or MPyV-specific CD8 T cells in the brain were observed in CD4 or CD8 antibody-treated mice, indicating that neither CD4 help nor replenishment from the circulation is needed to maintain this population (Fig. 2-2A). This finding parallels parabiosis experiments in which endogenous memory cells in the brain do not equilibrate with donor parabiont cells, suggesting that effector-phase T cells seed the memory population [143]. Next, we administered the thymidine analog BrdU to mice 60 h prior to sacrifice at 30 dpi. Approximately 15% of Db-LT359-specific CD8 T cells in both the brain and spleen incorporated BrdU (Fig. 2-2B), suggesting that *in situ* proliferation contributed to the long-term maintenance of brain-infiltrating memory CD8 T cells.

We asked whether the canonical CD62L^{lo} CD69^{hi} CD103⁺ phenotype used to define TRM cells in acute infection models applied to brain-infiltrating virus-specific CD8 T cells during persistent MPyV infection. Over 90% of Db-LT359-specific CD8 T cells in the brain upregulated CD69 by 15 dpi, but those in the spleen remained CD69^{-lo} at all time points examined (Fig. 2-2C). All MPyV-specific CD8 T cells in the brain and spleen were CD62L^{lo}, a phenotype expected in persistently infected hosts.

Notably, most MPyV-specific CD8 T cells in the brain remained CD69^{hi}, despite declining virus levels (Fig. 2-1A). Because CD69 antagonizes expression of S1P1 receptors, which must be downregulated for establishment of a T_{RM} compartment [53], CD69^{hi} appears to be an indispensable phenotype for T_{RM} cells. Beginning at 15 dpi, we observed a gradual increase in CD103 expression by D^b-LT359-specific CD8 T cells; however, even at 30 dpi, only one third of these cells were CD103⁺ (Fig. 2-2C), with no further increase in CD103 expression by 60 dpi (data not shown). This contrasts with acutely cleared VSV infection in the CNS, in which the CD103⁺ fraction increases from ~60 to 80% of VSV-specific CD8 T cells from 20 to 40 dpi [64]. Most MPyV-specific CD8 T cells in the brain were CD103⁻, despite being stably maintained, indicating that these cells were functionally brain-resident during persistent infection. Together, these data suggest that persistent antigen impedes CD103 upregulation, in line with other studies [56], but not establishment of a T_{RM} population. Evidence that CD103 expression by CD69^{hi} CD62L^{lo} CD8 T cells varies among non-lymphoid organs [53] further supports the likelihood that CD103 is not a reliable T_{RM} marker. The role of cytokines and antigen in development and retention of T_{RM} cells responding to low-level persistent infections remains to be determined. The gradual decline in virus levels during persistent infection and stability of MPyV-specific CD8 T cells imply that antigen may be dispensable for retention of these T_{RM} cells, as for skin-resident HSV-specific T_{RM} cells [144].

Brain- and kidney-infiltrating memory MPyV-specific CD8 T cells express high-affinity TCRs

MPyV-specific CD8 T cells in the brain showed a progressive increase in mean fluorescence intensity (MFI) of D^b-LT359 tetramer, whereas in the spleen, tetramer MFI stayed uniformly lower during persistent infection (Fig. 2-3A). We also observed that brain-infiltrating cells expressed significantly higher levels of CD8 co-receptors than did those in the spleen as early as 8 dpi, and they showed a progressive increase in MFI (Fig. 2-3B). The cooperative tri-molecular interactions among the TCR, CD8, and p-MHC complex obviate determination of affinity of a given TCR for its cognate p-MHC ligands [145]. Therefore, to determine whether MPyV-specific memory T cells in the spleen and brain differed in TCR affinity, we used the micropipette adhesion-frequency assay with D^b-LT359 monomers, in which the native $\alpha 3$ domain is replaced with that of HLA-A2, which cannot bind mouse CD8 [140]. This assay allows interrogation of the affinity of a single T cell for p-MHC in a physiologically relevant membrane-anchored context, and it can detect antigen-specific populations with affinities below detection by tetramers [141, 146, 147]. Reactivity to Db-LT359 was assessed for 56 CD8 T cells isolated from the brain, and 44 of which (78.6%) were determined to be Ag specific (Fig. 2-4A). In contrast, of 68 CD8 T cells isolated from the spleen, only 14 (20.6%) were found to be D^b-LT359 specific. The micropipette adhesion-frequency data confirmed the observations made with tetramers that D^b-LT359-specific CD8 T cells predominantly make up the brain T_{RM} pool.

Using the adhesion-frequency values, together with TCR and p-MHC surface densities, we calculated that brain T_{RM} cells have a 20-fold higher mean affinity for D^b-

LT359 than do cells in the spleen (Fig. 2-4B). To address whether increased TCR affinity was unique to T_{RM} cells in the brain, we assayed 69 kidney-infiltrating memory CD8 T cells and found that 55.1% were D^b -LT359 specific, with a mean TCR affinity that was significantly higher than that measured in the spleen ($p = 0.0029$). Cells in the brain and kidney occupied a 3-log range skewed toward higher affinities, in contrast to the spleen where affinities spanned 1-log (Fig. 2-4C). Notably, cells in the kidney did not differ significantly in affinity from those in the brain (Fig. 2-4B) and had higher MFIs for D^b -LT359 tetramer and CD8 antibody staining than did those in the spleen (Supplemental Fig. 2-1A). Approximately 70% of CD8 T cells in the kidney expressed CD69, suggesting that most are T_{RM} cells (Supplemental Fig. 2-1B). Elevated CD8 levels on T cells in both brain and kidney may constitute an additional phenotypic marker for T_{RM} cells. Together, these data show that MPyV-specific CD8 T_{RM} cells express higher-affinity TCRs, with cooperative binding by higher levels of CD8, than do memory cells in the spleen.

A number of studies documented that effector, but not memory, CD8 T cells are competent to enter non-lymphoid tissues [60, 64, 148]. Effector CD8 T cells generated *in vitro* express higher effective TCR affinity than do their naïve precursors [140]. Together, these findings raise the possibility that effector T cells in both lymphoid and non-lymphoid tissues may express high-affinity TCRs during acute infection. We compared the TCR affinities of virus-specific CD8 T cells in acutely infected mice. From the brain, TCR affinities for D^b -LT359 were determined for 40 of 53 cells assayed, a frequency of 75.4% (Supplemental Fig. 2-2A). In both the spleen and the kidney, the frequency of D^b -LT359-specific CD8 T cells was lower: 40 of 86 cells (46.5%) cells in the spleen and 15

of 33 (45.5%) cells from the kidney (Supplemental Fig. 2-2A). Unlike memory cells, effector T cells in all three organs expressed TCRs of similarly high affinity (geometric mean affinities: 7.72×10^{-4} , 5.20×10^{-4} , and $7.48 \times 10^{-4} \mu\text{m}^4$ for the brain, kidney, and spleen, respectively) (Fig. 2-4D). For both acute and persistent infection time points, splenic D^b-LT359-specific CD8 T cells had significantly higher TCR surface density than did those from the brain (Supplemental Fig. 2-2D, E), and this difference is taken into account when calculating TCR affinity [141]. Similar to memory cells in the brain and kidney, CD8 T cells from all organs isolated during acute infection spanned a 3-log range of affinities.

These findings suggest that high-affinity TRM cells originate from high-affinity effector cells that enter non-lymphoid tissues during acute infection; further, these data raise the possibility that the non-lymphoid microenvironment may be conducive for retaining T cells having high-affinity TCRs. High TCR affinity would improve the ability of T_{RM} cells to detect infected cells expressing low levels of antigen, not only during persistent polyomavirus infection, but also during early re-infection when rapid control may be critical in limiting injury to organs with a large population of essential, non-renewable cells (e.g., brain).

Acknowledgements

The authors were supported by the PML Consortium, LLC (to AEL), the National Multiple Sclerosis Society Grant RG4047 (to BDE), and the National Institutes of Health (R01 NS088367 and R01 AI102543 to AEL; F31 NS083336 to ELF; R01 AI096879 to BDE; T32 AI007610 and F31 NS081828 to AEK).

Disclosures

The authors have no financial conflicts of interest.

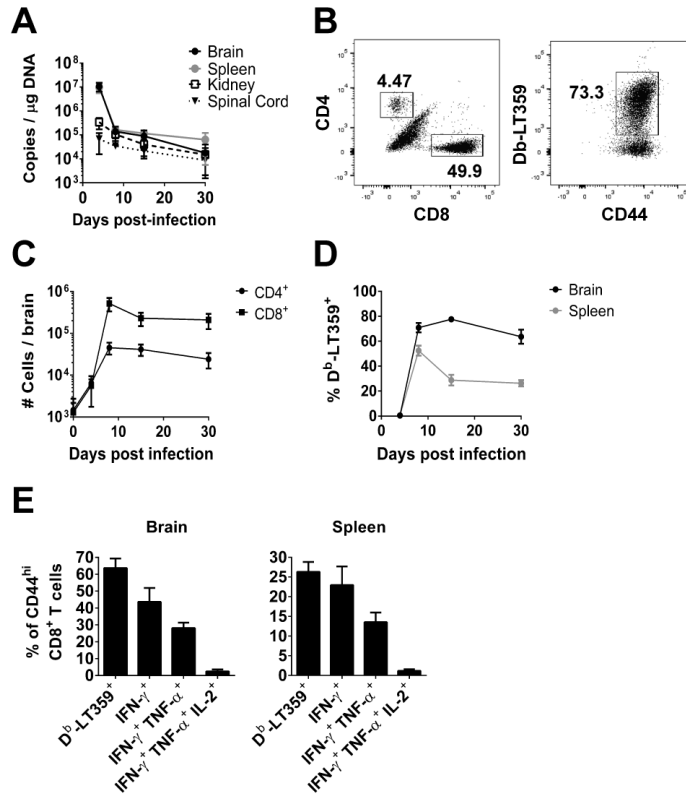


Figure 2-1. Characterization of MPyV replication and T cell responses in the brain.

(A) Kinetic analysis by qPCR of viral genome copy numbers in genomic DNA isolated from brain, spleen, kidney, and spinal cord at indicated timepoints post-infection. (B) Representative dot plot of T cell frequencies in brain-isolated mononuclear cells (left plot) and frequency of D^b-LT359-tetramer⁺ cells of total CD8 T cells (right plot) at 8 dpi by flow cytometry. (C) Kinetic analysis of the number of total CD8 and CD4 T cell responses in brain. (D) Frequency of D^b-LT359⁺ of CD44^{hi} CD8⁺ T cells in brain and spleen over the course of infection. (E) Frequency of cytokine-producing CD44^{hi} CD8 T cells in brain and spleen at 30 dpi following *ex vivo* stimulation with LT359 peptide. Data are cumulative from 3 independent experiments with 7-9 total mice/timepoint.

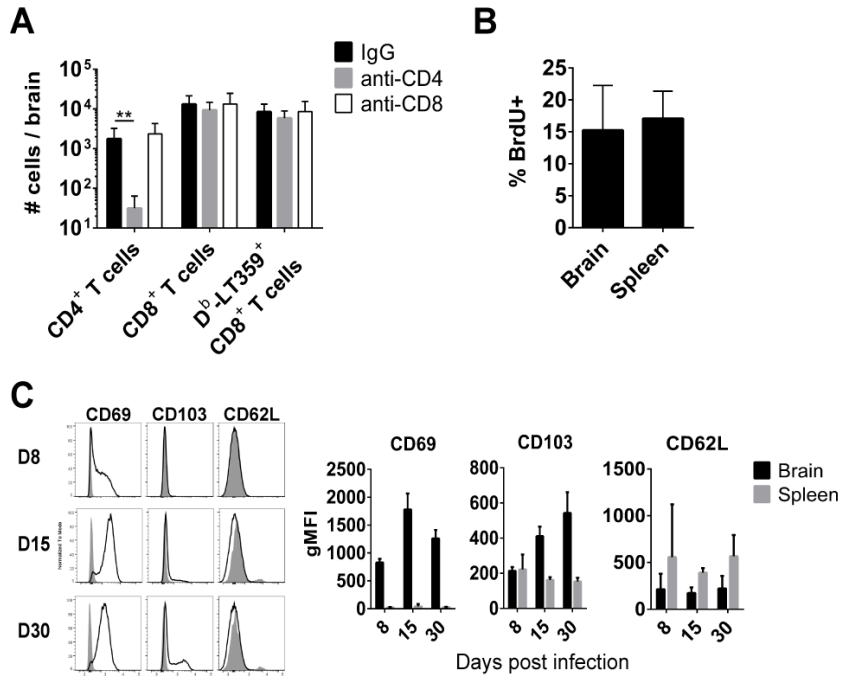


Figure 2-2. MPyV-specific CD8 T cells survive long-term in the brain. (A) Mice were antibody-depleted of circulating CD8 or CD4 T cells, and numbers of T cells infiltrating the brain were determined by flow cytometry. Data are cumulative from 2 independent experiments with 7-8 total mice/group. (B) Mice were given BrdU i.p. for 60 h prior to sacrifice at 30 dpi. Shown are the mean frequencies (\pm SD) of BrdU⁺ D^b-LT359⁺ CD8 T cells in brain and spleen. Data are cumulative from 2 independent experiments with 9 total mice. (C) Representative histograms (left panel) of expression of phenotypic markers of tissue-resident memory cells by brain-infiltrating (line) or splenic (shaded) D^b-LT359⁺ CD8 T cells at indicated timepoints post-infection. Mean (\pm SD) of the gMFI of each marker (right panel). Data are cumulative from 3 independent experiments of 7-9 mice/timepoint. **** p < 0.01**

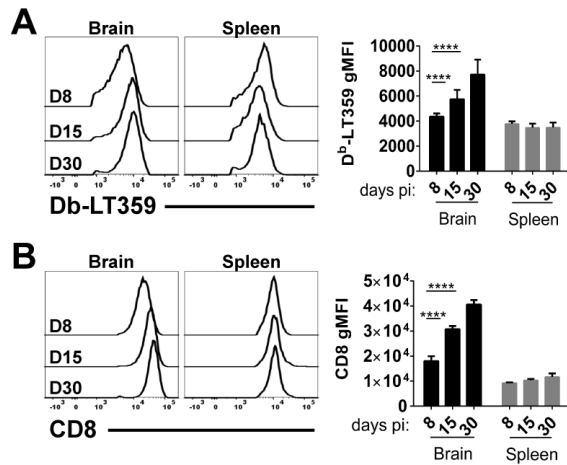


Figure 2-3. Increase in tetramer binding and CD8 expression by MPyV-specific CD8 T cells in the brain. CD8 T cells from brain and spleen were analyzed for geometric (g)MFI of staining by D^b-LT359 tetramers (A) and anti-CD8 α (B), shown by representative histograms (left panel) and bar graphs (mean \pm SD; right panel). Data are cumulative from 3 independent experiments of 7-9 mice/timepoint. *****, $p < 0.0001$.

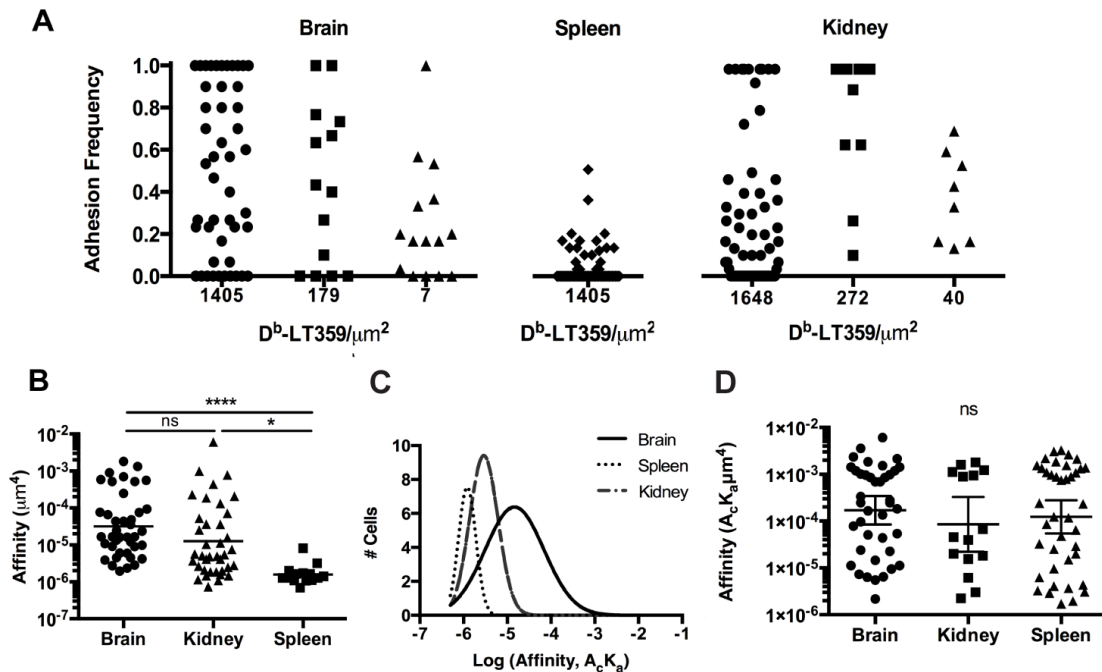


Figure 2-4. Comparison of TCR affinities of MPyV-specific CD8 T cells in brain,

kidney, and spleen. CD8 T cells pooled from each organ during persistent (A-C; 26-32

dpi) or acute (D; 8 dpi) infection were analyzed by micropipette adhesion frequency

assay. (A) Adhesion frequencies of CD8 T cells from the brain, spleen, and kidney using

RBCs coated with different pMHC surface densities. (B & D) Geometric mean \pm 95%

confidence interval of 2-dimensional binding affinity for $D^b\text{-LT359}$, where each mark

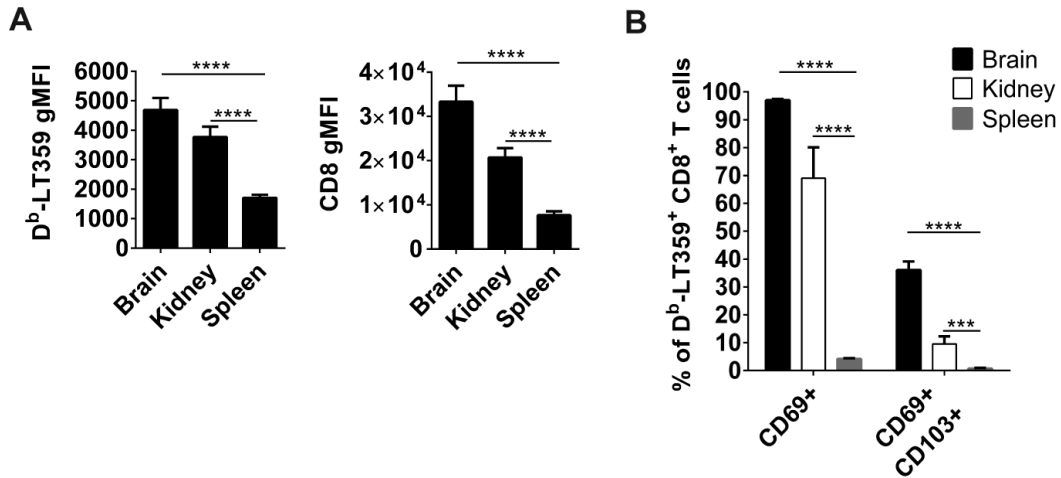
represents an individual CD8 T cell. (C) Frequency distributions of the log of affinities

for each organ examined. Gaussian curves were fitted to the data with r^2 values as

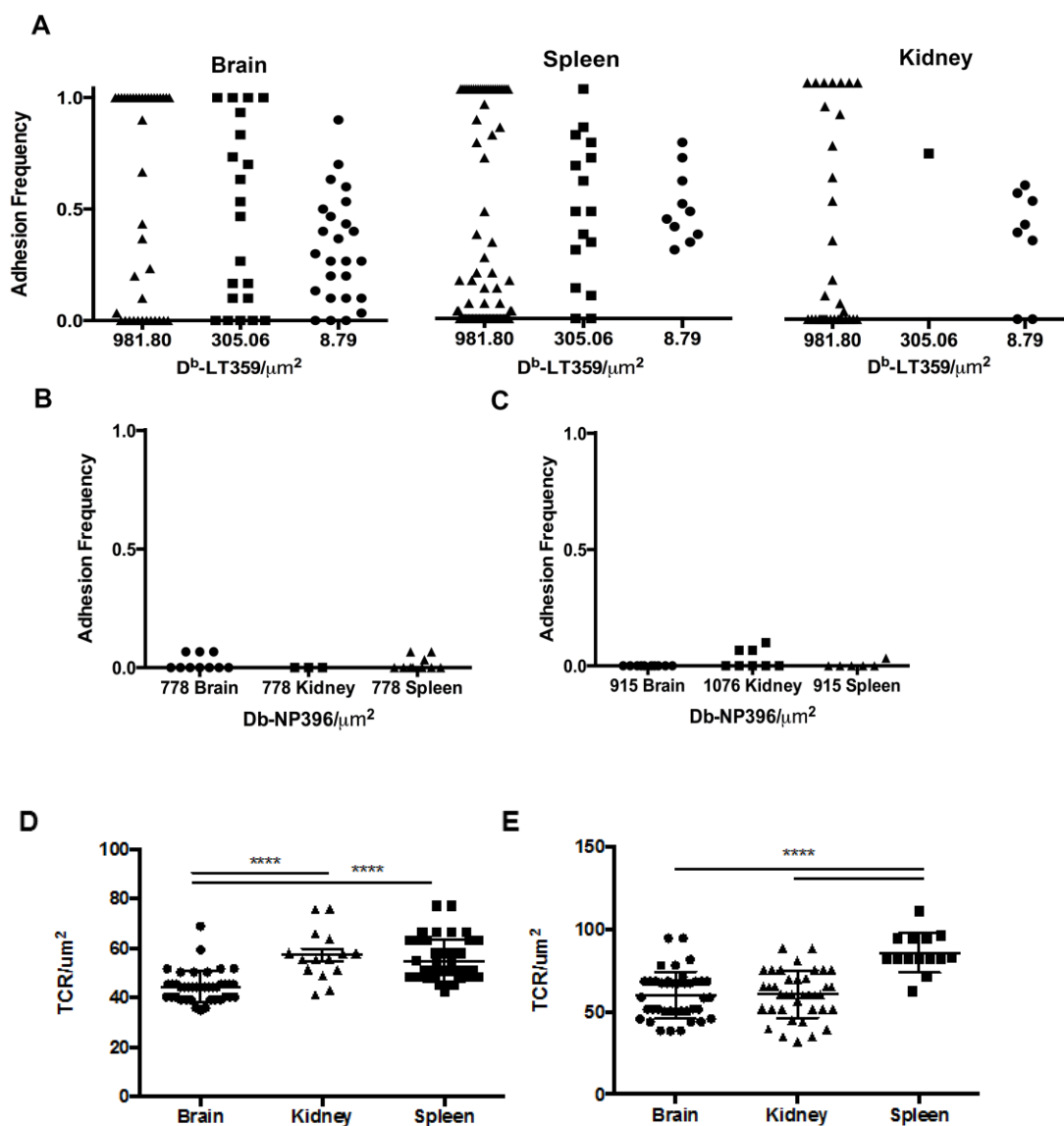
follows: spleen = 0.97; kidney = 0.71; brain = 0.64. Data are cumulative from 2

independent experiments with 5-7 mice/pool. ns = not significant; *, $p < 0.01$; ****, $p <$

0.0001.



Supplemental Figure 2-1. Kidney-infiltrating CD8 T cells have elevated CD8 expression and tetramer binding, and express T_{RM} markers. D^b-LT359⁺ CD8 T cells from brain, kidney, and spleen at 30 dpi showing (A) gMFI mean ± SD of D^b-LT359 tetramer (left) and CD8 (right) and (B) frequency of cells expressing CD69 alone and with CD103. Data are representative of 2 independent experiments of 4-5 mice/experiment. ***, $p < 0.0005$; ****, $p < 0.0001$.



Supplemental Figure 2-2. Adhesion frequency analyses of MPyV-specific effector and memory CD8 T cells from brain, kidney, and spleen. CD8 T cells pooled from brains, kidneys, and spleens during (A & B) acute infection (8 dpi) and (C) persistent infection (30 dpi) were analyzed by micropipette adhesion frequency assay. RBCs were coated at the indicated densities with (A) D^b -LT359 and (B & C) negative control LCMV D^b -NP396 monomers. Monomer surface densities are the mean from 2 independent

experiments. Mean \pm SEM of the TCR surface density at 8 dpi (D) and 30 dpi (E), determined by flow cytometry. Adhesion frequency and TCR density data are cumulative from 2 independent experiments of 5 mice/pool, with each point corresponding to the adhesion frequency of a single T cell. ****, $p < 0.0001$.

CHAPTER 3**PD-1^{hi} CD8 T cells in the brain remain functional during persistent****mouse polyomavirus infection**

Elizabeth L. Frost¹, Mesut Toprak², and Aron E. Lukacher³

¹Immunology and Molecular Pathogenesis Graduate Program, Emory University,
Atlanta, GA

²Department of Psychiatry, The Pennsylvania State University College of Medicine,
Hershey, PA

³Department of Microbiology and Immunology, The Pennsylvania State University
College of Medicine, Hershey, PA

Abstract

Programmed cell death-1 (PD-1) is a key marker and mediator of T cell exhaustion resulting from chronic antigenic stimulation from uncontrolled viral infection or tumors. Ligation of PD-1 by PD-L1 is required for negative regulation of T cell receptor stimulation. Here, we demonstrate sustained high levels of PD-1 expression by brain-infiltrating MPyV-specific CD8 T cells despite declining viral load. A fraction of these cells fail to produce interferon- γ (IFN- γ) after exposure to peptide *ex vivo*, and stimulation with PD-L1^{-/-} bone marrow-derived dendritic cells restores IFN- γ capability. However, comparison of PD-L1-sufficient mice with mice genetically deleted of PD-L1 or given intracerebroventricular anti-PD-L1 blockade shows no differences in cytokine functionality, control of viral load, or proliferative capacity. Absence of PD-1 signaling leads to an increase in the frequency of cells expressing CD103, a ligand for E-cadherin and marker, in some cases, of tissue-resident memory T cell phenotype. Examination of brain-infiltrating hematopoietic and brain-resident neural cells by flow cytometry revealed high PD-L1 expression by monocyte-derived cells in the acute phase of infection and a low frequency of PD-L1⁺ neural cells that are neither oligodendrocytes nor microglia. Although MPyV persists at a low level and PD-L1 expression in the persistent phase of infection is minimal, PD-1 expression by virus-specific T cells remains high. Our findings suggest that the brain microenvironment may contribute to maintenance of PD-1 levels, and are in line with recent reinterpretations of exhaustion as an altered state of memory T cell differentiation.

Introduction

The inhibitory receptor PD-1 is regarded as an indicator of T cell exhaustion, a progressive loss of T cell function resulting from repetitive antigen stimulation such as in chronic viral infection or tumor development [149]. Extensive work using experimental models of chronic infection (LCMV and SIV) as well as analysis of T cells from individuals infected with HIV, HCV, and HBV, demonstrate that PD-1 expression is not only associated with exhaustion but is actively responsible for T cell inhibition [150]. Engagement of PD-1 by its ligands PD-L1 or PD-L2 results in recruitment of SHP-phosphatases to the intracellular tyrosine inhibitory or switch motif domains of PD-1 proximal to the T cell receptor; these phosphatases inactivate kinase cascades induced by TCR signaling thereby inhibiting downstream pathways required for cytokine production, proliferation, and cytotoxicity, among others [151, 152]. The reversal of T cell exhaustion achieved by blockade of the PD-1:PD-L1 interaction provides further evidence of a direct inhibitory role for PD-1 [70], and is also the basis for checkpoint immunotherapy for various cancers [153].

Recent analyses of CD8 T cells examined *in situ* and immediately after isolation reveal that the impact of PD-1 on CD8 T cells is more complex and includes restricting T cell mobility in tissues [154] and having a trophic effect on T cells [155, 156]. That “exhausted” T cells in fact express effector activity is evidenced by the outgrowth of CD8 T cell epitope-escape HIV viruses late in infection [157] and the increase in viral titers after depletion of CD8 T cells in chronic SIV infection [158, 159]. Accumulating literature challenges the dogma that PD-1 expression is synonymous with cellular dysfunction and senescence [160-162], with new data supporting the concept that CD8 T

cell exhaustion is actually a state of differentiation adapted by T cells to enable them to survive and retain functionality during persistent infection [163, 164].

Although PD-1 has been extensively investigated as a central inhibitory receptor in driving dysfunction and subsequent deletion of virus-specific CD8 T cells in the setting of chronic viremic infection [70], only a few studies have investigated PD-1's impact on T cells responding to viral CNS infection [71, 73, 74]. We have previously reported that during low level persistent infection by mouse polyomavirus (MPyV), CD8 T cells primed during the acute phase of infection show signs of exhaustion, such as decreased functionality, poor memory generation, and eventual clonal deletion, but do so in the absence of PD-1 upregulation [165]. More recently, we have shown that brain-infiltrating MPyV-specific T cells retain a high affinity for antigen [166], which likely improves their ability to sense antigen but may also predispose them to exhaustion [167, 168].

Here, we demonstrate that T cells infiltrating the brain in response to MPyV infection upregulate and sustain high expression of PD-1, and do so despite declining virus levels. Moreover, a fraction of virus-specific CD8 T cells fails to produce IFN- γ . *Ex vivo* stimulation of brain-infiltrating MPyV-specific CD8 T cells with PD-L1^{-/-} antigen-presenting cells restores IFN- γ production. However, *in vivo*, neither PD-L1^{-/-} nor intracerebroventricular anti-PD-L1 blockade-treated mice shows improved cytokine functionality or viral control. In the absence of PD-1 signaling, MPyV-specific cells decrease as a percentage of total CD8 T cells in the brain and upregulate CD103, a ligand for E-cadherin and a presumptive marker of tissue resident memory cells. Failure to reverse loss of T cell functions with PD-L1 blockade was not due to severe exhaustion, as

the majority of MPyV-specific cells in C57BL/6 mice expressed Tbet, rather than Eomesodermin (Eomes). A low frequency of both hematopoietic and non-hematopoietic cells in the MPyV-infected brain express PD-L1, but taken with our other data, does not appear sufficient to inhibit PD-1^{hi} CD8 T cells. Together, our findings show that high PD-1 expression by CD8 T cells can be sustained under conditions of low-level antigen persistence and that PD-1 is not incontrovertibly associated with T cell functional exhaustion.

Materials and Methods

Mice and virus inoculation. C57BL/6NCr female mice purchased from the Frederick Cancer Research and Development Center of the National Cancer Institute (Frederick, MD) and B7-H1^{-/-} mice (generously provided by C.C. Bergmann with approval of L. Chen) were housed in accordance with the guidelines of the Institutional Animal Care and Use Committees and the Department of Comparative Medicine at the Pennsylvania State University College of Medicine. Here, B7-H1^{-/-} mice are termed PD-L1^{-/-} mice. At 7-12 weeks of age, anesthetized mice were intracerebrally (i.c.) inoculated by injecting the right frontal lobe with 2×10^6 PFU MPyV strain A2 in 30 μ l DMEM 5%FBS.

Quantitation of MPyV Genomes. TaqMan real-time PCR was performed in an ABI StepOnePlus (Applied Biosciences) with 10 μ g of template DNA purified from tissue using the Maxwell 16 Research Instrument (Promega, Madison, WI) according to the manufacturer's instructions. Primers and amplification parameters are previously described [125].

Bone marrow dendritic cell culture and peptide pulse. Bone marrow was flushed from the femurs and tibias of C57BL/6 and PD-L1^{-/-} mice using a 30-gauge needle and syringe loaded with DMEM 10% FBS. Red blood cells were lysed with ACK buffer. Bone marrow-derived cells were plated (5×10^6 cells in 100 mm Petri dish) and cultured in DMEM 10% FBS with GM-CSF (20 ng/ml) at 37°C with the media changed every 3 days. After 10 days, differentiated bone marrow dendritic cells (BMDCs) were harvested by gentle trypsinization (0.25% for <1 min) to release loosely adherent cells. BMDCs

were re-plated (3×10^6 cells per Petri dish in DMEM + 10% FBS) with 100 U/ml IFN- γ to induce antigen presentation and PD-L1 expression (phenotype verified by flow cytometry) and were incubated overnight at 37°C. BMDCs were transferred to a 96-well plate (3×10^5 cells/well) and incubated with 10 μ M LT359 peptide at 37° C for ~6 hr prior to co-culture with brain-isolated cells or splenocytes.

Cell isolation, stimulation for intracellular cytokine staining, and flow cytometry. For isolation of neural and mononuclear cells [169], anesthetized mice were perfused transcardially with 30 ml heparinized PBS (100 U/ml). Brains and spleens were collagenase digested for 15 min at 37° C. Single-step Percoll centrifugation was used to remove myelin from the brain homogenate. Cells were washed and incubated overnight with anti-O4 (Miltenyi, Bergisch Gladbach, Germany; 1:20 in FACS buffer) and surface stained with other antibodies the following day. For all other experiments, brains and spleens were harvested from mice intravascularly labeled for 3 min with 3 μ g anti-CD45 (30-F11) [138]. Brain mononuclear cells were isolated on Percoll gradients of collagenase-digested brains. Spleen and brain cells were exposed to Fixable Viability Dye (eBioscience, San Diego, CA) and Fc Block (BioLegend, San Diego, CA) prior to staining with D^b-LT359-638 tetramers (NIH Tetramer Core Facility, Atlanta, GA) and antibodies to the following molecules: CD8 α (53-6.7), CD4 (RM4-5), CD44 (IM7), CD11b (M1/70), CD45(30-F11), Ki67 (B56), CD69 (H1.2F3), CD103 (M290), IFN- γ (XMG1.2), and IL-2 (JES6-5H4), H-2D^b (KH95), and KLRG1 (2F1) purchased from BD Biosciences (San Diego, CA); and TNF- α (TN3-19.12), PD-1 (RMP1-30), PD-L1 (MIH5), Eomes (Dan11mag), MHC-II (M5/114.15.2), TIM3 (RMT3-23), 2B4

(eBio244F4), and Lag3 (eBioC9B7W) purchased from eBioscience; and Tbet (4B10), PD-L2 (TY25), CD11c (N418), and CD127 (A7R34) from Biolegend (San Diego, CA). Anti-GLAST was purchased from Miltenyi (clone ACSA-1; Bergisch Gladbach, Germany). BrdU (Sigma, St. Louis, MO) was injected i.p. (1 mg/24 h) and mice euthanized 60 h later. BrdU uptake was detected using the BrdU Flow Kit (BD Biosciences), per manufacturer's instructions. Brain and spleen cells were stimulated with 1 μ M LT359 peptide or no peptide or peptide-pulsed BMDCs for 5-6 h in the presence of brefeldin A, stained for viability and surface markers, fixed and permeabilized with CytoFix/CytoPerm (BD Biosciences), then stained for intracellular IFN- γ , TNF- α , and IL-2. Staining for these cytokine antibodies in absence of peptide was <1% of CD8⁺ CD44^{hi}-gated cells (data not shown). Samples were acquired on an LSR II or LSRFortessa (BD Biosciences) and data analyzed using FlowJo software (Tree Star, Ashland, OR).

Intracerebroventricular (i.c.v.) cannulation. Prior to surgery, ALZET osmotic pumps (Model 2002, DURECT Corporation, Cupertino, CA) were loaded with 6 mg/ml rat IgG or rat anti-PD-L1 (Clone 10F.9G2; BioXCell, West Lebanon, NH) according to manufacturer's instructions and connected to L-shaped cannulas (ALZET Brain Infusion Kit 3) with tubing trimmed to 2 cm. Pumps were incubated overnight at 37° C in sterile PBS to activate flow. Surgical procedures were performed similar to those previously described [170]. Following removal of soft tissues from the skull, the cannula was positioned into the left lateral ventricle (1.0 mm lateral to midline, 0.1 mm posterior to bregma, and 3.0 mm dorsoventral to the skull) and secured with ALZET Loctite

adhesive. The scalp was sutured over the cannula. I.c.v antibody administration lasted 14 days at a flow rate of 12 μ l/day, delivering 1 mg of antibody over the course of the experiment, as described for PD-L1 blockade experiments in LCMV-infected mice [70]. Delivery of antibody to the lateral ventricle was confirmed by cutting the brain at the site of cannulation and by measuring the volume of antibody remaining in the pump.

Statistical analysis. *P* values were determined by unpaired Student's *t*-test or one-way ANOVA using GraphPad Prism software (La Jolla, CA). All *P* values ≤ 0.05 were considered significant.

Results

High PD-1 expression correlates with decreased ex vivo cytokine production

CD8 T cells infiltrating the brain in response to persistent MPyV infection seed a population of tissue-resident memory T cells (T_{RM}) that retain high affinity T cell receptors and express increased levels of CD8 co-receptor [166]. These attributes likely aid T_{RM} cells in their role as a frontline defense against recurring pathogens by increasing their sensitivity to antigen; however, with continuous antigen exposure due to viral persistence, we hypothesized that heightened antigen sensing may drive upregulation of PD-1 on brain T_{RM} cells. In confirmation of this hypothesis, we observed that LT359-specific CD8 T cells isolated from brains of mice at 8 days post-infection (dpi) expressed PD-1, the levels of which peaked at 15 dpi and were sustained into the persistent phase of infection (Figure 3-1A) despite a drop in viral load [166]. Low levels of PD-1 were transiently expressed by LT359-specific splenic T cells at 8 dpi (Figure 1A), the peak of viral load in the spleen [166].

Because PD-1^{hi} cells are typically described as dysfunctional, we compared the percentage of CD8 T cells producing IFN- γ after *ex vivo* LT359 peptide stimulation to total antigen-specific cells as detected by D^b LT359 tetramers. When PD-1 expression levels were highest (i.e., 8 dpi for the spleen and 30 dpi for the brain)[166], the frequency of IFN- γ ⁺ cells was less than the frequency of D^b LT359 tetramer⁺ CD8 T cells (Figure 3-1B). Next, we asked whether engagement of PD-1 by its ligand PD-L1 inhibited *ex vivo* production of IFN- γ . Bone marrow-derived dendritic cells (BMDCs) cultured from C57BL/6 and PD-L1^{-/-} mice were treated with IFN- γ to maximize their PD-L1 expression (Supplemental Figure 3-1), then pulsed with LT359 peptide; these peptide-loaded

BMDCs were used to stimulate T cells isolated from brains and spleens. In the absence of PD-L1, LT359 peptide-stimulated T cells from brains had a greater frequency of IFN- γ ⁺ cells and higher gMFI for IFN- γ at both 8 and 30 dpi than using peptide-loaded BMDCs from wild type mice; in contrast, LT359-specific CD8 T cells from the spleen showed restoration in IFN- γ function only at 8 dpi when they expressed PD-1 (Figure 3-1C).

Taken together, these data point toward PD-1-mediated inhibition of MPyV-specific CD8 T cell function, as determined by *ex vivo* intracellular cytokine staining assays.

T cells from PD-L1-deficient mice do not show improved effector capabilities

In the chronic LCMV infection model, interfering with the PD-1 pathway via anti-PD-L1 antibody blockade resulted in a higher magnitude gp33-specific T cell response as well as recovery of cytokine production and improved control of viral load [70]. We therefore compared CD8 T cell responses in MPyV-infected C57BL/6 and PD-L1^{-/-} mice to ask if deficient PD-1 signaling *in vivo* restored the decreased IFN- γ production seen by *ex vivo* LT359 peptide stimulation at 30 dpi (Figure 3-1C). However, unlike LCMV clone 13-infected mice treated with PD-L1 blockade, MPyV-infected PD-L1^{-/-} mice showed a lower frequency, but no difference in number, of LT359-specific CD8 T cells in the brain at 30 dpi compared to controls (Figure 3-2A). A similar pattern was seen in the spleen, where PD-1 levels are low throughout MPyV infection. In the brain, PD-L1^{-/-} mice also showed a mismatch in percentage but not number of CD8 T cells producing IFN- γ compared to binding LT359 tetramer similar to C57BL/6 mice (Figure 3-2B), suggesting that PD-1 signaling is not responsible for IFN- γ dysfunction.

CD8 T cells show a progressive hierarchical loss of function as antigen load and strength of PD-1 signaling increase, starting with proliferation and IL-2 production, progressing to loss of cytotoxicity and TNF- α , followed by decreased IFN- γ , and ultimately, clonal deletion [69, 167]. Because PD-1 did not contribute to the decrease in IFN- γ capability, we asked whether PD-1 affected other aspects of T cell functionality. First, we found no difference in the number of cells producing TNF- α or IL-2 in PD-L1^{-/-} mice (Figure 3-2C). Furthermore, PD-L1^{-/-} mice showed no difference in viral load in the brain or spleen compared to C57BL/6 mice (Figure 3-2D). We next measured Ki67 expression as a marker of T cell proliferation and found that in the absence of PD-L1, the frequency of LT359-specific proliferating cells was unchanged (Figure 3-2E). Together, these data show that PD-1 signaling is not an impediment to function of MPyV-specific CD8 T cells or control of MPyV infection in the brain.

We also analyzed CD8 T cells in PD-L1^{-/-} mice for changes in phenotype. Interestingly, although we previously reported that CD103, a ligand for E-cadherin and marker of T_{RM} cells, is not required for MPyV-specific CD8 T cell residence in the brain [166], we observed an increase in the frequency of CD103⁺ cells in PD-L1^{-/-} mice (Figure 3-3A). We also assayed cells for expression of the additional inhibitory receptors Tim3, 2B4, and Lag3. No Lag3 upregulation was observed (data not shown). In C57BL/6 mice, the majority of PD-1⁺ MPyV-specific T cells co-expressed Tim3 and nearly half of these also expressed 2B4 (Figure 3-3B). The frequency of triple-positive (PD-1⁺ Tim3⁺ 2B4⁺) cells was significantly increased in PD-L1^{-/-}, and was primarily attributed to elevated levels of 2B4. We previously showed that levels of CD8 expression and to T cells in the brain but not the spleen increased over the course of MPyV infection, with a markedly

higher TCR affinity by the brain-resident MPyV-specific cells [166]. Examination of T cells in PD-L1^{-/-} mice revealed significantly higher geometric mean fluorescence intensity of LT359 tetramer than in C57BL/6 controls and a trend toward higher CD8 levels (Figure 3-3C). These data demonstrate that although PD-L1 deficiency *in vivo* did not affect MPyV-specific T cell function, there were alterations in expression of CD103 and inhibitory receptors, and possibly in TCR affinity.

To circumvent possible effects of genetic PD-1 deficiency on thymocyte selection and T cell differentiation, as well as compensatory T cell inhibitory mechanisms, we sought to develop an approach to block PD-1 signaling in the CNS. Because antibodies do not cross the blood-brain barrier and complete turnover of cerebrospinal fluid occurs multiple times per day [171], we used chronic intracerebroventricular (i.c.v.) administration of anti-PD-L1 or control IgG using cannulas attached to subcutaneously implanted osmotic pumps to continuously deliver antibodies into the brain at a rate of 0.5 $\mu\text{l/hr}$ over a 2-week course, which is the timeframe routinely used for systemic PD-1 blockade in mice [70]. Unlike in PD-L1^{-/-} mice, no significant change in frequency of tetramer⁺ cells was observed in PD-L1 blockade mice compared to IgG controls (Figure 3-4A). As in genetically deficient mice, PD-L1 blockade resulted in no change in number of MPyV-specific cells compared to rat IgG-treated control mice. PD-L1 blockade also did not improve proliferation or production of TNF- α or IL-2 (Supplemental Figure 3-2). Viral load was also unaffected (Figure 3-4B). PD-L1 blockade, however, increased the frequency of CD103⁺ cells as observed in PD-L1^{-/-} mice (Figure 3-4C).

Terminally exhausted CD8 T cells exhibit an Eomes⁺ PD-1^{hi} phenotype, whereas Tbet⁺PD-1^{int} cells are progenitors of exhausted cells and can be revived by PD-L1

blockade [161]. Because multiple functions were not restored when engagement of the PD-1 pathway was disrupted, we hypothesized that MPyV-specific CD8 T_{RM} cells may be severely exhausted and would exhibit high Eomes expression. Examination of Tbet and Eomes expression over time showed that in the brain the percentage of Tbet⁺ cells was constant from 8 to 30 dpi, but Eomes⁺ cells increased in frequency, coincident with increasing levels of PD-1 (Figure 3-5A). However, we compared the gMFI of PD-1 on Tbet⁺ and Eomes⁺ cells and found that the Tbet⁺PD-1^{int} vs Eomes⁺PD-1^{hi} dichotomy reported elsewhere was not evident in this MPyV infection model [161] (Figure 3-5B).

Brain-infiltrating macrophages and some neural cells upregulate PD-L1

PD-1 has two known ligands, PD-L1 (also called B7-H1 or CD274) and PD-L2 (CD273), which have different patterns of expression. PD-L1 is constitutively expressed by both hematopoietic and parenchymal cells and PD-L2 is inducibly expressed by macrophages and dendritic cells. Non-hematopoietic cells in the CNS do not typically express PD-L1 but it can be induced by type I and II interferons in the context of viral infection and in experimental autoimmune encephalomyelitis [73, 75, 172-174]. To determine which cell types in the brain may express PD-L1 or PD-L2 during MPyV infection, we isolated hematopoietic and neural cells from the brain for flow cytometric analysis [169] and found that the majority of CD45^{hi} infiltrating immune cells expressed PD-L1 (Figure 3-2A) but not PD-L2 (data not shown), and that their levels of PD-L1 were stable from 8 to 30 dpi. CD11b⁺ infiltrating monocyte-derived cells showed the highest level of expression, but this population declined significantly from 8 dpi to 30 dpi (Figure 3-2B). We asked whether the microenvironment of the infected brain contributed

to upregulation of PD-L1 by infiltrating immune cells, and found that monocyte-derived cells had highly elevated levels of PD-L1 compared to their splenic counterparts, whereas expression of PD-L1 by CD4 and CD8 T cells in the brain was only slightly higher than in the spleen (Figure 3-2A). Examination of neural cell populations showed that oligodendrocytes (CD45⁻ O4⁺) were negative for PD-L1 at both 8 and 30 dpi, but a low frequency of microglia (CD45^{lo} CD11b^{int}) and CD45⁻ O4⁻ cells were PD-L1⁺ at both timepoints (Figure 3-2C). Taken with our *in vitro* findings with PD-L1^{-/-} BMDCS, these data suggest that the amount of PD-1 ligands expressed in the MPyV-infected brain may be insufficient to inhibit virus-specific T cell function.

Discussion

PD-1 negatively regulates CD8 T cell responses in the setting of chronic antigen exposure, forging an armistice between the host immune response and viral pathogens or tumors with the benefit of lessened immunopathology. New studies suggest that PD-1-mediated exhaustion may be a state of memory T cell differentiation in the face of chronic antigenic stimulation rather than one exclusively intended to eliminate potentially immunopathologic T cells functionally or physically. Here, we show high levels of PD-1 expression by virus-specific CD8 T cells during low-level persistent MPyV infection limit IFN- γ production when cells are stimulated with PD-L1⁺ BMDCs. Although MPyV infection induces some expression of PD-L1 in the brain, T cells from PD-L1-deficient mice did not make more IFN- γ than those from wild type mice, as is reported in PD-L1 blockade-treated mice infected with LCMV. Furthermore, absence of PD-1 signaling *in vivo* did not bolster the MPyV-specific T cell response or reduce viral load in the brain. In mice genetically deficient in PD-L1, however, anti-MPyV CD8 T cells showed changes in phenotype with a higher frequency expressing CD103 and multiple inhibitory receptors. The mean fluorescence intensity of virus-specific tetramer was also elevated, which taken with our previous study of T_{RM} cells, points toward a link between PD-1 and TCR affinity. Together, these data are consistent with the concept that PD-1 is reflective of a persistent infection guided pathway of memory T cell differentiation that does not necessarily involve functional exhaustion.

Interfering with the PD-1:PD-L1 interaction did not have outcomes for PD-1^{hi} MPyV-specific CD8 T cells predicted based on studies with chronic LCMV infection. In the setting of clone 13 infection, engagement of PD-1 by PD-L1 expressed on the surface

of hematopoietic cells or non-hematopoietic cells resulted in differential loss of T cell effector functions, as reflected by decreased magnitude and profile of cytokines or impaired clearance of infected target cells, respectively [175]. Similarly, JMHV coronavirus-infected oligodendrocytes express PD-L1 and are protected from virus-specific T cell cytotoxicity, although at the expense of viral persistence [73]. Our finding that MPyV-infected PD-L1^{-/-} mice do not recover IFN- γ production or increase in number suggests that PD-L1⁺ brain-infiltrating monocyte-derived cells have little effect on T cells *in vivo* and therefore are not inducing T cell exhaustion. In contrast to LCMV and JMHV infections, we did not observe improved viral control. Thus, neither IFN- γ dysfunction among anti-MPyV CD8 T cells nor viral persistence in the brain is primarily due to inhibition by PD-1.

Our findings *in vivo* contrasted the increase in IFN- γ production observed using PD-L1^{-/-} BMDCS to stimulate brain-infiltrating cells. This could be due to expression of PD-L1 in the brain being too infrequent or because PD-L1⁺ cells are either not infected by MPyV or cross presenting MPyV antigens. PD-L1 ligation of PD-1 is inhibitory in the context of antigen-dependent TCR stimulation. Although MPyV can infect peritoneal macrophages and splenic dendritic cells [120], we have not evaluated brain-infiltrating cells of these types for infection. In a model of humanized glial chimeric mice, astrocytes predominantly support productive human JC polyomavirus replication early infection but oligodendrocytes are nonproductively infected late in infection [101]. Both astrocytes and oligodendrocytes are capable of inducibly upregulating PD-L1 [71, 73], but whether this occurs in MPyV-infected mice has not been determined. PD-L1 expression can be regulated by the PTEN pathway, which is targeted by MPyV middle T (MT) antigen

[176]. A mouse fibroblast cell line stimulated with IFN- γ upregulated PD-L1, but when infected with MPyV, PD-L1 levels did not increase relative to uninfected controls (data not shown). Although this result could be specific for this cell type and not applicable to monocyte-derived or neural cells in the MPyV-infected brain, it raises the possibility that PD-L1 expression by host cells *in vivo* is driven by cytokines and not in direct response to viral infection.

Although we did not observe functional defects of MPyV-specific cells as a result of the PD-1:PD-L1 interaction, there were some phenotypic changes, including upregulation of CD103 (integrin α_E) and the inhibitory receptors Tim3 and 2B4, as well as improved tetramer binding. However, with the exception of increased CD103 expression, these results were seen only in PD-L1^{-/-} and not in i.c.v. PD-L1 blockade-treated mice. Because antibody blockade was initiated at 14 dpi, these data suggest that our findings in genetically deficient mice are likely due to earlier events involving PD-L1. This also fits with the decrease in frequency of LT359 cells, perhaps due to increased priming of subdominant MPyV epitope-specific cells, not observed in blockade-treated mice, but seen in both the brain and spleen of PD-L1^{-/-} mice. Interestingly, CD103 is a ligand for E-cadherin and is important for memory T cell residence in tissues with prevalent epithelium. Epithelial cells in a variety of tissues are permissive for MPyV replication and tumorigenesis [119]. E-cadherin is expressed in ependymal cells of the CNS [177]. If MPyV upregulates PD-L1 in epithelial cells, it is possible that CD103 expression by T cells increases in its absence as a consequence of their tethering to infected ependymal cells.

Upregulation of PD-1 is initiated by TCR signaling and downregulated with loss of antigen availability. PD-1 expression is sustained in chronic infections by repetitive TCR stimulation, and signaling through PD-1 perpetuates its own expression through a positive-feedback loop [155]. It has recently been demonstrated that epigenetic regulation of *PDCDI*, the gene for PD-1 varies among CD8 T cells depending on their state of differentiation, with high methylation of the *PDCDI* promoter in naïve cells, demethylation in effector cells, and partial remethylation in memory cells [178]. Exhausted T cells fail to remethylate the *PDCDI* promoter, leaving the PD-1 locus available for transcription. Reports that PD-1 expression and the exhaustion phenotype are passed on to cells after homeostatic proliferation or pathogen rechallenge point toward chromatin remodeling as a mechanism for establishing a transcriptional program of T cell differentiation unique to cells exposed to chronic antigen [179, 180]. Exhausted cells show an array of differences in gene expression compared to functional memory cells, suggesting that PD-1, perhaps also Tim3 and 2B4, is part of a larger epigenetically controlled program. Furthermore, Zehn and colleagues advocate the idea that exhaustion represents a distinct state of memory T cell differentiation enabling them to retain anti-viral activity during chronic infection [163]. In MPyV infection, T cells in the spleen transiently expressed PD-1 at 8 dpi, but in the brain high PD-1 expression was sustained into the persistent phase, at which time viral loads were similar in the brain and spleen. This suggests that PD-1 levels in the brain are not exclusively antigen-driven, fitting with findings from examination of HIV-specific CD8 T cells, which had higher levels of PD-1 on cells from the CSF than those in the blood, despite lower titers of HIV RNA [79]. Taken with evidence that PD-1 expression can be maintained by some common γ -chain

cytokines and type I IFNs [80-82], it is possible that PD-1 expression in the CNS is determined by microenvironmental cues rather than or in addition to antigen.

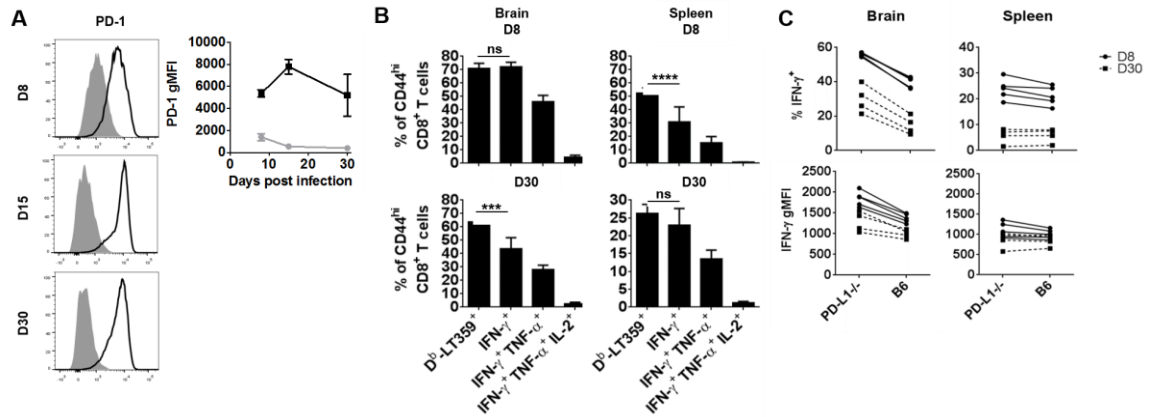


Figure 3-1. Analysis of PD-1 expression and cytokine production by MPyV-specific CD8 T cells in the brain and spleen. (A) Representative histograms (left panel) of PD-1 expression by brain-infiltrating (line) or splenic (shaded) D^b-LT359⁺ CD8 T cells at indicated timepoints post-infection. Mean (\pm SD) of the geometric mean fluorescence intensity (gMFI) of PD-1. (B) Frequency of cytokine-producing CD44^{hi} CD8 T cells in brain and spleen at 30 dpi following ex vivo stimulation with LT359 peptide. Data are cumulative from 3 independent experiments of 7-9 mice per timepoint. (C) Frequency (top panels) and gMFI (bottom panels) of IFN- γ -producing cells isolated from the brain and spleen at indicated timepoints following stimulation with LT359 peptide-pulsed dendritic cells derived from C57BL/6 and PD-L1^{-/-} bone marrow. Points connected by lines indicate cells from a single mouse. Data are cumulative from 2 independent experiments with 8-9 mice/timepoint. *** p <0.001, **** p <0.0001, ns = not significant.

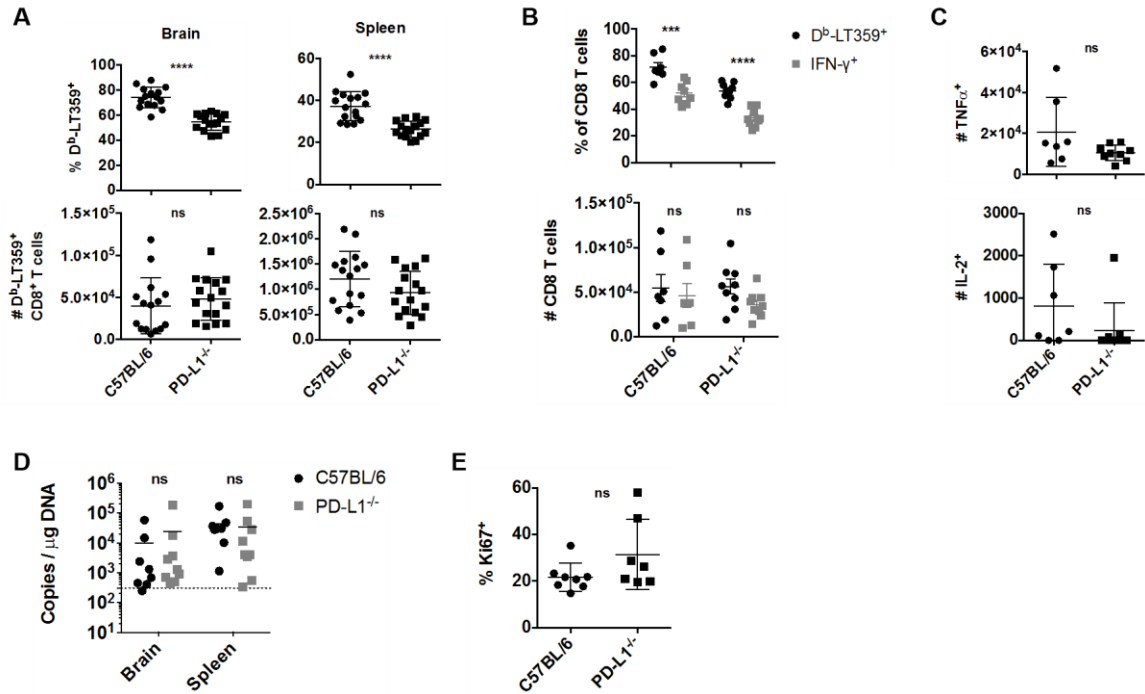


Figure 3-2. Comparison of T cell functionality in wild-type mice and mice genetically deficient for PD-L1. (A) Frequency (top panels) and number (bottom panels) of D^b-LT359⁺ cells of CD44^{hi} CD8⁺ T cells in the brain and spleen at 30 dpi. (B) Frequency (top panels) and number (bottom panels) of D^b-LT359 tetramer-binding cells and IFN- γ -producing cells (following *ex vivo* stimulation with LT359 peptide) in the brain at 30 dpi. Gated on CD44^{hi} CD8⁺ T cells. (C) Number of CD8 T cells in the brain at 30 dpi that produce TNF α (top) or IL-2 (bottom). (D) Analysis by qPCR of viral genome copy numbers in genomic DNA isolated from brain and spleens at 30 dpi. (E) Frequency of D^b-LT359⁺ CD8 T cells in the brain that express Ki67 at 30 dpi. Data are cumulative from 2-4 experiments with 3-5 mice/group. *** p <0.001, **** p <0.0001, ns = not significant.

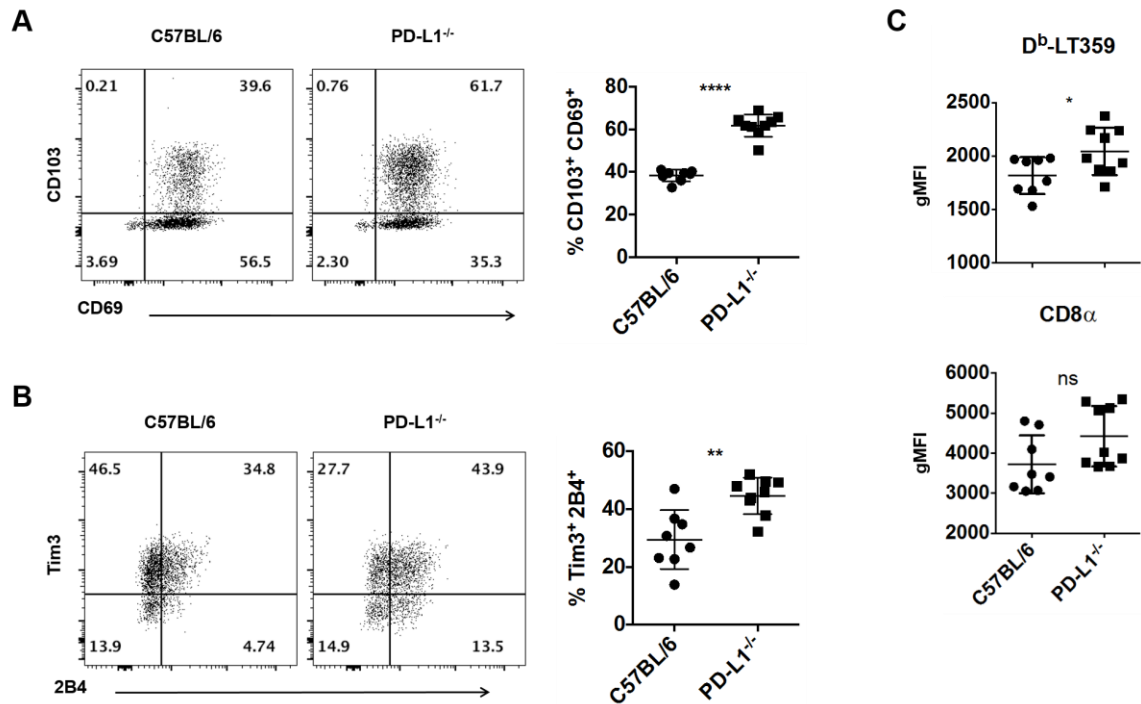


Figure 3-3. Comparison of T cell phenotype in wild-type mice and mice genetically deficient for PD-L1. (A) Representative dot plots (left panel) and mean (\pm SD; right panel) of frequencies of D^b-LT359⁺ CD8 T cells expressing CD103 and CD69 in the brain at 30 dpi. (B) Representative dot plots (left panel) and mean (\pm SD; right panel) of frequencies of PD-1^{hi} D^b-LT359⁺ CD8 T cells expressing Tim3 and 2B4 in the brain at 30 dpi. (C) Mean (\pm SD) of the geometric mean fluorescence intensity (gMFI) of staining by D^b-LT359 tetramers (top) and CD8 α (bottom). Data are cumulative from 2 experiments with 3-5 mice/group. * p <0.05, ** p <0.01, **** p <0.0001, ns = not significant.

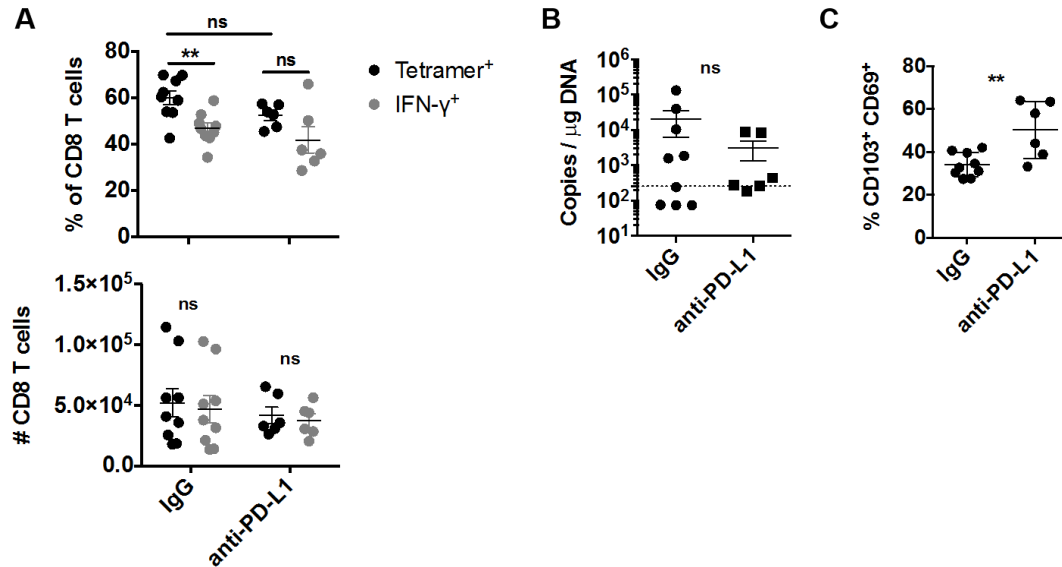


Figure 3-4. Comparison of T cell functionality and phenotype in the brain of PD-L1-blockade or rat IgG treated mice. Mice were surgically implanted with subcutaneous osmotic pumps connected to cannulas inserted into the left lateral ventricle. Pumps were loaded with 6 mg/ml of either anti-PD-L1 or rat IgG in phosphate buffered saline and delivered antibody at a rate of 12 μ l/day for 14 days. (A) Frequency (top panels) and number (bottom panels) of D^b-LT359 tetramer-binding cells and IFN- γ -producing cells (following *ex vivo* stimulation with LT359 peptide) in the brain at 30 dpi. Gated on CD44^{hi} CD8⁺ T cells. (B) Analysis by qPCR of viral genome copy numbers in genomic DNA isolated from brain tissue at 30 dpi. (C) Mean (\pm SD) of the frequency of D^b-LT359⁺ CD8 T cells expressing CD103 and CD69 in the brain at 30 dpi. Data are cumulative from 2 experiments with 2-5 mice/group. ** p <0.01, ns = not significant.

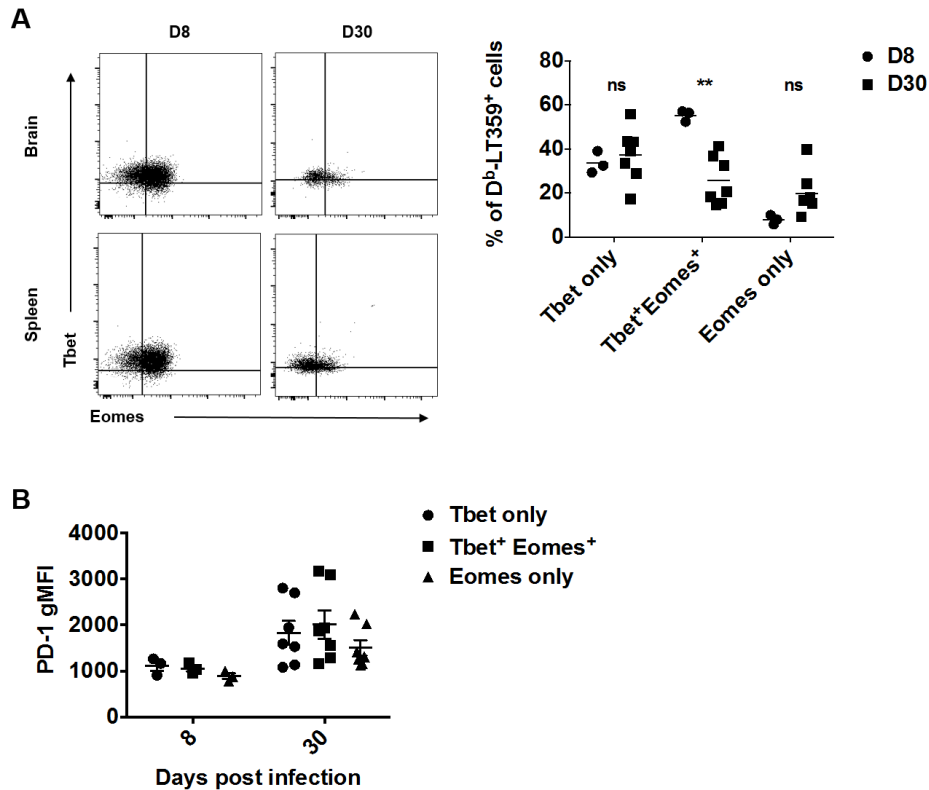


Figure 3-5. Expression of Tbet and Eomes transcription factors by LT359-specific CD8 T cells during acute and persistent MPyV infection. (A) Representative dot plots (left panel) of frequencies of D^b-LT359⁺ CD8 T cells expressing Tbet and Eomes in the brain and spleen at 8 and 30 dpi and the mean (\pm SD; right panel) of those frequencies in the brain. (B) Mean (\pm SD) of geometric mean fluorescence intensity (gMFI) of PD-1 expressed by indicated subsets of D^b-LT359⁺ CD8 T cells in the brain at 8 and 30 dpi. Data are from 1 experiment at 8 dpi and cumulative from 2 experiments at 30 dpi with 3-4 mice/group. ** $p < 0.01$, ns = not significant.

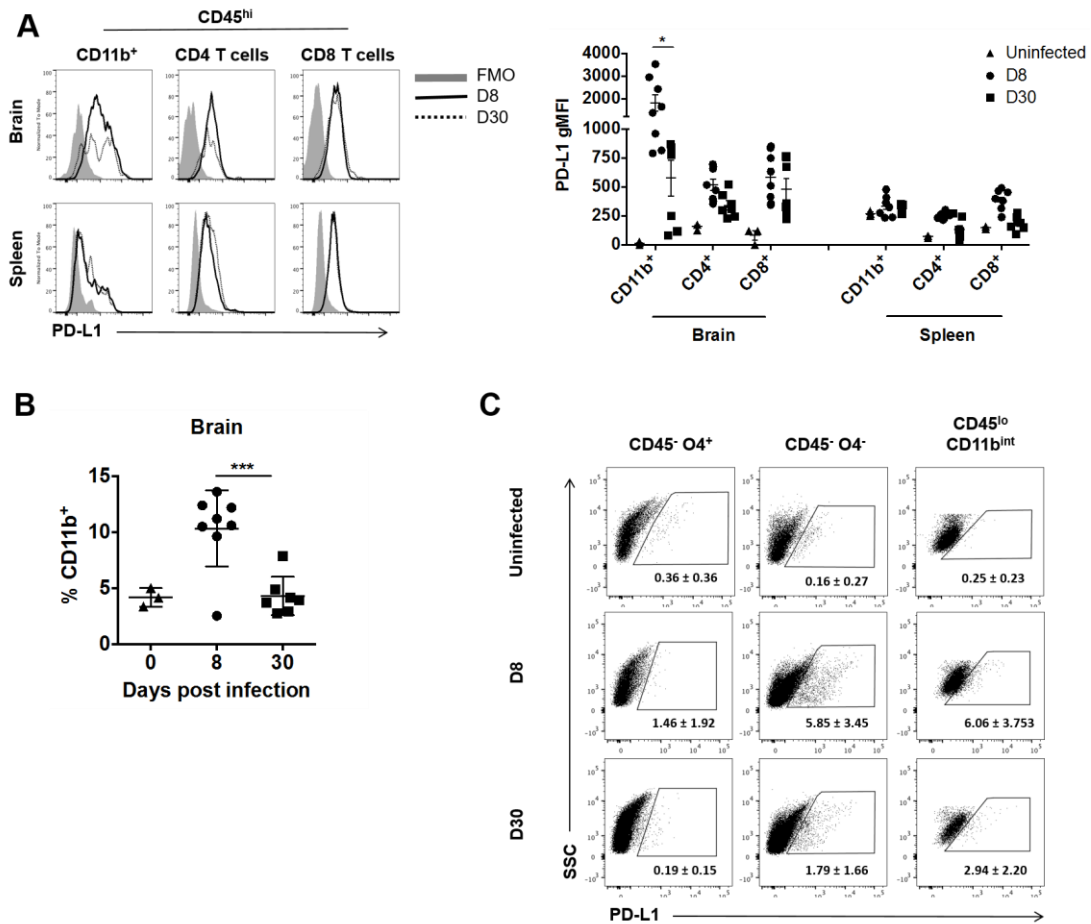
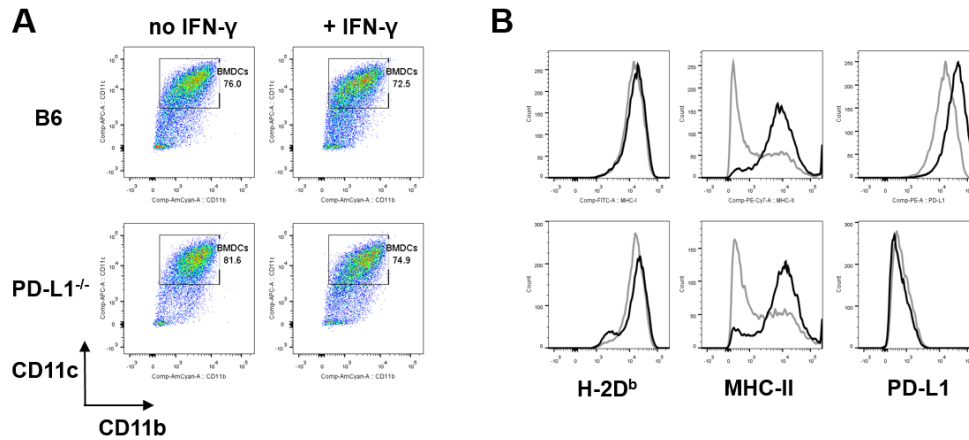


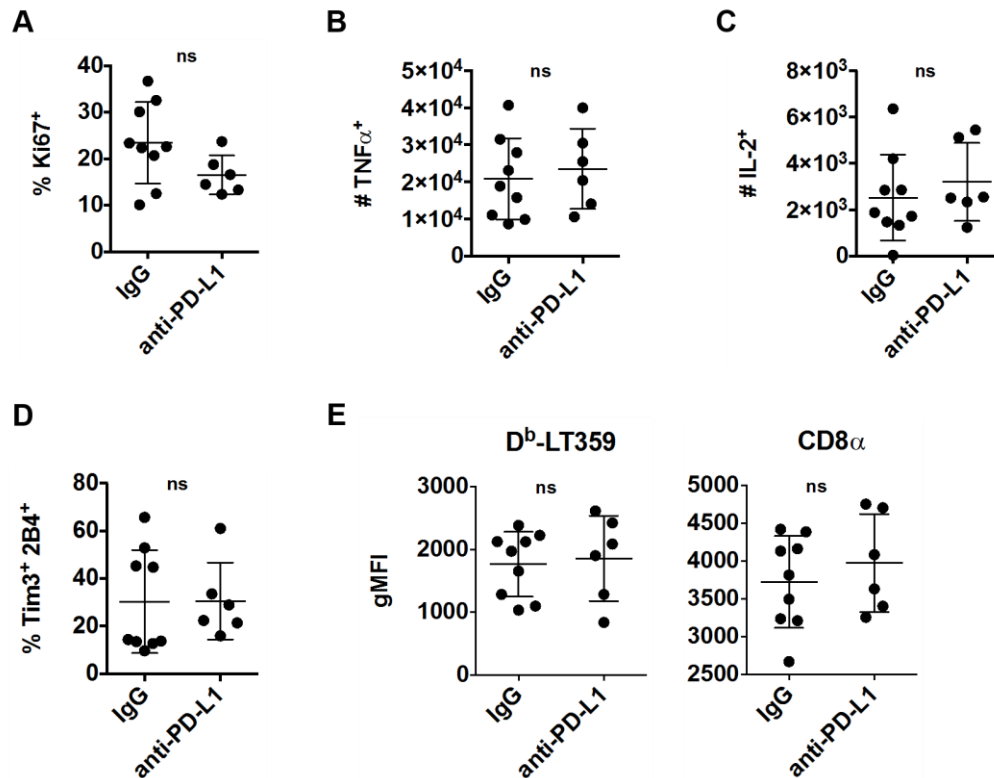
Figure 3-6. Expression of PD-L1 by hematopoietic and brain-resident non-hematopoietic cells during acute and persistent MPyV infection. (A) Representative histograms (left panel) of expression of PD-L1 by indicated cell types in the brain and spleen at 8 dpi (solid line) and 30 dpi (dashed line) compared to fluorescence minus-one (FMO) control (shaded); (Right panel) Mean (\pm SD) of geometric mean fluorescence intensity (gMFI) of PD-L1 in indicated cell types from brains and spleens of mice at 8 and 30 dpi and uninfected controls. (B) Mean (\pm SD) of the frequency of CD11b⁺ cells of total CD45^{hi} brain-infiltrating cells in mice at 8 and 30 dpi and uninfected controls. (C) Representative dot plots with mean (\pm SD) frequency of PD-L1⁺ cells in CD45⁺O4⁺ (oligodendrocytes), CD45⁻O4⁻ (other neural cells), and CD45^{lo}CD11b^{int} (microglia) in

uninfected controls and mice at 8 and 30 dpi. Data for uninfected controls are from 1 experiment and cumulative from 2 experiments for 8 and 30 dpi with 3-4 mice/group.

* $p < 0.05$, *** $p < 0.001$



Supplemental Figure 3-1. Expression of dendritic cell markers and antigen-presentation receptors in bone marrow-derived dendritic cell cultures. Cells from the bone marrow of C57BL/6 and PD-L1^{-/-} mice were harvested and cultured for 10 days in the presence of GM-CSF. Loosely adherent dendritic cells were then collected and cultured overnight with or without IFN- γ . Verification of dendritic cell phenotype (A) and expression of MHC-I and -II and PD-L1 was performed by flow cytometry prior to use of IFN- γ -stimulated cells as antigen presenting cells.



Supplemental Figure 3-2. Comparison of T cell functionality and phenotype in the brain of PD-L1-blockade or rat IgG treated mice. Mice were surgically implanted with subcutaneous osmotic pumps connected to cannulas inserted into the left lateral ventricle. Pumps were loaded with 6 mg/ml of either anti-PD-L1 or rat IgG in phosphate buffered saline and delivered antibody at a rate of 12 μ l/day for 14 days. (A) Frequency of D^b-LT359⁺ CD8 T cells in the brain that express Ki67 at 30 dpi. Number of CD8 T cells in the brain at 30 dpi that produce TNF α (B) or IL-2 (C). (D) Mean (\pm SD) of frequencies of PD-1^{hi} D^b-LT359⁺ CD8 T cells expressing Tim3 and 2B4 in the brain at 30 dpi. (E) Mean (\pm SD) of the geometric mean fluorescence intensity (gMFI) of staining by D^b-LT359 tetramers (left) and CD8 α (right). Data are cumulative from 2 experiments with 2-5 mice/group. ns = not significant.

CHAPTER 4

Mouse polyomavirus induces central nervous system demyelination and recruits CD8 T cells independent of VLA-4

Elizabeth L. Frost¹, Saumya Maru², Timothy K. Cooper³, and Aron E. Lukacher²

¹Immunology and Molecular Pathogenesis Graduate Program, Emory University,
Atlanta, GA

²Department of Microbiology and Immunology, The Pennsylvania State University
College of Medicine, Hershey, PA

³Department of Comparative Medicine, The Pennsylvania State University College of
Medicine, Hershey, PA

Abstract

Human JC polyomavirus (JCV) is the etiologic agent of progressive multifocal leukoencephalopathy (PML), an often fatal demyelinating disease of the central nervous system (CNS). The major risk factor for PML development is immunosuppression, therefore PML is a potential complication of natalizumab (anti-VLA-4 monoclonal antibody) therapy for multiple sclerosis. Lack of a tractable animal model due to strict species specificity of polyomaviruses has clouded understanding of early events and progression of PML. Successful humanized mouse models provide important insight into some aspects of disease, but cannot address interaction of the host immune response with viral infection in the CNS. Here, we used intracerebral inoculation of immunocompetent mice with mouse polyomavirus, a natural pathogen of this host, to determine whether the presence of infiltrating anti-viral T cell responses precludes demyelinating disease. Immunohistochemistry revealed infection of ventricular ependymal cells and white matter astrocytes and co-localization of responding T cells. Associated pathology included demyelination of the cingulum bundle and external capsule, enlargement of ventricles, edema, and astrogliosis, demonstrating that T cells are not sufficiently protective. Furthermore, genetic deletion of the α_4 integrin component of VLA-4 did not prevent MPyV-specific T cell migration into the CNS, raising questions about the presumed effects of natalizumab treatment on JCV immunity in cases of PML. Our work provides a novel system of polyomavirus-induced demyelination allowing manipulation of host immunity to better understand disease pathogenesis and a means for preclinical testing of potential treatment and prevention strategies for PML patients.

Introduction

Human JC polyomavirus (JCV) asymptotically and persistently infects the kidney and bone marrow of the majority of the population [1]; however immunosuppressed individuals, such as those with HIV/AIDS, hematological malignancies, and those undergoing monoclonal antibody therapies for autoimmune diseases, are at risk of opportunistic JCV infection of the central nervous system, resulting in a demyelinating disease known as progressive multifocal leukoencephalopathy (PML) [10, 11]. Diagnosis involves magnetic resonance imaging of demyelination, detection of JCV DNA in the cerebrospinal fluid, and sometimes confirmation by immunohistochemical staining of biopsy tissues for JCV proteins VP1 and large T antigen and/or *in situ* hybridization for JCV DNA [181-183]. Histological hallmarks of PML include oligodendrocytes at the borders of white matter lesions with “ground glass” nuclei full of viral inclusion bodies, “bizarre” astrocytes with enlarged, multilobed nuclei and shortened processes, and lipid-laden macrophages [184]. In some cases, JCV infection targets cerebellar granule cell neurons rather than glial cells [185]. Lytic infection of oligodendrocytes by JCV is thought to underlie demyelination [8, 9]. Once diagnosed, PML typically progresses rapidly resulting in debilitation or death, and the accepted histological hallmarks of PML are derived from examination of autopsy and biopsy tissue collected at a late stage of disease. Therefore, much of what is known about mechanisms of PML pathogenesis may not be applicable in earlier stages of disease prior to diagnosis.

Given that the most prevalent underlying risk factor for PML is immune suppression, it is thought that the absence of JCV-targeted surveillance in the CNS

promotes PML progression. Natalizumab is a monoclonal antibody therapy for multiple sclerosis that purportedly interferes with migration of myelin-specific T cells to the CNS by disrupting the interaction of very late antigen-4 (VLA-4) expressed by leukocytes with the ligand vascular cell adhesion molecule-1 (VCAM-1) on the surface of activated endothelium [186]. Natalizumab predisposes patients to PML risk by a largely unknown mechanism. Due to its efficacy in blocking migration of autoreactive cells to the CNS, JCV-specific CD8 T cells are also thought to be targeted by natalizumab and excluded from the brain. Because multiple hematopoietic cell types express VLA-4, natalizumab treatment is not directed at T cells alone but toward an entire concert of immune responses.

Much of what remains unknown about PML—such as the role of viral determinants (capsid mutations at host receptor binding sites and alterations in the non-coding regulatory region), mechanisms by which the host immune response contributes to prevention of demyelination, spread of JCV in the CNS, and the evolution of disease—would be best addressed in an animal model. Co-evolution of host species with polyomaviruses restricts productive replication to natural hosts [87]; consequently, inoculation of non-human primates and rodents with JCV results in tumor development rather than demyelinating disease because only the oncogenic early region viral T antigens are produced [91, 92, 96]. Recently, a humanized glial chimeric mouse model capable of supporting JCV replication and exhibiting demyelination of the corpus callosum demonstrated that astrocytes and glial precursor cells, rather than oligodendrocytes, are the predominant cell type infected [101]. Furthermore, infection in astrocytes was sufficient for propagation and spread of JCV, whereas JCV triggered

apoptosis in oligodendrocytes. This model has provided important insight into JCV infection of CNS cell types, but without a humanized immune system, it allows no examination of the intersection of host immunity and control of JCV.

Although improved outcome for PML is strongly correlated with JCV-specific T cell responses in the blood, effective immunity to JCV in the brain is largely uncharacterized. We have previously demonstrated that intracerebral (i.c.) inoculation of immunocompetent mice with mouse polyomavirus results in persistent viral infection in the brain despite recruitment of a stable and functional high-affinity CD8 T cell response. Here, we use this model to address whether the presence of MPyV-specific T cells sufficiently controls infection to prevent CNS pathology, as is thought for protection from PML. We show that MPyV productively replicates in the CNS in ependymal cells lining the ventricle as well as in white matter astrocytes and that infiltrating T cells are located at sites of viral infection. Despite this anatomic co-localization of T cells and infected cells, loss of myelin occurs in the external capsule and cingulum bundle beginning with appearance of T cell infiltrates, with demyelination increasing over time despite reduction in virus levels. At the latest stage examined, enlargement of the ventricles, edema, and gemistocytic (reactive) astrocytosis were also apparent. However, in the most severe lesions in the cingulum bundle, no evidence of ongoing infection or lingering T cells was observed early or late in disease. In addition, to address the role of natalizumab in promoting polyomavirus-induced demyelination, we used mice selectively deficient of the α_4 integrin component of VLA-4 in cells of hematopoietic origin. Unexpectedly, we found that neither CD4 T cells nor MPyV-specific CD8 T cells require VLA-4 expression to enter the CNS and that they express other integrins

including P selectin glycoprotein ligand-1 (PSGL-1) and CD11a, a component of lymphocyte function-associated antigen-1 (LFA-1). Our findings demonstrate that intracerebral MPyV infection provides a novel model of polyomavirus-induced CNS disease that can improve understanding of antiviral immunity in the brain.

Materials and Methods

Mice and virus inoculation. C57BL/6NCR female mice purchased from the Frederick Cancer Research and Development Center of the National Cancer Institute (Frederick, MD), Tie2Cre and α_4 -floxed ($\alpha_4^{fl/fl}$) mice generously provided by Thalia Papayannopoulou (University of Washington), and β_2 -microglobulin knockout ($\beta_2m^{-/-}$; B6.129P2- $B2m^{tmlUnc/J}$) purchased from the Jackson Laboratory (Bar Harbor, ME) were housed and bred in accordance with the guidelines of the Institutional Animal Care and Use Committees and the Department of Comparative Medicine at the Pennsylvania State University College of Medicine. At 7-12 weeks of age, mice were inoculated intravenously (i.v.) via the tail vein with 2×10^6 PFU MPyV strain A2 in 100 μ l or anesthetized and intracerebrally (i.c.) inoculated by injecting the right frontal lobe with 2×10^6 PFU MPyV strain A2 or with a previously described recombinant hemagglutinin-tagged MPyV [187] in 30 μ l DMEM 5% FBS. Heat-inactivated (70°C for 30 min) MPyV stock had no infectious virus by plaque assay (limit of detection 5 PFU/ml; data not shown).

Quantitation of MPyV Genomes. TaqMan real-time PCR was performed in an ABI StepOnePlus (Applied Biosciences) with 10 μ g of template DNA purified from tissue using the Maxwell 16 Research Instrument (Promega, Madison, WI) according to the manufacturer's instructions. Primers and amplification parameters are previously described [125].

Cell isolation, staining, verification of serum anti-VLA-4 and flow cytometry. Blood samples were lysed with ACK buffer prior to staining for flow cytometry. Cell numbers were determined using 50 μ l blood whole blood ACK lysed and stained for flow cytometry and 75 μ l Absolute Count Standard beads (Bangs Laboratories, Inc., Fishers, IN) per the manufacturer's instructions. Brains and spleens were harvested from mice intravascularly labeled for 3 min with 3 μ g anti-CD45 (30-F11) [138]. Brain mononuclear cells were isolated on Percoll gradients of collagenase-digested brains. Spleen and brain cells were exposed to Fixable Viability Dye (eBioscience, San Diego, CA) and Fc Block (BioLegend, San Diego, CA) prior to staining with D^b-LT359-68 tetramers (NIH Tetramer Core Facility, Atlanta, GA) and antibodies to the following molecules: CD8 α (53-6.7), CD11b (M1/70), CD45(30-F11), NK1.1 (PK136), CD162 (2PH1) purchased from BD and CD4 (RM4-5), CD19 (6D5), CD11a (M17/4), CD146 (ME-9F1), CD49d (MFR4.B), and CD3 ϵ (145-2C11) from Biolegend (San Diego, CA). For measurement of anti-VLA-4 mAb in the serum, whole blood from mice treated with control rat IgG or anti-VLA-4 was harvested at various timepoints post-infection then centrifuged and the pellet discarded. Serum and stock anti-VLA-4 mAb (positive control) were diluted 1:100 and incubated with VLA-4^{hi} splenocytes from 8 dpi infected mice. Next, cells were stained with fluorescently conjugated goat anti-rat secondary antibody (BD Biosciences, San Diego, CA) and co-stained for CD49d. Samples were acquired on an LSRFortessa (BD Biosciences) and data analyzed using FlowJo software (Tree Star, Ashland, OR).

RNA in situ hybridization, immunohistochemistry, and immunofluorescent staining. At sacrifice, anesthetized mice were transcardially perfused with PBS then by 10% neutral buffered formalin (NBF). The brain was harvested and cut coronally into 3-mm pieces using a cutting matrix prior to immersion fixation overnight in 10% NBF and embedding in paraffin. For RNA *in situ* hybridization (ISH), 10 μ m formalin-fixed, paraffin-embedded (FFPE) brain sections were processed and stained using the ViewRNA ISH Tissue 2-Plex Assay Kit (Affymetrix, Santa Clara, CA) with probes specific for MPyV T antigen (Accession #AF442959), MPyV VP1 (M34958), or the housekeeping gene ubiquitin C (NM_019639) according to manufacturer's instructions. For immunohistochemistry (IHC), 10 μ m FFPE brain sections were deparaffinized and rehydrated prior to antigen retrieval in 10 mM sodium citrate buffer (pH 6.0). Sections were permeabilized with 1% TritonX-100 and stained with primary antibodies overnight at 4°C with rabbit polyclonal anti-VP1 (generously provided by Robert L. Garcea, University of Colorado, Boulder), anti-HA (Clone 3F10, Roche, Basel, Switzerland), or anti-CD3 (Clone SP7, Abcam, Cambridge, UK) or for 1 hour at RT with anti-GFAP (Dako, Carpinteria, CA), then with biotinylated goat anti-rabbit or anti-rat (Vector, Burlingame, CA), followed by avidin-conjugated horse radish peroxidase (VECTASTAIN Elite ABC Kit, Vector, Burlingame, CA). Staining was developed using the VECTOR NovaRED Peroxidase substrate kit (Vector, Burlingame, CA). For immunofluorescent staining (IF), 10 μ m FFPE brain sections were deparaffinized and rehydrated prior to antigen retrieval in 10 mM sodium citrate buffer (pH 6.0). Staining for anti-APC (Clone CC-1, Abcam, Cambridge, UK) and anti-NeuN (Clone A60, Millipore, Darmstadt, Germany) was done for 30 min at RT in conjunction with the Mouse-on-

Mouse Fluorescein Staining Kit (Vector, Burlingame, CA), prior to overnight staining with anti-VP1 followed by secondary antibody incubation (donkey anti-rabbit conjugated to AlexaFluor594; Jackson ImmunoResearch, West Grove, PA). Staining for astrocytes was performed using directly conjugated anti-GFAP (Clone GA5, ebioscience, San Diego, CA). Tissue sections were counterstained with modified Mayer's hematoxylin (Thermo Scientific, Waltham, MA) and mounted with VectaMount permanent mounting media (Vector, Burlingame, CA) for ISH and IHC or ProLong Gold Anti-Fade Reagent with DAPI (Life Technologies, Carlsbad, CA) for ISH and IF. Images were acquired using a Leica DM4000 B LED microscope (Leica-Camera, Wetzlar, Germany).

Histology. Demyelination was determined by Luxol fast blue-periodic acid Schiff-hematoxylin (LFB-PAS-H) staining of 10 μm FFPE brain sections.

Antibody administration. Mice were injected intraperitoneally (i.p.) with 250 μg rat anti-VLA-4 (PS/2, Bio X Cell, West Lebanon, NH) or ChromPure whole rat IgG (Jackson ImmunoResearch, West Grove, PA) at 0 and 2 days post infection (dpi) and weekly thereafter.

Results

Our previous work examining T cell responses to MPyV infection in the brain utilized i.c. inoculation [166], as a means to bypass the blood brain barrier as is done in other models of CNS viral infection [72, 142]. Because JCV spreads to the brain hematogenously from reservoirs of persistent infection such as the kidney and bone marrow [102], we asked whether intravenous injection of MPyV could be used to model PML in mice. Levels of virus in the brain of i.v. inoculated mice were approximately 1.5 logs lower than in i.c. infected mice, whereas the reverse was seen in the spleen, supporting that viral replication is higher near sites of inoculation (Supplemental Figure 4-1A). Comparison of immune cell population numbers in the blood and spleen of i.c. and i.v. inoculated mice at 8 days post-infection (dpi) showed few differences (Supplemental Figure 4-1B and C); in the brain, however, total infiltrating immune cell numbers were decreased by more than one log, with only a few hundred CD4 T cells and a few thousand CD8 T cells responding to peak infection (Supplemental Figure 4-1D). We chose the i.c. over the i.v. inoculation route because it yielded higher acute and persistent MPyV CNS infection levels.

MPyV actively replicates in the brain, evident by a nearly 2-log increase in viral genome copies from 1 dpi to 4 dpi with untreated virus stock but not with heat-inactivated virus (Supplemental Figure 4-2A). Furthermore, in brain tissue sections from 5 dpi, we were able to detect both viral mRNA transcripts and proteins by *in situ* hybridization (ISH) using T antigen- and VP1-specific probes and immunohistochemistry (IHC), respectively (Supplemental Figure 4-2B and C). Interestingly, at this timepoint,

many infected cells were found in the white matter tract of the external capsule, suggesting that the CNS tropism of MPyV may be similar to that of JCV.

Next we used IHC to identify brain structures supporting MPyV replication at various timepoints post-infection. At 4 dpi, ependymal cells lining the ventricles as well as some cells in the adjacent white matter tracts were VP1⁺ (Figure 4-1A). At 9 dpi, infection involved the external capsule extending toward the cingulum bundle, but by 30 dpi, little productive infection was detected (Figure 4-1A and C). Infiltrating T cells were present at 9 and 30 dpi but not at 4 dpi, in line with kinetic analysis by flow cytometry (Chapter 2), and they co-localized with viral infection at the ventricles and in the white matter tracts (Figure 4-1B and C). We next asked which cell types in the white matter were infected using immunofluorescent staining to detect co-localization of VP1 with several cell-specific CNS antigens: adenomatous polyposis coli (APC) for mature oligodendrocytes, glial fibrillary acidic protein (GFAP) for astrocytes, and NeuN for neurons. VP1 was not detected in either oligodendrocytes or neurons, but astrocytes were VP1⁺, supporting the conclusion that they were productively infected (Figure 4-2). Although not addressed in this study, it may be important to determine whether microglia harbor MPyV infection or are reactive to infection in the CNS. JCV replication has not been reported in microglia in cases of PML, but this glial cell type may be involved in early disease events. Microglia in MPyV-infected brains upregulate MHC-II upon stimulation by IFN- γ produced by CD8 T cells [data not shown] and may play a critical role in orchestrating host immune responses.

Having confirmed that T cells co-localized with virally infected cells in white matter structures, we next asked whether this protected animals from polyomavirus-

associated pathology, as is thought to protect against PML in humans. We examined MPyV infected brains over time for demyelination using Luxol fast blue staining. It should be noted that a needle track was detected histologically being contiguous with a lateral ventricle, demonstrating that the method of i.c. injection used here delivers virus directly into the CSF (Figure 4-3A, top left panel). Vehicle-injected controls and mice sacrificed at 4 dpi showed intact myelin (Figure 4-3A). Small foci of demyelination and vacuolation were apparent in the cingulum bundle and the external capsule at 9 dpi and had progressed by 30 dpi with enlargement of the ventricles and development of edema in this white matter tract (Figure 4-3A). MPyV-induced CNS disease also featured gemistocytic astrocytosis with some multinucleate cells, sharing some characteristics with the bizarre phenotype described in PML (Figure 4-3B). The incidence of this pathology was high—100% of infected mice (n = 12) examined in 3 experiments. Less frequently, we also observed corpus callosum demyelination, perivascular cuffing of lymphocytes, acute focal hemorrhage, neuronal necrosis, and gemistocyte foci in the thalamus. Because most of the damage was in the cingulum bundle, we examined that site for virally infected cells and T cell infiltrates. Interestingly, at 30 dpi no virally infected cells or T cells were found in this area (data not shown), suggesting that these neuropathologic changes were not directly caused by viral infection of neural cells.

Next, we sought to model natalizumab treatment in MPyV-infected animals to determine whether conditions of immune suppression resulted in CNS pathology more closely resembling that of human PML. Initial experiments administering α_4 integrin-specific rat monoclonal antibody (clone PS/2) at 0 and 2 dpi and weekly thereafter showed a significant decrease in brain-infiltrating CD8 T cells at 8 dpi and a co-incident

increase in viral load in the brain and spinal cord compared to control rat IgG-treated mice; however, a decrease in MPyV-specific T cells in the spleen and blood was also observed (data not shown). This suggested that the decrease in T cell number in the brain could be a consequence of a globally diminished T cell response rather than due to antibody blockade. Because VLA-4 is a component of the peripheral supramolecular activation complex of the immune synapse, we hypothesized that injecting PS/2 at these timepoints interfered with T cell priming [188], which contributed to the differences we observed between PS/2- and IgG-treated mice.

Furthermore, the effects on T cell numbers in the brain and viral load were absent at 15 and 30 dpi. Because the PS/2 antibody is raised in rats, we hypothesized that anti-rat IgG humoral immune responses were clearing this antibody from the serum. Splenocytes from 8 dpi, which are high for VLA-4, were incubated with serum from mice treated with rat IgG or PS/2 over the course of infection and followed with a fluorescently labelled anti-rat secondary antibody for analysis by flow cytometry. At D4 and D8 pi, the gMFI of the anti-rat secondary was similar to that of the positive control PS/2 stock antibody, but at 15 dpi through 30 dpi the amount of PS/2 antibody in the serum declined significantly (Supplemental Figure 4-3). Such humoral clearance renders long-term use of PS/2 antibody as blockade for VLA-4 ineffective.

To circumvent this issue, we utilized mice with loxP sites flanking α_4 integrin locus, which can be crossed with Tie2Cre mice to selectively excise the α_4 gene from hematopoietic and endothelial cells [189]. This system allows study of the long-term effects of VLA-4 inhibition on immune cells responding to MPyV infection in the brain, which is important because risk of PML increases with prolonged natalizumab therapy

[17]. Infection of these α_4 -deficient ($\alpha_4^{\Delta/\Delta}$) mice and Cre-negative ($\alpha_4^{+/+}$) littermate controls with MPyV induced comparable B cell, NK cell, monocyte, and T cell immune responses in the blood (Figure 4-4A). Furthermore, similar numbers of MPyV-specific CD8 T cells were measured in both the blood and the spleen, indicating that deletion of VLA-4 did not interfere with T cell priming. Interestingly, there was no change in the numbers of total infiltrating immune cells, CD4 T cells, or total or virus-specific CD8 T cells in the brain of $\alpha_4^{\Delta/\Delta}$ mice compared to $\alpha_4^{+/+}$ littermates. To determine whether these cells were merely associated with the brain tissue, for example by retention in the choroid plexus or meninges, brain tissue sections from mice at 8 dpi were stained for CD3. T cells were found in the white matter tracts of both $\alpha_4^{\Delta/\Delta}$ mice and $\alpha_4^{+/+}$ controls (Figure 4-4B). Moreover, levels of virus were unchanged (Figure 4-4C). These data show that VLA-4 is dispensable for entry of polyoma-virus specific T cells to the CNS.

Because T cell infiltration of the brain in this model does not depend on VLA-4, we hypothesized that expression of other integrins may mediate T cell entry. It was reported recently that in natalizumab-treated patients, migration into the CNS is not hindered but instead is shifted toward entrance via the choroid plexus in a manner dependent on PSGL-1, the ligand for P selectin [87]. This study also demonstrated that T_H17 cells rely on MCAM to infiltrate the CNS in mice with EAE administered VLA-4 blockade. In addition, LFA-1 is the target of efalizumab, a monoclonal antibody treatment for plaque psoriasis that was removed from the market due to its risk of PML as a side effect [20]. Therefore, we assayed MPyV-specific CD8 T cells from the blood and brain of $\alpha_4^{\Delta/\Delta}$ and $\alpha_4^{+/+}$ mice at 8 dpi for levels of CD162 (PSGL-1), CD11a (a component of LFA-1), and CD146 (MCAM). As expected, cells in the blood and brains of $\alpha_4^{\Delta/\Delta}$ mice

were negative for CD49d (Figure 4-4D). Levels of CD162 were higher on brain-infiltrating D^bLT359 tetramer⁺ CD8 T cells than those in the blood, with no difference between $\alpha_4^{\Delta/\Delta}$ mice and control $\alpha_4^{+/+}$ mice. CD11a was also upregulated on these cells in the brain compared to blood and was elevated on $\alpha_4^{\Delta/\Delta}$ floxed cells compared to $\alpha_4^{+/+}$ mice, but only in the brain. Cells were negative for CD146. Total CD4 T cells in the blood and brain showed an expression profile similar to MPyV-specific CD8 T cells, with the exception that no difference in CD11a levels was seen between $\alpha_4^{\Delta/\Delta}$ and $\alpha_4^{+/+}$ mice (Supplemental Figure 4-4). These findings demonstrate that other integrins, particularly CD11a, may control T cell entry of the polyomavirus-infected brain, and further suggest that JCV-specific T cells may bypass natalizumab-mediated blockade of CNS entry.

Discussion

Previous attempts to model PML in animals have been hindered by the strict species specificity of *Polyomaviridae* family members. Adoptive transfer of human fetal glial cells and infection with JCV has proven successful for studying viral replication, tropism and spread in the CNS; however, this model cannot be used to understand the interplay of host immune responses with polyoma infection in the brain. Similarly, another humanized mouse model involved implantation of human bone marrow and thymus to study T cells, but in the absence of appropriate target cells. Here we use mouse polyomavirus, a natural pathogen that has co-evolved with its host, requiring no manipulation of target cells to support viral replication and in the setting of unaltered host immunity. We demonstrate that, when directly injected into the CNS of immunocompetent mice, MPyV productively infects astrocytes in white matter tracts, similar to JCV in mice colonized by human glia, and recruits T cells to the brain in a manner independent of VLA-4.

Focal lesions in PML appear to radiate outwardly as JCV spreads to new oligodendrocytes, creating a region of demyelination bordered by JCV infected cells with recruitment of CD8 T cells if the patient is not severely immunosuppressed [46]. Immunofluorescent staining for MPyV capsid protein VP1 and the oligodendrocyte marker APC did not show co-localization. We also did not observe virally infected cells or infiltrating T cells at sites of severe myelin loss in the cingulum bundle. This further supports the idea that demyelination in our system may occur by an indirect mechanism, perhaps as a result of excessive cytokine production by infiltrating immune cells or lack of support for oligodendrocytes due to astrocyte reactivity or loss of axons. Alternatively,

ventriculitis and edema may be the primary antecedents of demyelination rather than virus-induced death of oligodendrocytes; this possibility seems less likely because compression injury and atrophy of the cerebral cortex were not observed.

A potential modification of our present model is the use of strains of MPyV with mutations orthologous to those associated with PML. JCV isolates from CSF of PML patients are known to carry mutations in the host receptor binding site of VP1 as well as duplications and deletions in the non-coding control region (NCCR). In this preliminary model, we have used a wild-type strain of MPyV. Goldman and colleagues infected humanized mice with JCV Mad-1, a strain isolated from a patient with PML that has NCCR changes compared to archetype virus strains typically found in the urine [101]. Over the course of infection, JCV Mad-1 acquired VP1 capsid mutations, some of which were identical to PML JCV isolates; however, no changes in tropism among glial cell types were conferred.

Evidence that JCV strains with PML-associated capsid mutations lose ability to bind typically used sialylated host receptors, and therefore binding to erythrocytes and kidney tubular epithelial cells, suggests that VP1 mutations may shift tropism away from non-glial cell types, restricting polyomavirus infection to glial cells [25]. Because we have used an unmutated strain of MPyV, it is possible that ependymal cells serve as a sink, diverting viral replication away from astrocytes and oligodendrocytes. This may be supported by the fact that ependymal cells are neural stem cells in the adult mammalian brain and proliferate in response to CNS injury [190] and that MPyV replicates efficiently in cells with a high rate of turnover.

Prolonged natalizumab therapy in patients with multiple sclerosis increases their risk of developing PML, but the effects of natalizumab on JCV-directed immune surveillance in the CNS have not been elucidated. Interference of VLA-4-mediated leukocyte rolling and arrest at activated endothelium is the predicted mechanism of natalizumab [186]. This is thought to extend to JCV-specific CD8 and CD4 T cells, which have a strong positive correlation with improved PML outcome, as well as any other VLA-4-expressing immune cell types that may be involved in mitigating PML progression (i.e., macrophages, B cells, NK cells). Here, we demonstrated that CD4 T cells and MPyV-specific CD8 T cells infiltrate the brain despite deletion of α_4 integrin. Furthermore, these cells express the integrins CD162 (PSGL-1) and CD11a, which is in line with recent evidence that natalizumab treatment increases expression of PSGL-1 and MCAM thereby altering routes of immune cell entry to the CNS [191]. Together these findings necessitate examination of peripheral blood JCV-specific T cell responses for expression of integrins other than VLA-4, and bring into question the concept that natalizumab impairs CNS immunosurveillance for JCV.

We previously demonstrated that high-affinity MPyV-specific CD8 T cells establish a long-lived brain-resident population, independent of replenishment from circulating cells and capable of homeostatic proliferation *in situ* [166]. Despite the presence of virus-specific immunity, MPyV persists systemically and in the brain. Similarly, JCV persists lifelong in peripheral organs, including the kidney and bone marrow, which are also surveyed by the host antiviral immune response. These findings imply a host-pathogen standoff; whether this is preferable to the current notion of uncontrolled lytic polyomavirus infection in the brain, as immune responses may

participate in driving PML pathology, has yet to be determined. Our work has laid a foundation for an animal model that could help uncover mechanisms of polyomavirus-induced CNS disease and improve treatment outcomes for patients with PML. Unlike humanized systems, this model provides a means of studying the interplay between host immunity and infection by polyomavirus in the CNS and could be used to identify immunomodulatory therapeutic strategies and for preclinical *in vivo* drug testing for candidate agents with anti-viral activity in tissue culture.

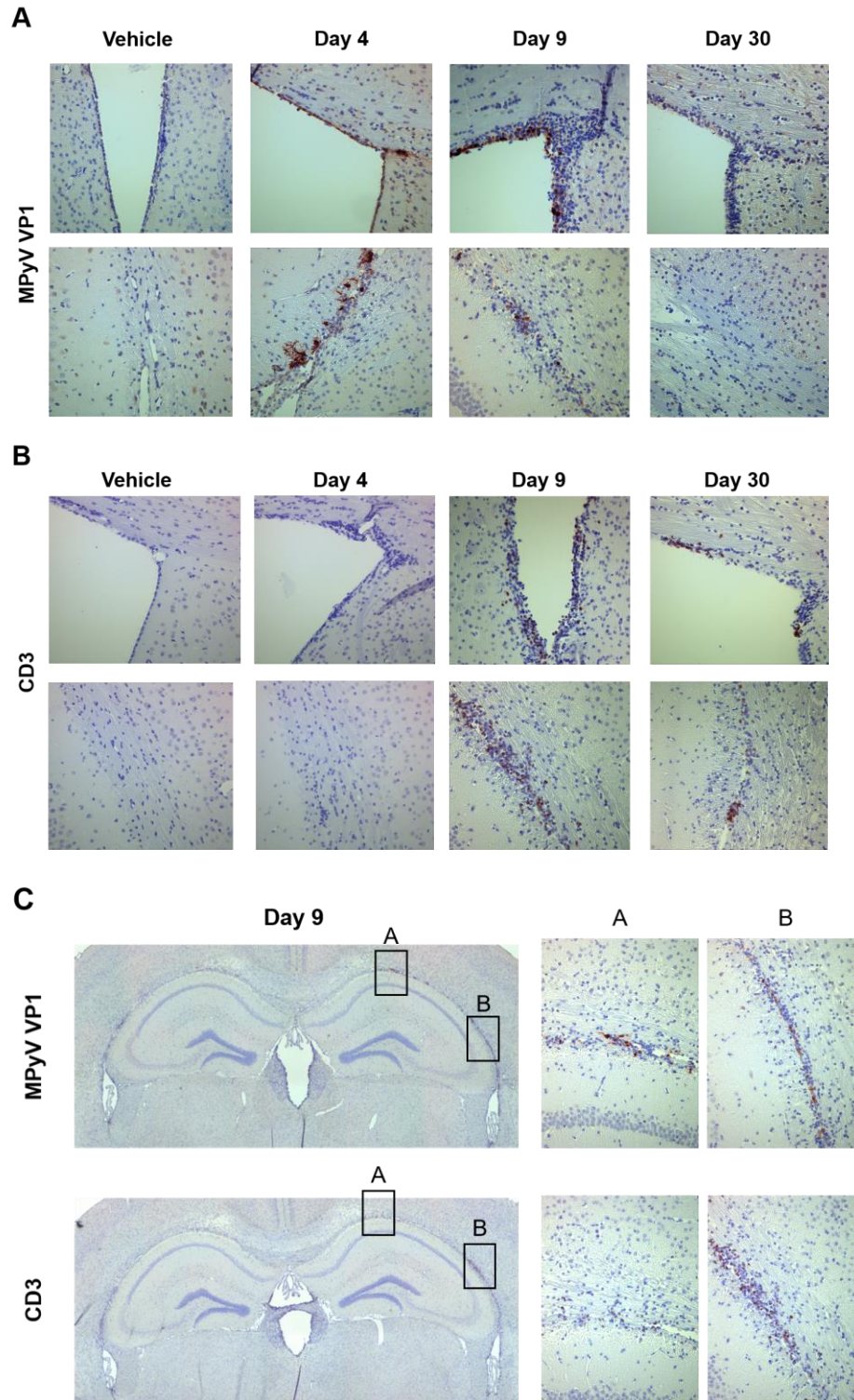


Figure 4-1. Kinetic analysis of location of MPyV-infected cells and T cell infiltrate in the brain by immunohistochemistry. Photomicrographs of formalin-fixed, paraffin-

embedded (FFPE) brain tissue sections from mice sacrificed at indicated timepoints post-infection stained with antibodies specific for (A) MPyV capsid protein VP1 (red) and (B) CD3 (red) and counterstained with hematoxylin. Sections imaged were cut near bregma +0.2 mm (top rows) and bregma -2 to -2.7 mm (bottom rows). Magnification 200X. (C) Photomicrographs of FFPE brain sections at 9 dpi stained for VP1 (top) or CD3 (bottom) with boxes in left panels (50X) indicating areas shown at higher magnification in right panels (200X). Bregma -2.0 mm. Images are representative of 3 mice/timepoint from 1 experiment.

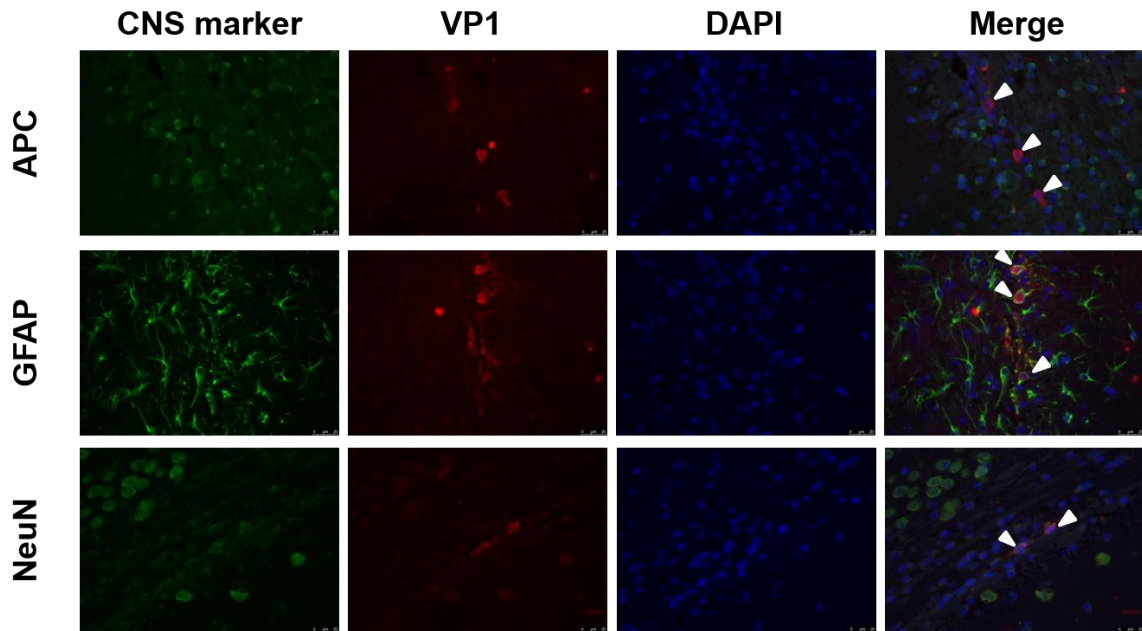


Figure 4-2. Identification of MPyV-infected CNS cell types by immunofluorescent staining. Fluorescence micrographs of formalin-fixed, paraffin-embedded (FFPE) brain tissue sections from mice sacrificed at 4 days post-infection stained with antibodies specific for CNS antigens (green) for identification of oligodendrocytes (APC), astrocytes (GFAP), and neurons (NeuN) as well as for MPyV capsid protein VP1 (red). Nuclei were counterstained with DAPI (blue). White arrows in merged images indicate VP1⁺ cells. Magnification 400X. Images are representative of 3 mice from 1 experiment.

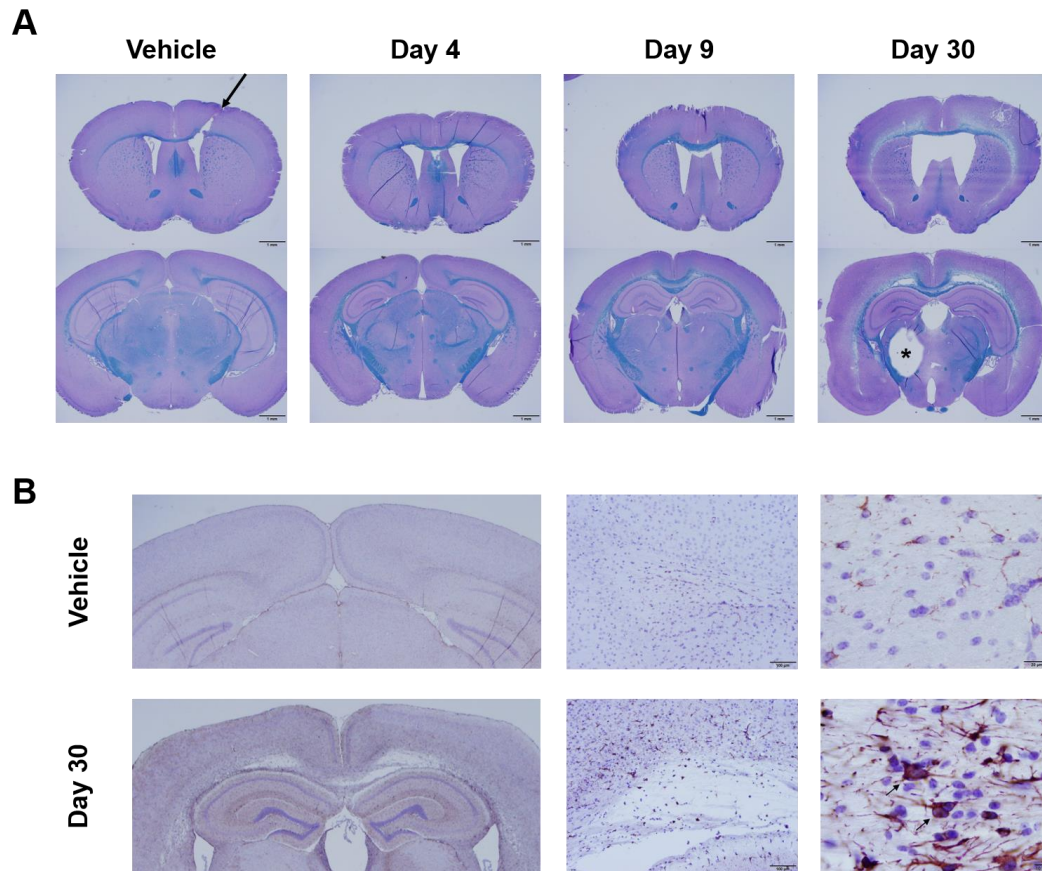


Figure 4-3. Kinetic analysis of demyelination and evidence of astrogliosis in MPyV-infected mice. (A) Photomicrographs of Luxol fast blue-periodic acid Schiff-hematoxylin stained formalin-fixed paraffin-embedded (FFPE) brain sections from mice at indicated timepoints post-infection. Arrow in the top left panel indicates the needle track at the site of intracerebral injection. Asterisk in bottom right panel indicates significant cutting artifact. Sections imaged were cut near bregma +0.2 mm (top rows) and bregma -2 to -2.7 mm (bottom rows). Scale bars indicate 1 mm. Representative of 15 mice from 4 experiments. (B) Photomicrographs from FFPE brain sections (bregma -2 to -2.7 mm) 30 days post-infection stained with antibody specific for the astrocyte marker GFAP (red) and counterstained with hematoxylin. Magnification 50X (left panels). Scale

bars indicate 100 μm (center panels), 20 μm (top right panel), and 10 μm (bottom right panel). Images are representative of 3 mice from 1 experiment.

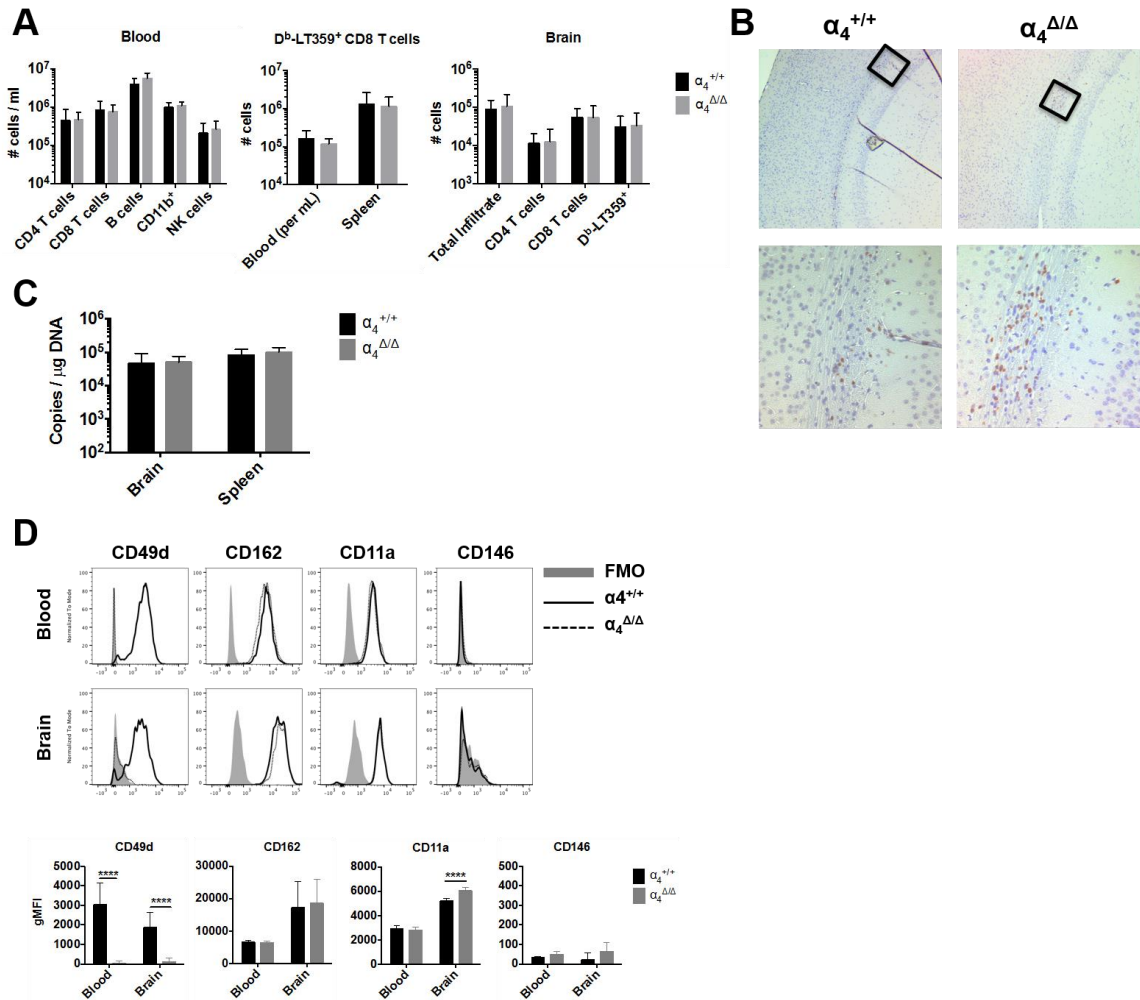
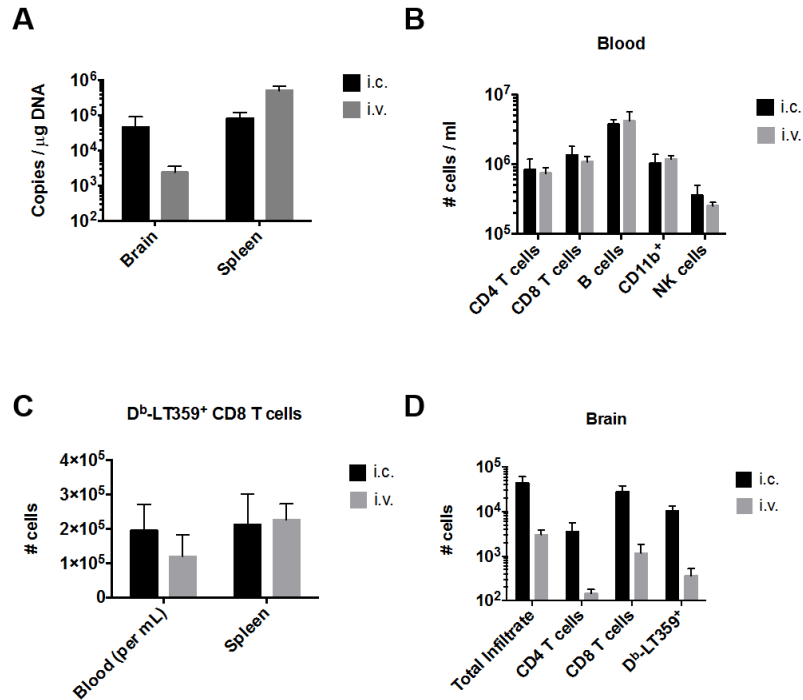


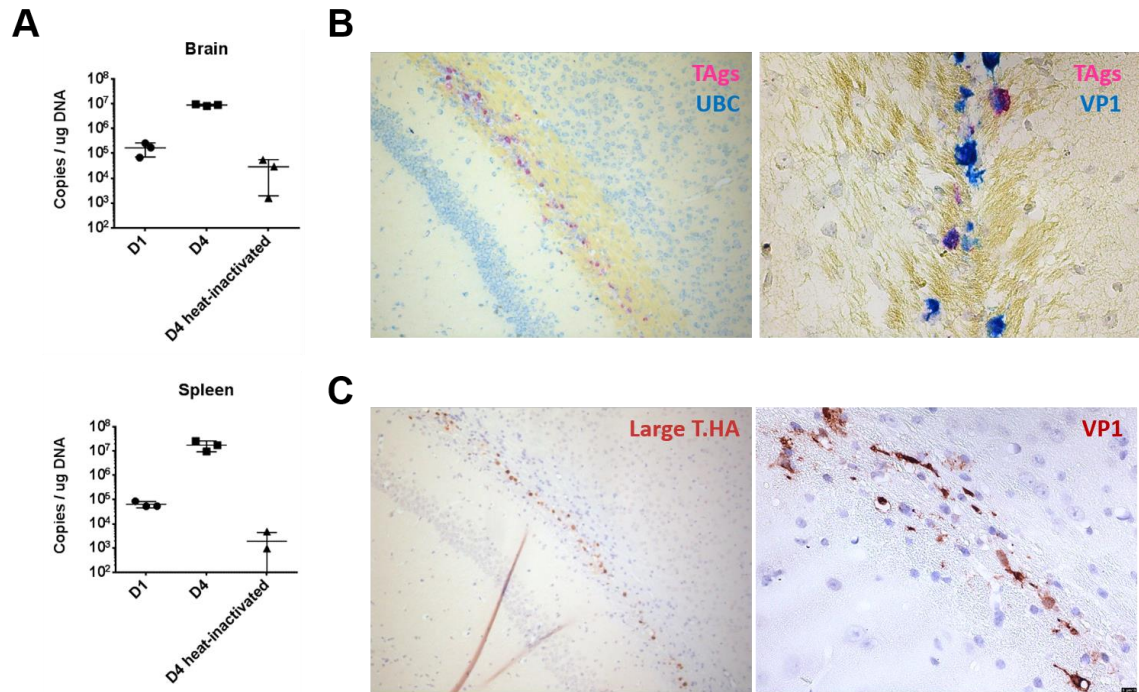
Figure 4-4. Comparison of immune responses and T cell infiltration of the brain in MPyV-infected VLA-4-deficient and -sufficient mice during acute infection. (A) Mean (\pm SD) of the number of immune cells of indicated populations in the blood, spleen, and brain at 8 days post-infection (dpi). (B) Photomicrographs of formalin-fixed, paraffin-embedded (FFPE) brain tissue sections from Cre-negative ($\alpha_4^{+/+}$; left panels) and α_4 integrin-deficient ($\alpha_4^{\Delta/\Delta}$; right panels) mice stained with anti-CD3 (red) and counterstained with hematoxylin. Bregma -2.7 mm; magnification in top panels is 50X with boxes indicating area shown in bottom panels at 200X. Images are representative of 4 mice/group from 1 experiment. (C) Mean (\pm SD) of viral genome copies in total

genomic DNA isolated from brain and spleen quantified by qPCR. (D) Expression of integrins VLA-4 (CD49d), PSGL-1 (CD162), LFA-1 (CD11a) and MCAM (CD146) by D^b-LT359⁺ CD8 T cells in the blood and brain of Cre-negative and α_4 integrin-deficient mice shown as representative histograms (top panel) compared to fluorescence minus one controls (shaded) and bar graphs of the mean (\pm SD) of the geometric mean fluorescence intensity (gMFI) of each integrin (bottom panel) with background subtracted. qPCR and flow cytometry data are cumulative from 2 experiments with 8 mice/group.

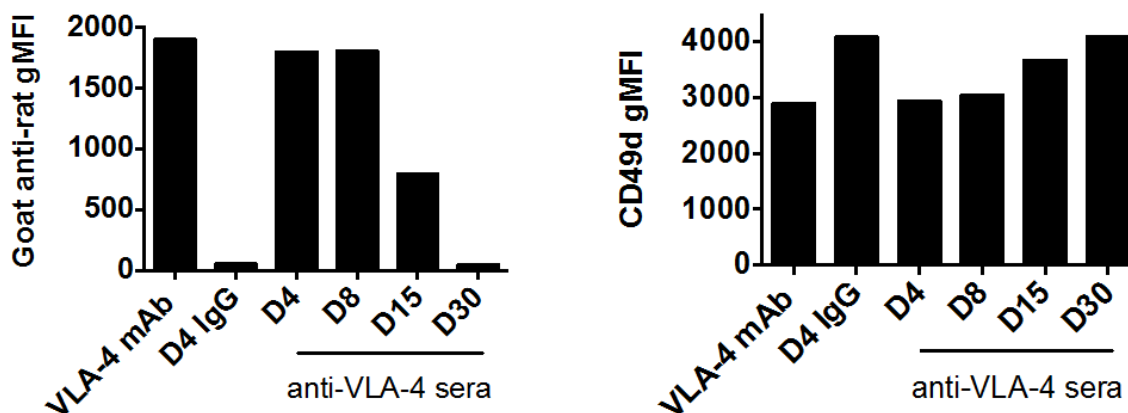
**** $p < 0.0001$



Supplemental Figure 4-1. Comparison of viral load and immune responses following intracerebral and intravenous inoculation with MPyV. (A) Mean (\pm SD) of viral genome copies in total genomic DNA isolated from brain and spleen of intracerebral (i.c.) and intravenous (i.v.) infected mice at 8 days post-infection quantified by qPCR. Mean (\pm SD) of the number of cells of indicated populations in the (B) blood, (C) blood and spleen, and (D) brain. Data are from 3 mice/group from 1 experiment.

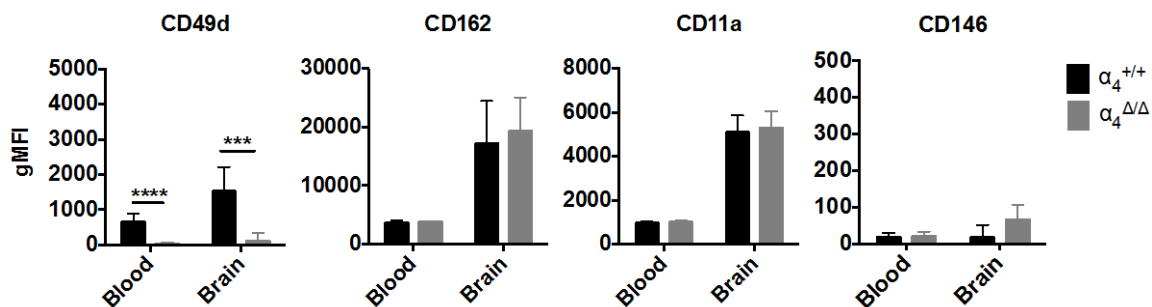


Supplemental Figure 4-2. Detection of MPyV replication in the brain following intracerebral inoculation. (A) Mean (\pm SD) of viral genome copies in total genomic DNA isolated from brains of mice at 1 day post-infection (input genomes) and 4 days post-infection (dpi) with untreated or heat-inactivated virus quantified by qPCR. (B) RNA in situ hybridization (ISH) for transcripts of MPyV T antigens (red) or the housekeeping gene ubiquitin C (blue) (left panel) in formalin-fixed paraffin-embedded (FFPE) brain sections. Magnification 100X. ISH for transcripts of MPyV T antigens (red) and VP1 (blue) in FFPE brain sections at 5 dpi (right panel). Magnification 400X. (C) Immunohistochemistry with antibodies specific for hemagglutinin-tagged MPyV Large T antigen (red; left panel) and MPyV VP1 (red; right panel) in FFPE brain sections at 5 dpi. Magnification 100X and 200X, respectively.



Supplemental Figure 4-3. Detection of anti-VLA-4 monoclonal antibody in sera.

MPyV infected mice were administered 250 μ g of anti-VLA-4 (clone PS/2) or control rat IgG at 0 and 2 days post-infection (dpi). Serum was collected from whole blood of mice at indicated timepoints and diluted 1:100 prior to incubation with splenocytes from untreated mice at 8 dpi (which express VLA-4). Splenocytes were stained with secondary goat anti-rat antibody for analysis by flow cytometry. Gated on VLA-4^{hi} CD8 T cells. (Left panel) Geometric mean fluorescence intensity of goat anti-rat secondary antibody following incubation of splenocytes with stock VLA-4 mAb (1:100) or serum from IgG or anti-VLA-4 treated mice at indicated timepoints post-infection. Data is from pooled sera of 4 mice/group. (Right panel) Geometric mean fluorescence intensity of CD49d (anti- α_4 integrin) staining of samples from left panel. Data demonstrate different binding sites of the two anti-VLA-4 antibodies but some steric hindrance. Data are from 1 experiment.



Supplemental Figure 4-4. Comparison of integrin expression profiles of CD4 T cells in MPyV-infected VLA-4-deficient and wild-type mice during acute infection.

Shown are the means (\pm SD) of the geometric mean fluorescent intensity of VLA-4 (CD49d), PSGL-1 (CD162), LFA-1 (CD11a) and MCAM (CD146) in total CD4 T cells in blood and brain of Cre-negative ($\alpha_4^{+/+}$) and α_4 integrin-deficient ($\alpha_4^{\Delta\Delta}$) mice.

Background fluorescence is subtracted. Data are cumulative from 2 experiments with 8 mice/group. *** p <0.001; **** p <0.0001.

CHAPTER 5

DISCUSSION

Progressive multifocal leukoencephalopathy is thought to be caused by uncontrolled lytic infection of oligodendrocytes by JC virus due to the absence of JCV-specific immune surveillance in the CNS. Much of what is known about the pathogenesis of PML is derived from studies at a late stage of disease, leaving early events that contribute to PML progression poorly understood. Without a tractable animal model due to strict species specificity of polyomaviruses, these questions regarding the evolution of PML have remained unanswered. Therefore, our aim was to generate a mouse model of CNS disease using mouse polyomavirus, a natural pathogen in this host, in order to study the contribution of virus-specific CD8 T cells in control or exacerbation of polyomavirus-induced demyelination. Here, we show that intracerebral inoculation of mice with MPyV leads to productive viral replication in epithelial cells of the ependyma as well as astrocytes in white matter tracts and that infection recruits virus-specific CD8 T cells in a VLA-4 independent manner, which are retained long-term in the CNS as a brain-resident memory population. Pathological consequences of MPyV infection in immunocompetent mice include demyelination, edema, ventriculitis, and astrocytosis. While the pathology observed is not fully consistent with that of PML, once optimized, this system may provide a tractable animal model of PyV-induced CNS disease. These findings raise important questions about whether or not the PML brain is immune-deficient with regard to JCV and whether the currently accepted mechanisms of JCV-mediated CNS damage are correct.

Demyelination can occur by both direct and indirect mechanisms of oligodendrocyte death. Examples of direct killing of oligodendrocytes include induction of their apoptosis or lysis due to infection and CD8 T cell cytotoxicity upon recognition of viral or self-antigen (ex. myelin) presented on the cell surface. Survival of mature myelinating oligodendrocytes also depends upon the presence of neuronal axons and supporting signals and factors from other glial cells, including astrocytes [192]; thus, any damage done to these cell types could have indirect and negative consequences on the welfare of oligodendrocytes. Presently, we have yet to determine how myelin is lost in this model of MPyV-induced CNS disease. The site of major demyelination, the cingulum bundle, was devoid of infected cells and T cell infiltrate at the latest timepoint examined as well as at the onset of myelin loss with the appearance of T cells at 9 days post-infection, suggesting death of oligodendrocytes by an indirect mechanism. However, negative immunohistochemical staining of biopsied tissue from lesions visualized by MRI has occurred in some cases of PML [184]. MPyV-infected brain sections should be evaluated at additional timepoints between 9 and 30 days post-infection to determine whether viral infection occurs in sites of severe demyelination.

Examination of brain tissue sections from infected mice by immunofluorescent staining did not reveal co-localization of the viral capsid protein VP1 and the mature oligodendrocyte marker APC. In cells that were infected with MPyV (VP1⁺), staining for Large T antigen (LT) was barely detectable. As a non-structural regulatory protein, LT is required for expression of VP1 and production of virions [193], making it unlikely that VP1⁺ cells would be LT⁻ and suggesting that sensitivity of our assay may not be sufficient or that the cells were at a late stage of infection after virion assembly.

Furthermore, immunohistochemistry (IHC) showed superior staining for viral antigens compared to immunofluorescence (IF) used for identification of infected CNS cell types, possibly due to amplification with streptavidin-peroxidase in addition to secondary antibody. Our current approach may be improved upon using the RNA in situ hybridization system mentioned in Chapter 4 which uses a specialized scaffold to significantly amplify the signal of the probe such that individual transcripts are detectable, or perhaps by flow cytometry. Alternatively, *in vitro* assays could offer an ancillary approach to determine whether oligodendrocytes are capable of supporting MPyV replication. Inoculation of the immortalized N19 oligodendrocyte cell line yielded few productively infected cells. Infection of primary oligodendrocytes may provide a more definitive answer as to the permissivity of these glial cells.

Alternatively, the extensive demyelination we observe in MPyV-infected mice could derive from inoculation of the CSF and a high frequency of infected ependymal cells. Infection itself as well as recruitment of T cells to the ventricles likely compromises their integrity. The resultant edema could distress neurons or astrocytes, which we have observed are highly reactive in the MPyV-infected brain although frequency of infection is low, and lead to indirect oligodendrocyte death and demyelination. Using such a model complicates determination of whether demyelination precedes edema or inability to compartmentalize fluid vacuolates the white matter. To circumvent this, stereotaxic injections of small volumes (2 μ l) of virus stock into the brain parenchyma could be evaluated as a means of inducing pathology more closely approximating that of PML. It is possible that with this approach the profile of MPyV-induced pathology may change dramatically from what is reported here and is therefore an area of critical importance in

refining this model. Although white matter structures in mice and humans are very different and recapitulation of all characteristics of PML lesions may not be achieved in an animal model, stereotactically inoculated JCV-infected humanized mice show punctate demyelination of the corpus callosum [101], which may arise in a manner mechanistically similar to radial PML lesions. If such pathology were reproduced in MPyV-infected mice, we could better address whether CD8 T cells and other immune responses protect against or contribute to demyelination.

Our route of virus stock administration has implications for infiltration of the brain by virus-specific CD8 T cells as well. T cell entry of the brain is precluded by three distinct anatomical obstacles-- the blood-brain barrier (BBB), the blood-cerebrospinal fluid barrier (BCSFB), and the blood-leptomeningeal barrier (BLMB) [194]. The basic morphology of the BBB and BLMB barriers consists of tight junctions between endothelial cells in the blood vessels, a perivascular space (or the CSF-filled subarachnoid space in the BLMB) containing antigen-presenting pericytic macrophages or dendritic cells, and the glia limitans, a layer of astrocyte endfeet that serves as the last line of separation from the brain parenchyma. Multistep adhesion, arrest, and extravasation of lymphocytes occurs along endothelial cells in the brain as for other activated endothelia, requiring upregulation of selectins and addressins, including P-selectin, VCAM-1, and ICAM-1, induced by pericytes. Once lymphocytes have entered the perivascular space, they must encounter pericytes displaying their antigen before proceeding across the glia limitans, a process regulated by laminins.

MPyV-specific CD8 T cells and CD4 T cells (of undetermined specificity) infiltrating the brain do not depend on binding of VLA-4 to its ligand VCAM-1 for their

migration, as determined by comparison of T cell numbers in the brains of MPyV-infected IgG- and VLA-4 blockade treated mice as well as in α_4 -floxed mice and wild-type α_4 controls. This contrasts with the presumed mechanism of treatment of multiple sclerosis (MS) patients with natalizumab (humanized anti-VLA-4) and mice with experimental autoimmune encephalomyelitis (EAE) given VLA-4 blockade, as in both cases, autoreactive cells are effectively excluded from the CNS [186, 195]. In MPyV-infected mice, T lymphocytes expressed high levels of the integrins CD162 (PSGL-1) and CD11a (a component of LFA-1), which given our findings, may sufficiently compensate for blockade or absence of VLA-4. Based on these findings, it may be valuable to screen the blood of natalizumab-treated MS patients for expression of integrins other than α_4 by JCV-specific T cells.

However, there is also the possibility that cells infiltrating the MPyV-infected brain enter by traversing the BCSFB, which involves P-selectin mediated exit of fenestrated capillaries into the choroid plexus, a villus epithelial structure in the ventricles that produces CSF [194]. The BCSFB is established by tight junctions between epithelial cells of the choroid plexus. It is not known how cells cross this barrier, but ICAM-1 and VCAM-1 are expressed only on the apical side of the epithelium, and therefore are not available for use in transmigration into the CSF [196, 197]. All that separates the CSF from the brain parenchyma is a single layer of ependymal cells lining the ventricles, which we have demonstrated are highly susceptible to MPyV infection and disruption in mice inoculated via the CSF. As such, it stands to reason that MPyV-specific T cells in these mice could use PSGL-1 to mediate entry of the choroid plexus and cross the BCSFB into the CSF, where they destroy the infected ependyma and advance to the brain

parenchyma, all independent of VLA-4. Thus, comparison of T cell trafficking in α_4 -floxed and wild-type mice must be repeated in a version of the model that is optimized such that ventriculitis is not a confounding variable. This, again, can likely be achieved using stereotaxic injections of small volumes of virus, possibly with strains carrying capsid mutations for reasons mentioned in Chapter 4, and may also require titration of virus dose.

This hypothesized entry of T cells through the choroid plexus does not account for the cessation in CD8 T cell migration after 8-10 dpi. We show in Chapter 2 that CD8 T cells are not replenished from the circulation after their peak infiltration, whereas CD4 T cells continuously infiltrate, suggesting that these cell types may use different routes of migration into the CNS or may depend on differentially regulated addressins.

Ventriculitis did not resolve by 30 dpi. If the choroid plexus was the portal of CD8 T cell entry, there would be no physical means to bar the entry of new cells during the persistent phase, which raises the question of what bars CD8 T cells entry at time points late in infection. One possibility is that cells in the periphery change their integrin expression profile in the persistent phase such that they are no longer capable of homing to the brain through the choroid plexus. MPyV infection may also trigger production of inflammatory factors by microglia and gemistocytic astrocytes, inducing activation of the endothelium; but, as virus-induced inflammation decreases over time, so does endothelial cell expression of the ligands T cells require for extravasation. If this were the case, then the amount of viral replication in the brain likely has important implications for T cell recruitment and it would be useful to determine the profile of adhesion molecules

upregulated by endothelial cells and their expression level in mice infected with varying doses of MPyV.

Presently, very little is understood about the timing of events leading to PML progression. JCV is ubiquitous in the human population and a member of the human virome [1, 2, 198]. Whether or not JCV traffics to and replicates in the brains of healthy individuals is controversial, but there have been reports of JCV DNA found in the brains of individuals without PML [199]. It is important to know whether innocuous polyomavirus replication in the brain is capable of recruiting JCV-specific T cells to the CNS. We have found in our model, that MPyV-specific CD8 T cells in the brain establish a stable resident memory population that is capable of *in situ* homeostatic proliferation, independent of survival signals provided by CD4 T cells. These results demonstrate the potential for establishment of JCV immune surveillance in the CNS that would be unaffected by blockade of VLA-4. If lack of JCV immunity in the brain does drive PML risk and progression and if indeed there are CNS resident JCV-specific T cells in humans, it could account for the low incidence of PML as a risk factor in natalizumab-treated patients. That is, individuals with JCV infection in the CNS that recruited virus-specific T cells prior to natalizumab treatment would adequately control JCV, preventing development of PML. Furthermore, the durability of brain T_{RM} cells may account for the increased risk of PML associated with prolonged natalizumab treatment (>2 years). If the resident memory population declines around this time and needs to be replaced by circulating cells, natalizumab could interfere with this process if JCV-specific cells require VLA-4. Additional insight into the survival factors for brain T_{RM} cells could help develop PML prevention strategies.

Further study of brain T_{RM} cells is needed to better understand their role in long-term protection of the CNS. When T_{RM} cells in the female reproductive tract (FRT) are reactivated by peptide challenge, they secrete IFN- γ leading to activation of vascular endothelium, upregulation of VCAM-1, and recruitment of circulating memory T cells regardless of antigen specificity [61, 200]. They also sound the alarm to the innate immune response via cytokines, inducing dendritic cell maturation with TNF- α and granzyme B production by NK cells with IL-2; together, these effects of pathogen detection by T_{RM} cells promote an antiviral state [200]. It is noteworthy that the cytokines employed by T_{RM} cells are typical of protective polyfunctional T cell responses, and that a high frequency of MPyV-specific brain T_{RM} cells produce IFN- γ and TNF- α upon *ex vivo* peptide stimulation.

T_{RM} cells in the polyomavirus-infected brain may have a unique role due to stasis between low-level persistent infection and anti-viral CD8 T cells, which we have shown are functional and have heightened sensitivity to antigen through high-affinity TCRs. For brain T_{RM} cells to ring alarm bells as is described for those of the FRT upon antigen recognition in a persistent infection setting would likely result in immune pathology. In an organ with numerous non-regenerative cells, such as neurons, this would be deleterious to the host. Additionally, much of the work describing T_{RM} cells is focused on populations in barrier tissues, such as the mucosa, skin, and lungs, where T_{RM} cells are a front-line defense against pathogen invasion. Although polyomavirus is neither cleared nor latent, “reactivation” of JCV in the kidney is thought to occur in humans with certain immune suppressive conditions, increasing the chance of virus trafficking to the brain. It

would be interesting to know how brain T_{RM} cells at the battlefield react to resurgence of viral load in the brain.

Challenge experiments after primary infection with MPyV typically require a heterologous virus, such as vaccinia or vesicular stomatitis virus, to carry the CD8 T cell epitope, because humoral responses to MPyV are highly neutralizing [201]; we have observed occasional plasma cells near the ventricles, indicating the same considerations may need to be taken with CNS challenge. Alternatively, peptide-based challenge could be used by either i.c. injection of LT359 itself or by peptide-pulsed dendritic cells. Because balance of immunity with pathology is likely crucial for brain T_{RM}, it would be interesting to test whether the context in which antigen is presented at challenge influences the recall response. An altered profile of inflammatory cytokines from challenge with heterologous virus or injection of dendritic cells that have not differentiated in the CNS could yield results that are not reflective of polyomavirus reactivation but could give insight into T_{RM} responses. It would also be of interest to determine whether IFN- γ produced by reactivated T_{RM} cells in the brain induces vascular endothelial upregulation of VCAM-1. Perhaps in situations of increased viral replication, T_{RM} cells need reinforcement from circulating polyoma-specific cells, and if VLA-4 is dependent for migration those cells to the CNS, natalizumab might interfere. Another possibility is that, if T_{RM} cells are not tightly regulated, they may recruit memory cells similar to FRT T_{RM} cells and induce inflammation reminiscent of that seen in PML immune reconstitution inflammatory syndrome (IRIS).

In addition to providing a model with which to investigate immunity to polyomavirus infection in the CNS, our work contributes to the fields of tissue resident

memory cells and T cell exhaustion. Our study was the first to show that memory cells residing in non-lymphoid tissues, but not in secondary lymphoid organs, maintain heightened affinity for antigen. High affinity is a property of effector T cells, evident by similar patterns of binding to peptide:MHC-I in cells of the spleen, kidney, and brain at 8 dpi. Affinity of MPyV-specific CD8 T cells declined in the spleen over time, suggesting that high affinity cells were lost during the contraction phase. Similarly, effector cells in both the brain and spleen express PD-1, but it is only sustained by memory cells in the brain and does not induce exhaustion. In the kidney, viral load in the persistent phase is very low with i.c. inoculation, but T_{RM} cells exhibited intermediate levels of PD-1. Taken together with negative staining for both killer-cell lectin-like receptor G1 (KLRG1; a marker of T cell senescence) and the IL-7 receptor, T_{RM} cells in the brain and kidney possess several phenotypic traits of effector cells. An overall effector-like state may specially adapt T_{RM} cells to detect antigen rapidly and to survive in non-lymphoid organs. Future work with this model could focus on the role of CD103, which unlike in the setting of acutely cleared VSV-infection, was not required to maintain brain residence of MPyV-specific cells but interestingly was tied to PD-1 expression. Additional insight into CD4 T cell specificity, phenotype, and cytokine profile would also be of interest.

We have laid the groundwork for a long-awaited animal model for study of polyomavirus-induced demyelinating disease in the central nervous system. Although some modifications may be necessary for improved approximation of pathology with that of PML, we have demonstrated that this model is useful for investigation of disease mechanisms and the role of T cell responses and immunity as a whole. Further inquiry of

these areas may reveal which aspects of immunity are beneficial and which contribute to PML progression, allowing treatment and possibly prevention of PML.

REFERENCES

1. Egli, A., et al., *Prevalence of polyomavirus BK and JC infection and replication in 400 healthy blood donors*. J Infect Dis, 2009. **199**(6): p. 837-46.
2. Berger, J.R., et al., *JC virus antibody status underestimates infection rates*. Ann Neurol, 2013. **74**(1): p. 84-90.
3. Kean, J.M., et al., *Seroepidemiology of human polyomaviruses*. PLoS Pathog, 2009. **5**(3): p. e1000363.
4. Monaco, M.C., et al., *JC virus infection of hematopoietic progenitor cells, primary B lymphocytes, and tonsillar stromal cells: implications for viral latency*. J Virol, 1996. **70**(10): p. 7004-12.
5. Bofill-Mas, S. and R. Girones, *Excretion and transmission of JCV in human populations*. J Neurovirol, 2001. **7**(4): p. 345-9.
6. Berger, J.R., et al., *JC virus detection in bodily fluids: clues to transmission*. Clin Infect Dis, 2006. **43**(1): p. e9-12.
7. Padgett, B.L., et al., *Cultivation of papova-like virus from human brain with progressive multifocal leukoencephalopathy*. Lancet, 1971. **1**(7712): p. 1257-60.
8. Itoyama, Y., et al., *Distribution of papovavirus, myelin-associated glycoprotein, and myelin basic protein in progressive multifocal leukoencephalopathy lesions*. Ann Neurol, 1982. **11**(4): p. 396-407.
9. Zu Rhein, G.M., *Association of papova-virions with a human demyelinating disease (progressive multifocal leukoencephalopathy)*. Prog Med Virol, 1969. **11**: p. 185-247.
10. Astrom, K.E., E.L. Mancall, and E.P. Richardson, Jr., *Progressive multifocal leukoencephalopathy; a hitherto unrecognized complication of chronic lymphatic leukaemia and Hodgkin's disease*. Brain, 1958. **81**(1): p. 93-111.
11. Major, E.O., *Progressive multifocal leukoencephalopathy in patients on immunomodulatory therapies*. Annu Rev Med, 2010. **61**: p. 35-47.
12. Gheuens, S., et al., *Progressive multifocal leukoencephalopathy in individuals with minimal or occult immunosuppression*. J Neurol Neurosurg Psychiatry, 2010. **81**(3): p. 247-54.
13. Ferenczy, M.W., et al., *Molecular biology, epidemiology, and pathogenesis of progressive multifocal leukoencephalopathy, the JC virus-induced demyelinating disease of the human brain*. Clin Microbiol Rev, 2012. **25**(3): p. 471-506.
14. Kleinschmidt-DeMasters, B.K. and K.L. Tyler, *Progressive multifocal leukoencephalopathy complicating treatment with natalizumab and interferon beta-1a for multiple sclerosis*. N Engl J Med, 2005. **353**(4): p. 369-74.
15. Langer-Gould, A., et al., *Progressive multifocal leukoencephalopathy in a patient treated with natalizumab*. N Engl J Med, 2005. **353**(4): p. 375-81.
16. Van Assche, G., et al., *Progressive multifocal leukoencephalopathy after natalizumab therapy for Crohn's disease*. N Engl J Med, 2005. **353**(4): p. 362-8.
17. Bloomgren, G., et al., *Risk of natalizumab-associated progressive multifocal leukoencephalopathy*. N Engl J Med, 2012. **366**(20): p. 1870-80.
18. von Andrian, U.H. and B. Engelhardt, *Alpha4 integrins as therapeutic targets in autoimmune disease*. N Engl J Med, 2003. **348**(1): p. 68-72.
19. Stuve, O., et al., *Immune surveillance in multiple sclerosis patients treated with natalizumab*. Ann Neurol, 2006. **59**(5): p. 743-7.

20. Carson, K.R., et al., *Monoclonal antibody-associated progressive multifocal leukoencephalopathy in patients treated with rituximab, natalizumab, and efalizumab: a Review from the Research on Adverse Drug Events and Reports (RADAR) Project*. *Lancet Oncol*, 2009. **10**(8): p. 816-24.
21. Melet, J., et al., *Rituximab-induced T cell depletion in patients with rheumatoid arthritis: association with clinical response*. *Arthritis Rheum*, 2013. **65**(11): p. 2783-90.
22. Leon, B., et al., *Prolonged antigen presentation by immune complex-binding dendritic cells programs the proliferative capacity of memory CD8 T cells*. *J Exp Med*, 2014.
23. Clifford, D., *Progressive multifocal leukoencephalopathy therapy*. *Journal of NeuroVirology*, 2014: p. 1-5.
24. Johnson, T. and A. Nath, *Immune reconstitution inflammatory syndrome and the central nervous system*. *Curr Opin Neurol*, 2011. **24**(3): p. 284-90.
25. Gorelik, L., et al., *Progressive multifocal leukoencephalopathy (PML) development is associated with mutations in JC virus capsid protein VP1 that change its receptor specificity*. *J Infect Dis*, 2011. **204**(1): p. 103-14.
26. Sunyaev, S.R., et al., *Adaptive mutations in the JC virus protein capsid are associated with progressive multifocal leukoencephalopathy (PML)*. *PLoS Genet*, 2009. **5**(2): p. e1000368.
27. Reid, C.E., et al., *Sequencing and analysis of JC virus DNA from natalizumab-treated PML patients*. *J Infect Dis*, 2011. **204**(2): p. 237-44.
28. Pietropaolo, V., et al., *Rearrangement patterns of JC virus noncoding control region from different biological samples*. *J Neurovirol*, 2003. **9**(6): p. 603-11.
29. Gosert, R., et al., *Polyomavirus BK with rearranged noncoding control region emerge in vivo in renal transplant patients and increase viral replication and cytopathology*. *J Exp Med*, 2008. **205**(4): p. 841-52.
30. Chen, B.J. and W.J. Atwood, *Construction of a novel JCV/SV40 hybrid virus (JCSV) reveals a role for the JCV capsid in viral tropism*. *Virology*, 2002. **300**(2): p. 282-90.
31. Maginnis, M.S., et al., *Progressive multifocal leukoencephalopathy-associated mutations in the JC polyomavirus capsid disrupt lactoseries tetrasaccharide c binding*. *MBio*, 2013. **4**(3): p. e00247-13.
32. Murata, H., et al., *Identification of a neutralization epitope in the VP1 capsid protein of SV40*. *Virology*, 2008. **381**(1): p. 116-22.
33. Pastrana, D.V., et al., *Neutralization serotyping of BK polyomavirus infection in kidney transplant recipients*. *PLoS Pathog*, 2012. **8**(4): p. e1002650.
34. Luo, C., et al., *VP-1 quasispecies in human infection with polyomavirus BK*. *J Med Virol*, 2012. **84**(1): p. 152-61.
35. Berger, J.R., *The clinical features of PML*. *Cleve Clin J Med*, 2011. **78 Suppl 2**: p. S8-12.
36. Du Pasquier, R.A., et al., *JCV-specific cellular immune response correlates with a favorable clinical outcome in HIV-infected individuals with progressive multifocal leukoencephalopathy*. *J Neurovirol*, 2001. **7**(4): p. 318-22.
37. Koralnik, I.J., R.A. Du Pasquier, and N.L. Letvin, *JC virus-specific cytotoxic T lymphocytes in individuals with progressive multifocal leukoencephalopathy*. *J Virol*, 2001. **75**(7): p. 3483-7.
38. Koralnik, I.J., et al., *Association of prolonged survival in HLA-A2+ progressive multifocal leukoencephalopathy patients with a CTL response specific for a commonly recognized JC virus epitope*. *J Immunol*, 2002. **168**(1): p. 499-504.
39. Weber, T., et al., *Analysis of the systemic and intrathecal humoral immune response in progressive multifocal leukoencephalopathy*. *J Infect Dis*, 1997. **176**(1): p. 250-4.

40. Guillaume, B., C.J. Sindic, and T. Weber, *Progressive multifocal leukoencephalopathy: simultaneous detection of JCV DNA and anti-JCV antibodies in the cerebrospinal fluid*. Eur J Neurol, 2000. **7**(1): p. 101-6.
41. Du Pasquier, R.A., et al., *A prospective study demonstrates an association between JC virus-specific cytotoxic T lymphocytes and the early control of progressive multifocal leukoencephalopathy*. Brain, 2004. **127**(Pt 9): p. 1970-8.
42. Gasnault, J., et al., *Critical role of JC virus-specific CD4 T-cell responses in preventing progressive multifocal leukoencephalopathy*. AIDS, 2003. **17**(10): p. 1443-9.
43. Lima, M.A., et al., *Frequency and phenotype of JC virus-specific CD8+ T lymphocytes in the peripheral blood of patients with progressive multifocal leukoencephalopathy*. J Virol, 2007. **81**(7): p. 3361-8.
44. Du Pasquier, R.A., et al., *Detection of JC virus-specific cytotoxic T lymphocytes in healthy individuals*. J Virol, 2004. **78**(18): p. 10206-10.
45. Du Pasquier, R.A., et al., *Low frequency of cytotoxic T lymphocytes against the novel HLA-A*0201-restricted JC virus epitope VP1(p36) in patients with proven or possible progressive multifocal leukoencephalopathy*. J Virol, 2003. **77**(22): p. 11918-26.
46. Wuthrich, C., et al., *Characterization of lymphocytic infiltrates in progressive multifocal leukoencephalopathy: co-localization of CD8(+) T cells with JCV-infected glial cells*. J Neurovirol, 2006. **12**(2): p. 116-28.
47. Achim, C.L. and C.A. Wiley, *Expression of major histocompatibility complex antigens in the brains of patients with progressive multifocal leukoencephalopathy*. J Neuropathol Exp Neurol, 1992. **51**(3): p. 257-63.
48. Murali-Krishna, K., et al., *Counting antigen-specific CD8 T cells: a reevaluation of bystander activation during viral infection*. Immunity, 1998. **8**(2): p. 177-87.
49. Yousef, S., et al., *TCR bias and HLA cross-restriction are strategies of human brain-infiltrating JC virus-specific CD4+ T cells during viral infection*. J Immunol, 2012. **189**(7): p. 3618-30.
50. Jameson, S.C. and D. Masopust, *Diversity in T cell memory: an embarrassment of riches*. Immunity, 2009. **31**(6): p. 859-71.
51. Sallusto, F., et al., *Two subsets of memory T lymphocytes with distinct homing potentials and effector functions*. Nature, 1999. **401**(6754): p. 708-12.
52. Masopust, D. and J.M. Schenkel, *The integration of T cell migration, differentiation and function*. Nat Rev Immunol, 2013. **13**(5): p. 309-20.
53. Skon, C.N., et al., *Transcriptional downregulation of S1pr1 is required for the establishment of resident memory CD8+ T cells*. Nat Immunol, 2013. **14**(12): p. 1285-93.
54. Matloubian, M., et al., *Lymphocyte egress from thymus and peripheral lymphoid organs is dependent on S1P receptor 1*. Nature, 2004. **427**(6972): p. 355-60.
55. Pauls, K., et al., *Role of integrin alphaE(CD103)beta7 for tissue-specific epidermal localization of CD8+ T lymphocytes*. J Invest Dermatol, 2001. **117**(3): p. 569-75.
56. Casey, K.A., et al., *Antigen-independent differentiation and maintenance of effector-like resident memory T cells in tissues*. J Immunol, 2012. **188**(10): p. 4866-75.
57. Graham, J.B., A. Da Costa, and J.M. Lund, *Regulatory T cells shape the resident memory T cell response to virus infection in the tissues*. J Immunol, 2014. **192**(2): p. 683-90.
58. Wakim, L.M., et al., *CD8(+) T-cell attenuation of cutaneous herpes simplex virus infection reduces the average viral copy number of the ensuing latent infection*. Immunol Cell Biol, 2008. **86**(8): p. 666-75.
59. Masopust, D., *Developing an HIV cytotoxic T-lymphocyte vaccine: issues of CD8 T-cell quantity, quality and location*. J Intern Med, 2009. **265**(1): p. 125-37.

60. Masopust, D., et al., *Dynamic T cell migration program provides resident memory within intestinal epithelium*. J Exp Med, 2010. **207**(3): p. 553-64.
61. Schenkel, J.M., et al., *Sensing and alarm function of resident memory CD8(+) T cells*. Nat Immunol, 2013. **14**(5): p. 509-13.
62. Gebhardt, T., et al., *Memory T cells in nonlymphoid tissue that provide enhanced local immunity during infection with herpes simplex virus*. Nat Immunol, 2009. **10**(5): p. 524-30.
63. Masopust, D. and L.J. Picker, *Hidden memories: frontline memory T cells and early pathogen interception*. J Immunol, 2012. **188**(12): p. 5811-7.
64. Wakim, L.M., A. Woodward-Davis, and M.J. Bevan, *Memory T cells persisting within the brain after local infection show functional adaptations to their tissue of residence*. Proc Natl Acad Sci U S A, 2010. **107**(42): p. 17872-9.
65. Fox, R.J. and J.A. Cohen, *Multiple sclerosis: the importance of early recognition and treatment*. Cleve Clin J Med, 2001. **68**(2): p. 157-71.
66. Ransohoff, R.M. and B. Engelhardt, *The anatomical and cellular basis of immune surveillance in the central nervous system*. Nat Rev Immunol, 2012. **12**(9): p. 623-35.
67. Tan, C.S., et al., *Increased program cell death-1 expression on T lymphocytes of patients with progressive multifocal leukoencephalopathy*. J Acquir Immune Defic Syndr, 2012. **60**(3): p. 244-8.
68. Keir, M.E., et al., *PD-1 and its ligands in tolerance and immunity*. Annu Rev Immunol, 2008. **26**: p. 677-704.
69. Wei, F., et al., *Strength of PD-1 signaling differentially affects T-cell effector functions*. Proc Natl Acad Sci U S A, 2013. **110**(27): p. E2480-9.
70. Barber, D.L., et al., *Restoring function in exhausted CD8 T cells during chronic viral infection*. Nature, 2006. **439**(7077): p. 682-7.
71. Schachtele, S.J., et al., *Glial cells suppress postencephalitic CD8+ T lymphocytes through PD-L1*. Glia, 2014. **62**(10): p. 1582-94.
72. Parra, G.I., et al., *Gamma interferon signaling in oligodendrocytes is critical for protection from neurotropic coronavirus infection*. J Virol, 2010. **84**(6): p. 3111-5.
73. Phares, T.W., et al., *Target-dependent B7-H1 regulation contributes to clearance of central nervous system infection and dampens morbidity*. J Immunol, 2009. **182**(9): p. 5430-8.
74. Phares, T.W., et al., *Enhanced antiviral T cell function in the absence of B7-H1 is insufficient to prevent persistence but exacerbates axonal bystander damage during viral encephalomyelitis*. J Immunol, 2010. **185**(9): p. 5607-18.
75. Salama, A.D., et al., *Critical role of the programmed death-1 (PD-1) pathway in regulation of experimental autoimmune encephalomyelitis*. J Exp Med, 2003. **198**(1): p. 71-8.
76. Zhu, B., et al., *Differential role of programmed death-ligand 1 [corrected] and programmed death-ligand 2 [corrected] in regulating the susceptibility and chronic progression of experimental autoimmune encephalomyelitis*. J Immunol, 2006. **176**(6): p. 3480-9.
77. Schreiner, B., et al., *PD-1 ligands expressed on myeloid-derived APC in the CNS regulate T-cell responses in EAE*. Eur J Immunol, 2008. **38**(10): p. 2706-17.
78. Kroner, A., et al., *Accelerated course of experimental autoimmune encephalomyelitis in PD-1-deficient central nervous system myelin mutants*. Am J Pathol, 2009. **174**(6): p. 2290-9.

79. Sadagopal, S., et al., *Enhanced PD-1 expression by T cells in cerebrospinal fluid does not reflect functional exhaustion during chronic human immunodeficiency virus type 1 infection*. J Virol, 2010. **84**(1): p. 131-40.
80. Kinter, A.L., et al., *The common gamma-chain cytokines IL-2, IL-7, IL-15, and IL-21 induce the expression of programmed death-1 and its ligands*. J Immunol, 2008. **181**(10): p. 6738-46.
81. Terawaki, S., et al., *IFN-alpha directly promotes programmed cell death-1 transcription and limits the duration of T cell-mediated immunity*. J Immunol, 2011. **186**(5): p. 2772-9.
82. Gerner, M.Y., et al., *Cutting edge: IL-12 and type I IFN differentially program CD8 T cells for programmed death 1 re-expression levels and tumor control*. J Immunol, 2013. **191**(3): p. 1011-5.
83. Jin, Y.H., et al., *The role of interleukin-6 in the expression of PD-1 and PDL-1 on central nervous system cells following infection with Theiler's murine encephalomyelitis virus*. J Virol, 2013. **87**(21): p. 11538-51.
84. Nakamichi, K., et al., *Long-term infection of adult mice with murine polyomavirus following stereotaxic inoculation into the brain*. Microbiol Immunol, 2010. **54**(8): p. 475-82.
85. DeCaprio, J.A., *How the Rb tumor suppressor structure and function was revealed by the study of Adenovirus and SV40*. Virology, 2009. **384**(2): p. 274-84.
86. Tikhanovich, I. and H.P. Nasheuer, *Host-specific replication of BK virus DNA in mouse cell extracts is independently controlled by DNA polymerase alpha-primase and inhibitory activities*. J Virol, 2010. **84**(13): p. 6636-44.
87. Bruckner, A., et al., *The mouse DNA polymerase alpha-primase subunit p48 mediates species-specific replication of polyomavirus DNA in vitro*. Mol Cell Biol, 1995. **15**(3): p. 1716-24.
88. Chia, W. and P.W. Rigby, *Fate of viral DNA in nonpermissive cells infected with simian virus 40*. Proc Natl Acad Sci U S A, 1981. **78**(11): p. 6638-42.
89. Hacker, D. and M.M. Fluck, *High-level recombination specific to polyomavirus genomes targeted to the integration-transformation pathway*. Mol Cell Biol, 1989. **9**(3): p. 995-1004.
90. Israel, M.A., et al., *Biological activity of polyoma viral DNA in mice and hamsters*. J Virol, 1979. **29**(3): p. 990-6.
91. London, W.T., et al., *Viral-induced astrocytomas in squirrel monkeys*. Prog Clin Biol Res, 1983. **105**: p. 227-37.
92. Major, E.O., P. Mourrain, and C. Cummins, *JC virus-induced owl monkey glioblastoma cells in culture: biological properties associated with the viral early gene product*. Virology, 1984. **136**(2): p. 359-67.
93. Nagashima, K., et al., *Induction of brain tumors by a newly isolated JC virus (Tokyo-1 strain)*. Am J Pathol, 1984. **116**(3): p. 455-63.
94. Gordon, J., et al., *Pituitary neoplasia induced by expression of human neurotropic polyomavirus, JCV, early genome in transgenic mice*. Oncogene, 2000. **19**(42): p. 4840-6.
95. Khalili, K., et al., *Human neurotropic polyomavirus, JCV, and its role in carcinogenesis*. Oncogene, 2003. **22**(33): p. 5181-91.
96. Krynska, B., et al., *Identification of a novel p53 mutation in JCV-induced mouse medulloblastoma*. Virology, 2000. **274**(1): p. 65-74.
97. Trapp, B.D., et al., *Dysmyelination in transgenic mice containing JC virus early region*. Ann Neurol, 1988. **23**(1): p. 38-48.

98. Tan, C.S., et al., *Detection of JC virus-specific immune responses in a novel humanized mouse model*. PLoS One, 2013. **8**(5): p. e64313.
99. Windrem, M.S., et al., *Neonatal chimerization with human glial progenitor cells can both remyelinate and rescue the otherwise lethally hypomyelinated shiverer mouse*. Cell Stem Cell, 2008. **2**(6): p. 553-65.
100. Sim, F.J., et al., *CD140a identifies a population of highly myelinogenic, migration-competent and efficiently engrafting human oligodendrocyte progenitor cells*. Nat Biotechnol, 2011. **29**(10): p. 934-41.
101. Kondo, Y., et al., *Human glial chimeric mice reveal astrocytic dependence of JC virus infection*. J Clin Invest, 2014. **124**(12): p. 5323-36.
102. Van Loy, T., et al., *JC virus quasispecies analysis reveals a complex viral population underlying progressive multifocal leukoencephalopathy and supports viral dissemination via the hematogenous route*. J Virol, 2015. **89**(2): p. 1340-7.
103. Chapagain, M.L., et al., *Polyomavirus JC infects human brain microvascular endothelial cells independent of serotonin receptor 2A*. Virology, 2007. **364**(1): p. 55-63.
104. Dorries, K., et al., *Infection of human polyomaviruses JC and BK in peripheral blood leukocytes from immunocompetent individuals*. Virology, 1994. **198**(1): p. 59-70.
105. Atwood, W.J., et al., *Interaction of the human polyomavirus, JCV, with human B-lymphocytes*. Virology, 1992. **190**(2): p. 716-23.
106. Lindberg, R.L., et al., *Natalizumab alters transcriptional expression profiles of blood cell subpopulations of multiple sclerosis patients*. J Neuroimmunol, 2008. **194**(1-2): p. 153-64.
107. Marshall, L.J., et al., *Lymphocyte gene expression and JC virus noncoding control region sequences are linked with the risk of progressive multifocal leukoencephalopathy*. J Virol, 2014. **88**(9): p. 5177-83.
108. Houff, S.A., J. Berger, and E.O. Major, *Response to Linberg et al. Natalizumab alters transcriptional expression profiles of blood cell subpopulations of multiple sclerosis patients*. J Neuroimmunol, 2008. **204**(1-2): p. 155-6; author reply 157.
109. Houff, S.A. and J.R. Berger, *The bone marrow, B cells, and JC virus*. J Neurovirol, 2008. **14**(5): p. 341-3.
110. Chapagain, M.L. and V.R. Nerurkar, *Human polyomavirus JC (JCV) infection of human B lymphocytes: a possible mechanism for JCV transmigration across the blood-brain barrier*. J Infect Dis, 2010. **202**(2): p. 184-91.
111. Bonig, H., et al., *Increased numbers of circulating hematopoietic stem/progenitor cells are chronically maintained in patients treated with the CD49d blocking antibody natalizumab*. Blood, 2008. **111**(7): p. 3439-41.
112. Craddock, C.F., et al., *Antibodies to VLA4 integrin mobilize long-term repopulating cells and augment cytokine-induced mobilization in primates and mice*. Blood, 1997. **90**(12): p. 4779-88.
113. Papayannopoulou, T. and B. Nakamoto, *Peripheralization of hemopoietic progenitors in primates treated with anti-VLA4 integrin*. Proc Natl Acad Sci U S A, 1993. **90**(20): p. 9374-8.
114. Krumbholz, M., et al., *Natalizumab disproportionately increases circulating pre-B and B cells in multiple sclerosis*. Neurology, 2008. **71**(17): p. 1350-4.
115. Zohren, F., et al., *The monoclonal anti-VLA-4 antibody natalizumab mobilizes CD34+ hematopoietic progenitor cells in humans*. Blood, 2008. **111**(7): p. 3893-5.

116. Fluck, M.M. and B.S. Schaffhausen, *Lessons in signaling and tumorigenesis from polyomavirus middle T antigen*. Microbiol Mol Biol Rev, 2009. **73**(3): p. 542-63, Table of Contents.
117. Rowe, W.P., *The epidemiology of mouse polyoma virus infection*. Bacteriol Rev, 1961. **25**: p. 18-31.
118. Carroll, J., et al., *Receptor-binding and oncogenic properties of polyoma viruses isolated from feral mice*. PLoS Pathog, 2007. **3**(12): p. e179.
119. Dawe, C.J., et al., *Variations in polyoma virus genotype in relation to tumor induction in mice. Characterization of wild type strains with widely differing tumor profiles*. Am J Pathol, 1987. **127**(2): p. 243-61.
120. Drake, D.R., 3rd, et al., *Polyomavirus-infected dendritic cells induce antiviral CD8(+) T lymphocytes*. J Virol, 2000. **74**(9): p. 4093-101.
121. Freund, R., et al., *A single-amino-acid substitution in polyomavirus VP1 correlates with plaque size and hemagglutination behavior*. J Virol, 1991. **65**(1): p. 350-5.
122. Bauer, P.H., et al., *Genetic and structural analysis of a virulence determinant in polyomavirus VP1*. J Virol, 1995. **69**(12): p. 7925-31.
123. De Mattei, M., et al., *High incidence of BK virus large-T-antigen-coding sequences in normal human tissues and tumors of different histotypes*. Int J Cancer, 1995. **61**(6): p. 756-60.
124. Drake, D.R., 3rd and A.E. Lukacher, *Beta 2-microglobulin knockout mice are highly susceptible to polyoma virus tumorigenesis*. Virology, 1998. **252**(1): p. 275-84.
125. Kembal, C.C., et al., *Late priming and variability of epitope-specific CD8+ T cell responses during a persistent virus infection*. J Immunol, 2005. **174**(12): p. 7950-60.
126. Vezys, V., et al., *Continuous recruitment of naive T cells contributes to heterogeneity of antiviral CD8 T cells during persistent infection*. J Exp Med, 2006. **203**(10): p. 2263-9.
127. Lukacher, A.E., et al., *Pyvs: a dominantly acting gene in C3H/BiDa mice conferring susceptibility to tumor induction by polyoma virus*. Virology, 1993. **196**(1): p. 241-8.
128. Beltrami, S. and J. Gordon, *Immune surveillance and response to JC virus infection and PML*. J Neurovirol, 2014. **20**(2): p. 137-49.
129. Dalianis, T. and H.H. Hirsch, *Human polyomaviruses in disease and cancer*. Virology, 2013. **437**(2): p. 63-72.
130. Han Lee, E.D., et al., *A mouse model for polyomavirus-associated nephropathy of kidney transplants*. Am J Transplant, 2006. **6**(5 Pt 1): p. 913-22.
131. Albrecht, J.A., et al., *Adaptive immunity rather than viral cytopathology mediates polyomavirus-associated nephropathy in mice*. Am J Transplant, 2012. **12**(6): p. 1419-28.
132. McCance, D.J., *The types of mouse brain cells susceptible to polyoma virus infection in vitro*. J Gen Virol, 1984. **65** (Pt 1): p. 221-6.
133. Sebesteny, A., et al., *Demyelination and wasting associated with polyomavirus infection in nude (nu/nu) mice*. Lab Anim, 1980. **14**(4): p. 337-45.
134. McCance, D.J., et al., *A paralytic disease in nude mice associated with polyoma virus infection*. J Gen Virol, 1983. **64** (Pt 1): p. 57-67.
135. Harper, J.S., 3rd, et al., *Paralysis in nude mice caused by polyomavirus-induced vertebral tumors*. Prog Clin Biol Res, 1983. **105**: p. 359-67.
136. Steinert, E.M., et al., *Quantifying Memory CD8 T Cells Reveals Regionalization of Immunosurveillance*. Cell, 2015. **161**(4): p. 737-49.
137. Schenkel, J.M. and D. Masopust, *Tissue-resident memory T cells*. Immunity, 2014. **41**(6): p. 886-97.

138. Anderson, K.G., et al., *Intravascular staining for discrimination of vascular and tissue leukocytes*. Nat Protoc, 2014. **9**(1): p. 209-22.
139. Wakim, L.M., et al., *The molecular signature of tissue resident memory CD8 T cells isolated from the brain*. J Immunol, 2012. **189**(7): p. 3462-71.
140. Huang, J., et al., *The kinetics of two-dimensional TCR and pMHC interactions determine T-cell responsiveness*. Nature, 2010. **464**(7290): p. 932-6.
141. Sabatino, J.J., Jr., et al., *High prevalence of low affinity peptide-MHC II tetramer-negative effectors during polyclonal CD4+ T cell responses*. J Exp Med, 2011. **208**(1): p. 81-90.
142. Johnson, A.J., et al., *Prevalent class I-restricted T-cell response to the Theiler's virus epitope Db:VP2121-130 in the absence of endogenous CD4 help, tumor necrosis factor alpha, gamma interferon, perforin, or costimulation through CD28*. J Virol, 1999. **73**(5): p. 3702-8.
143. Klonowski, K.D., et al., *Dynamics of blood-borne CD8 memory T cell migration in vivo*. Immunity, 2004. **20**(5): p. 551-62.
144. Mackay, L.K., et al., *The developmental pathway for CD103(+)CD8+ tissue-resident memory T cells of skin*. Nat Immunol, 2013. **14**(12): p. 1294-301.
145. Jiang, N., et al., *Two-stage cooperative T cell receptor-peptide major histocompatibility complex-CD8 trimolecular interactions amplify antigen discrimination*. Immunity, 2011. **34**(1): p. 13-23.
146. Kersh, A.E., L.J. Edwards, and B.D. Evavold, *Progression of relapsing-remitting demyelinating disease does not require increased TCR affinity or epitope spread*. J Immunol, 2014. **193**(9): p. 4429-38.
147. Blanchfield, J.L., S.K. Shorter, and B.D. Evavold, *Monitoring the Dynamics of T Cell Clonal Diversity Using Recombinant Peptide:MHC Technology*. Front Immunol, 2013. **4**: p. 170.
148. Hofmann, M. and H. Pircher, *E-cadherin promotes accumulation of a unique memory CD8 T-cell population in murine salivary glands*. Proc Natl Acad Sci U S A, 2011. **108**(40): p. 16741-6.
149. Virgin, H.W., E.J. Wherry, and R. Ahmed, *Redefining chronic viral infection*. Cell, 2009. **138**(1): p. 30-50.
150. Wherry, E.J., *T cell exhaustion*. Nat Immunol, 2011. **12**(6): p. 492-9.
151. Okazaki, T., et al., *PD-1 immunoreceptor inhibits B cell receptor-mediated signaling by recruiting src homology 2-domain-containing tyrosine phosphatase 2 to phosphotyrosine*. Proc Natl Acad Sci U S A, 2001. **98**(24): p. 13866-71.
152. Chemnitz, J.M., et al., *SHP-1 and SHP-2 associate with immunoreceptor tyrosine-based switch motif of programmed death 1 upon primary human T cell stimulation, but only receptor ligation prevents T cell activation*. J Immunol, 2004. **173**(2): p. 945-54.
153. Pauken, K.E. and E.J. Wherry, *Overcoming T cell exhaustion in infection and cancer*. Trends Immunol, 2015. **36**(4): p. 265-76.
154. Zinselmeyer, B.H., et al., *PD-1 promotes immune exhaustion by inducing antiviral T cell motility paralysis*. J Exp Med, 2013. **210**(4): p. 757-74.
155. Staron, M.M., et al., *The transcription factor FoxO1 sustains expression of the inhibitory receptor PD-1 and survival of antiviral CD8(+) T cells during chronic infection*. Immunity, 2014. **41**(5): p. 802-14.
156. Odorizzi, P.M., et al., *Genetic absence of PD-1 promotes accumulation of terminally differentiated exhausted CD8+ T cells*. J Exp Med, 2015. **212**(7): p. 1125-37.
157. Price, D.A., et al., *T cell receptor recognition motifs govern immune escape patterns in acute SIV infection*. Immunity, 2004. **21**(6): p. 793-803.

158. Schmitz, J.E., et al., *Control of viremia in simian immunodeficiency virus infection by CD8+ lymphocytes*. Science, 1999. **283**(5403): p. 857-60.
159. Jin, X., et al., *Dramatic rise in plasma viremia after CD8(+) T cell depletion in simian immunodeficiency virus-infected macaques*. J Exp Med, 1999. **189**(6): p. 991-8.
160. Duraiswamy, J., et al., *Phenotype, function, and gene expression profiles of programmed death-1(hi) CD8 T cells in healthy human adults*. J Immunol, 2011. **186**(7): p. 4200-12.
161. Paley, M.A., et al., *Progenitor and terminal subsets of CD8+ T cells cooperate to contain chronic viral infection*. Science, 2012. **338**(6111): p. 1220-5.
162. Hong, J.J., et al., *Re-evaluation of PD-1 expression by T cells as a marker for immune exhaustion during SIV infection*. PLoS One, 2013. **8**(3): p. e60186.
163. Speiser, D.E., et al., *T cell differentiation in chronic infection and cancer: functional adaptation or exhaustion?* Nat Rev Immunol, 2014. **14**(11): p. 768-74.
164. Wherry, E.J. and M. Kurachi, *Molecular and cellular insights into T cell exhaustion*. Nat Rev Immunol, 2015. **15**(8): p. 486-99.
165. Wilson, J.J., et al., *CD8 T cells recruited early in mouse polyomavirus infection undergo exhaustion*. J Immunol, 2012. **188**(9): p. 4340-8.
166. Frost, E.L., et al., *Cutting Edge: Resident Memory CD8 T Cells Express High-Affinity TCRs*. J Immunol, 2015. **195**(8): p. 3520-4.
167. Wherry, E.J., et al., *Viral persistence alters CD8 T-cell immunodominance and tissue distribution and results in distinct stages of functional impairment*. J Virol, 2003. **77**(8): p. 4911-27.
168. Blattman, J.N., et al., *Impact of epitope escape on PD-1 expression and CD8 T-cell exhaustion during chronic infection*. J Virol, 2009. **83**(9): p. 4386-94.
169. Legroux, L., et al., *An optimized method to process mouse CNS to simultaneously analyze neural cells and leukocytes by flow cytometry*. J Neurosci Methods, 2015. **247**: p. 23-31.
170. DeVos, S.L. and T.M. Miller, *Direct intraventricular delivery of drugs to the rodent central nervous system*. J Vis Exp, 2013(75): p. e50326.
171. Johanson, C.E., et al., *Multiplicity of cerebrospinal fluid functions: New challenges in health and disease*. Cerebrospinal Fluid Res, 2008. **5**: p. 10.
172. Lafon, M., et al., *Detrimental contribution of the immuno-inhibitor B7-H1 to rabies virus encephalitis*. J Immunol, 2008. **180**(11): p. 7506-15.
173. Lipp, M., et al., *PD-L1 (B7-H1) regulation in zones of axonal degeneration*. Neurosci Lett, 2007. **425**(3): p. 156-61.
174. Magnus, T., et al., *Microglial expression of the B7 family member B7 homolog 1 confers strong immune inhibition: implications for immune responses and autoimmunity in the CNS*. J Neurosci, 2005. **25**(10): p. 2537-46.
175. Mueller, S.N., et al., *PD-L1 has distinct functions in hematopoietic and nonhematopoietic cells in regulating T cell responses during chronic infection in mice*. J Clin Invest, 2010. **120**(7): p. 2508-15.
176. He, J., et al., *Development of PD-1/PD-L1 Pathway in Tumor Immune Microenvironment and Treatment for Non-Small Cell Lung Cancer*. Sci Rep, 2015. **5**: p. 13110.
177. Karpowicz, P., et al., *E-Cadherin regulates neural stem cell self-renewal*. J Neurosci, 2009. **29**(12): p. 3885-96.
178. Youngblood, B., et al., *Chronic virus infection enforces demethylation of the locus that encodes PD-1 in antigen-specific CD8(+) T cells*. Immunity, 2011. **35**(3): p. 400-12.
179. Youngblood, B., C.W. Davis, and R. Ahmed, *Making memories that last a lifetime: heritable functions of self-renewing memory CD8 T cells*. Int Immunol, 2010. **22**(10): p. 797-803.

180. Utzschneider, D.T., et al., *T cells maintain an exhausted phenotype after antigen withdrawal and population reexpansion*. Nat Immunol, 2013. **14**(6): p. 603-10.
181. Stoner, G.L., et al., *A monoclonal antibody to SV40 large T-antigen labels a nuclear antigen in JC virus-transformed cells and in progressive multifocal leukoencephalopathy (PML) brain infected with JC virus*. J Neuroimmunol, 1988. **17**(4): p. 331-45.
182. Stoner, G.L., et al., *A double-label method detects both early (T-antigen) and late (capsid) proteins of JC virus in progressive multifocal leukoencephalopathy brain tissue from AIDS and non-AIDS patients*. J Neuroimmunol, 1988. **19**(3): p. 223-36.
183. Aksamit, A.J., J.L. Sever, and E.O. Major, *Progressive multifocal leukoencephalopathy: JC virus detection by in situ hybridization compared with immunohistochemistry*. Neurology, 1986. **36**(4): p. 499-504.
184. Gheuens, S., C. Wuthrich, and I.J. Koralnik, *Progressive multifocal leukoencephalopathy: why gray and white matter*. Annu Rev Pathol, 2013. **8**: p. 189-215.
185. Koralnik, I.J., et al., *JC virus granule cell neuronopathy: A novel clinical syndrome distinct from progressive multifocal leukoencephalopathy*. Ann Neurol, 2005. **57**(4): p. 576-80.
186. Bauer, M., et al., *Beta1 integrins differentially control extravasation of inflammatory cell subsets into the CNS during autoimmunity*. Proc Natl Acad Sci U S A, 2009. **106**(6): p. 1920-5.
187. Wilson, J.J., et al., *Gamma interferon controls mouse polyomavirus infection in vivo*. J Virol, 2011. **85**(19): p. 10126-34.
188. Mittelbrunn, M., et al., *VLA-4 integrin concentrates at the peripheral supramolecular activation complex of the immune synapse and drives T helper 1 responses*. Proc Natl Acad Sci U S A, 2004. **101**(30): p. 11058-63.
189. Priestley, G.V., T. Ulyanova, and T. Papayannopoulou, *Sustained alterations in biodistribution of stem/progenitor cells in Tie2Cre+ alpha4(f/f) mice are hematopoietic cell autonomous*. Blood, 2007. **109**(1): p. 109-11.
190. Johansson, C.B., et al., *Identification of a neural stem cell in the adult mammalian central nervous system*. Cell, 1999. **96**(1): p. 25-34.
191. Schneider-Hohendorf, T., et al., *VLA-4 blockade promotes differential routes into human CNS involving PSGL-1 rolling of T cells and MCAM-adhesion of TH17 cells*. J Exp Med, 2014. **211**(9): p. 1833-46.
192. Bradl, M. and H. Lassmann, *Oligodendrocytes: biology and pathology*. Acta Neuropathol, 2010. **119**(1): p. 37-53.
193. An, P., M.T. Saenz Robles, and J.M. Pipas, *Large T antigens of polyomaviruses: amazing molecular machines*. Annu Rev Microbiol, 2012. **66**: p. 213-36.
194. Engelhardt, B. and R.M. Ransohoff, *Capture, crawl, cross: the T cell code to breach the blood-brain barriers*. Trends Immunol, 2012. **33**(12): p. 579-89.
195. Polman, C.H., et al., *A randomized, placebo-controlled trial of natalizumab for relapsing multiple sclerosis*. N Engl J Med, 2006. **354**(9): p. 899-910.
196. Steffen, B.J., et al., *ICAM-1, VCAM-1, and MAdCAM-1 are expressed on choroid plexus epithelium but not endothelium and mediate binding of lymphocytes in vitro*. Am J Pathol, 1996. **148**(6): p. 1819-38.
197. Wolburg, K., et al., *Ultrastructural localization of adhesion molecules in the healthy and inflamed choroid plexus of the mouse*. Cell Tissue Res, 1999. **296**(2): p. 259-69.
198. De Vlaminck, I., et al., *Temporal response of the human virome to immunosuppression and antiviral therapy*. Cell, 2013. **155**(5): p. 1178-87.

199. White, F.A., 3rd, et al., *JC virus DNA is present in many human brain samples from patients without progressive multifocal leukoencephalopathy*. J Virol, 1992. **66**(10): p. 5726-34.
200. Schenkel, J.M., et al., *T cell memory. Resident memory CD8 T cells trigger protective innate and adaptive immune responses*. Science, 2014. **346**(6205): p. 98-101.
201. Swanson, P.A., 2nd, A.E. Lukacher, and E. Szomolanyi-Tsuda, *Immunity to polyomavirus infection: the polyomavirus-mouse model*. Semin Cancer Biol, 2009. **19**(4): p. 244-51.